KALMAN FILTER BASED ORBIT OBSERVABILITY STUDY

by

ROY ROBERT SHORTEN

B.Eng., Sir George Williams University, 1972

A THESIS SUBMITTED IN PARTIAL FULFILLMENT OF
THE REQUIREMENTS FOR THE DEGREE OF

MASTER OF APPLIED SCIENCE

in

THE FACULTY OF GRADUATE STUDIES

(Department of Electrical Engineering)

We accept this thesis as conforming
to the required standard.

THE UNIVERSITY OF BRITISH COLUMBIA

June, 1979

In presenting this thesis in partial fulfilment of the requirements for an advanced degree at the University of British Columbia, I agree that the Library shall make it freely available for reference and study. I further agree that permission for extensive copying of this thesis for scholarly purposes may be granted by the Head of my Department or by his representatives. It is understood that copying or publication of this thesis for financial gain shall not be allowed without my written permission.

Department of Electrical Engineering

The University of British Columbia
2075 Wesbrook Place
Vancouver, Canada
V6T 1W5

Date June 27, 1979

ABSTRACT

An Extended Kalman filter simulation technique was used to determine the observability of satellite orbits from one or two earth stations. It was found that range and range-rate measurements alone were insufficient for orbit determination. Either azimuth angle or elevation angle information were also required before an acceptable orbital estimate was obtained. However, range and range-rate measurements alone proved to be sufficient to improve the state estimates of approximately known orbits. Also if simultaneous range and range-rate measurements were available from two stations, orbit determination was possible. Various common orbital types were used throughout the study and only one pass of data was considered.

TABLE OF CONTENTS

LIST OF TABLES

LIST OF FIGURES

ACKNOWLEDGEMENTS

I would like to express my thanks to my supervisor Dr. E.V. Bohn and Dr. A.C. Soudack for their assistance in preparing and help in reviewing this thesis. I would also like to thank Dr. V.J. Modi for his help and encouragement.

CHAPTER I

INTRODUCTION TO SATELLITE TRACKING

1. Observable?

A system is observable if from a given set of measurements you can distinguish the states of the system. If the system in question happens to be a satellite in orbit around the earth, the states can be considered its position and velocity. Determining a satellite's position and velocity is called orbit determination. Newton's inverse square law, which relates the distance between two masses to the force of attraction between them, is the primary effect governing satellite motion. It also makes the problem non-linear.

Observability for a linear system is relatively simple to determine. It has been proven that the rank of the observability matrix determines whether the system is observable or not. In the non-linear case however, observability is much more difficult to determine [3]. Currently the primary method of determining non-linear observability is simulation. This is the approach taken in this thesis. A quasi-realistic model is employed and simulation runs are performed using various types of measurements in order to determine if the states can be distinguished. The model is quasi-realistic because as with any model assumptions were made and secondary effects neglected. A simulation is only as good as its assumptions and model. A discussion of these limitations is presented in chapter II.

2. Geometry

Satellites of the earth describe paths which are conic sections. We shall concern ourselves only with circular and elliptical orbits. All orbits describe a plane in space called the orbital plane which, in the presence of a purely central force, is fixed in inertial space. Measurements of satellite position along this orbit are obtained from a station on the surface of the earth, which is itself rotating. This rotation of the earth complicates the measurement process as the position and velocity of the measurer must continually be updated and taken into account. Only a small part of the orbit can be seen from any one earth station. The rest of the orbit is hidden behind the earth. This brings in the concept of 'pass', a pass being the portion of an orbit during which the satellite is above the horizon of the measuring station. A pass can last from zero minutes in the case of a satellite which is forever hidden from some station, to millions of years as in the case of a geosynchronous satellite. The length of time the satellite is in view affects its observability.

3. Measurement Methods

Historically the first method used to track satellites was visual sighting. It was used by the ancients to track the moon, the planets, and the stars, all of which they believed circled the earth. Visual tracking can supply angular information only. It is impossible to estimate range visually as can be seen from ancient estimates of the distance to the moon. The angular accuracy of visual tracking is surprisingly good, but it is difficult during daylight to track anything with less brightness than the moon. The visual method was later

augmented by the use of optical equipment such as telescopes. These enabled much better accuracy to be obtained and also allowed daylight measurements, but significantly increased the cost. When cameras were added to the optical tracking equipment, extremely high accuracies were obtained by measurements relative to known stellar background positions.

The recent introduction of radar to track satellites has drastically changed the type and quantity of measurements that can be performed. While the angular information supplied from radars is not nearly as accurate as from optical methods, radar does supply an accurate range and range-rate measurement.

If the satellite we wish to track is active, that is if it carries on board a radio transceiver which will receive and transmit radio signals, other types of tracking equipment can be used. Large phased antenna arrays and/or large steerable dish antennas can be used to obtain angular information, however both of these are extremely expensive. Conversely range and range rate measurements are relatively inexpensive. To measure range one only has to accurately measure a signal's round trip travel time to and from the satellite. The accuracy is determined by the time resolution possible. Accuracies of fifty centimeters are possible using sophisticated laser techniques [7]. Inexpensive equipment could resolve to about one kilometer without major problems. Range-rate measurements are accomplished by measuring the Doppler shift caused by satellite motion. Again relatively inexpensive equipment can resolve to about three meters per second.

4. Basic Problem Studied

Given that range and range-rate measurements were relatively inexpensive while angular measurements either by optical methods or radar were very expensive, the question arose as to whether range and range-rate were sufficient for orbit determination. From the control standpoint, the question was: "Is the system observable?". If the system were not observable, what was the minimum number of measurements required to make it observable, and how much could be accomplished using range and range-rate alone? Were angular measurements of satellite position required for satellite tracking? And finally, "What technique could be developed to answer the above questions?"

5. Method

The first problem encountered when one is attempting to determine observability is one of method. How does one show observability? As mentioned earlier the theoretical approach is extremely arduous for non-linear systems. Simulation offers the only alternative. An algorithm must be chosen such that if it fails to observe the system, the system is, to a high probability, not observable. The algorithm must be relatively simple so that program complexity is not a problem, and yet sophsticated enough to handle the measurement noise expected and the system model used. Escobal [1] treats a number of the classical methods of orbit determination, however all are deterministic and do not allow noise. If we consider the problem of contaminated measurements we have a choice between least squares, Kalman filtering and some form of parameter estimation. Since it can be shown that the sequential algorithms obtained from least squares are essentially the same as those

obtained from Kalman filtering [8], and since the non-linearity of the problem makes parameter estimation particularly difficult, the Kalman filter was chosen as the basic examination tool. The basic Kalman filter is an algorithm whereby measurements are weighted as they arrive according to the error in the state estimate (error covariance estimate). As estimates of the state derived from a system model get worse, the measurements are weighted higher. As the state estimates get better, the measurements are weighted lower and therefore have less affect on future state estimates. Chapter III further expands on the Kalman filter.

The method decided on therefore consists of writing a number of Kalman filter based smoothers to test various combinations of measurements.

CHAPTER II

THE SYSTEM MODEL

1. Limitations

State of the art orbit determination programs such as [5], take into account many factors of second and third order. These include earth gravitational anomalies, lunar and solar gravity, solar wind, atmospheric drag, earthshine etc. The model used in this study is the classical Newtonian central force model. The inclusion of secondary and tertiary effects would add little to the basic question of observability, while causing a complexity which would obscure basic problems and effects.

All the measurements were assumed to have been made from the same location on the earth. The location chosen was the Hector McLeod Building of the University of British Columbia. This represents an intermediate latitude of approximately 50 degrees, so it is believed that results obtained with this station will hold true for most other latitudes. The station coordinates are assumed to be known exactly. Noise with a normal distribution was impressed on all measurements. The standard deviation being tailored to the type of measurement. It is assumed throughout that the satellite is active and will return a signal sent to it with a known delay, and it was with this measurement technique in mind that the noise standard deviations were chosen.

2. Units

The geocentric system of units is used throughout this thesis. This system avoids the use of large numbers and is a more "natural"

system. It uses units defined by the system itself. The geocentric system has as its unit of distance the radius of the earth (E.R.). One E.R. is equal to 6,378.15 km. Its unit of time is the mean solar day, and its unit of mass is the mass of the earth. The gravitational constant (k) in the geocentric system is 107.0867 E.R. $^{3/2}$/Day.

3. Coordinates

3.1 Azimuth-Elevation Coordinate System

Measurements from a station on the surface of the earth of a satellite's position are referenced initially to the azimuth-elevation coordinate system. This is a rotating coordinate system which has as its origin the observing station, see Figure II.1.

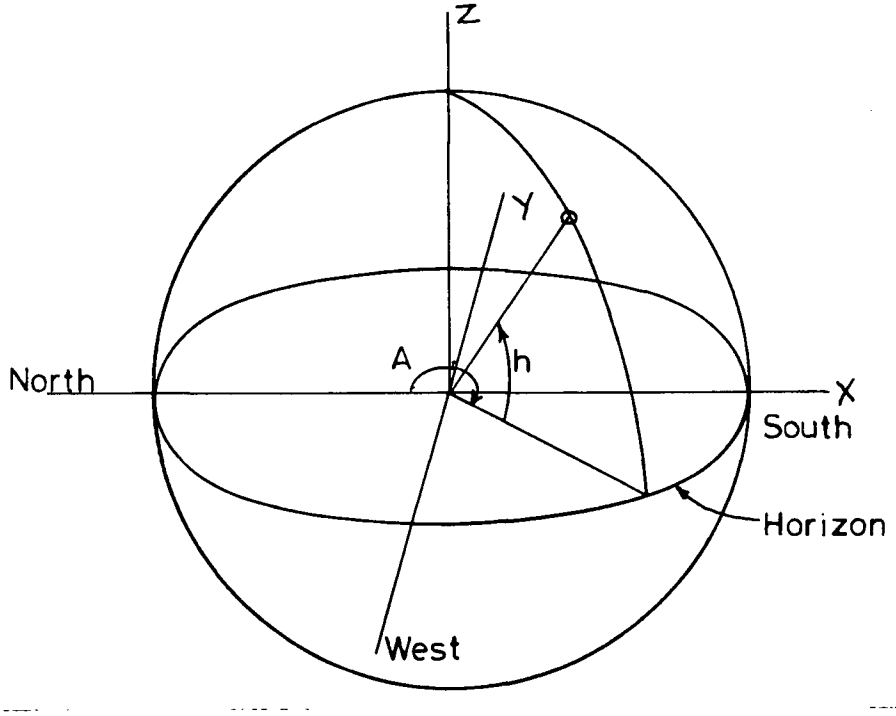

Azimuth-Elevation Coordinate System.

Figure II.1

The fundamental plane is defined as being tangential to the earth at the

observer. This means that the local vertical is normal to the fundamental plane. The positive X direction is defined as being due South. The positive Y direction is therefore due East and positive Z is straight up. Two angles which define the direction of the satellite in this system are the elevation and azimuth angles. The elevation is the angle between the satellite and the fundamental plane measured in a plane perpendicular to the fundamental plane. The azimuth is the angle measured from North in the fundamental plane to the projection of the satellite radial onto the fundamental plane. Range is simply the distance of the satellite from the origin measured along the radial.

3.2 Right Ascension Declination Coordinate System

The right ascension declination coordinate system is an inertial or fixed system. Its center is taken as the center of the earth, but it does not rotate with the earth. The fundamental plane is the plane of the equator and the positive X direction points toward the vernal equinox, see Figure II.2. The positive Z direction is up through the North pole and the Y direction completes the right handed system. There are two ways to define a location in this system. The first is to simply specify the X, Y, and Z coordinates. This is the system used in the system model. The second is to specify the right ascension, the declination and the range. The range is simply the distance from the center to the location to be specified. The right ascension is the angle measured in the fundamental plane between the X axis and the projection of the radial vector onto the fundamental plane. The declination is the angle between the location and the equator measured in a plane normal to the equator.

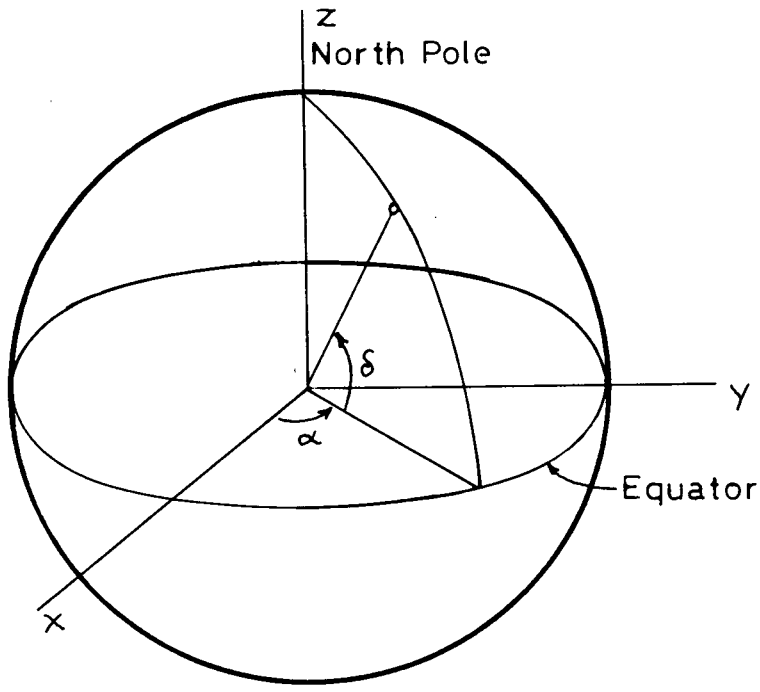

Right Ascension Declination Coordinate System.

Figure II.2

3.3 Orbital Plane Coordinate System

It is often much easier to analyze an orbital problem from a system which takes as its fundamental plane, the orbital plane of the satellite. Such a system is fixed in inertial space if there are no perturbations. Realistically, however, there are always perturbations and the orbital plane will gradually drift. Since it is annoying to have the coordinate system drift the fundamental plane is usually taken as the orbital plane at some epoch time. The center of this system is the center of the earth. The positive X axis points towards the perifocus. One of the angles defined in this coordinate system is of some importance. This is the eccentric anomaly (E). See Figure II.3

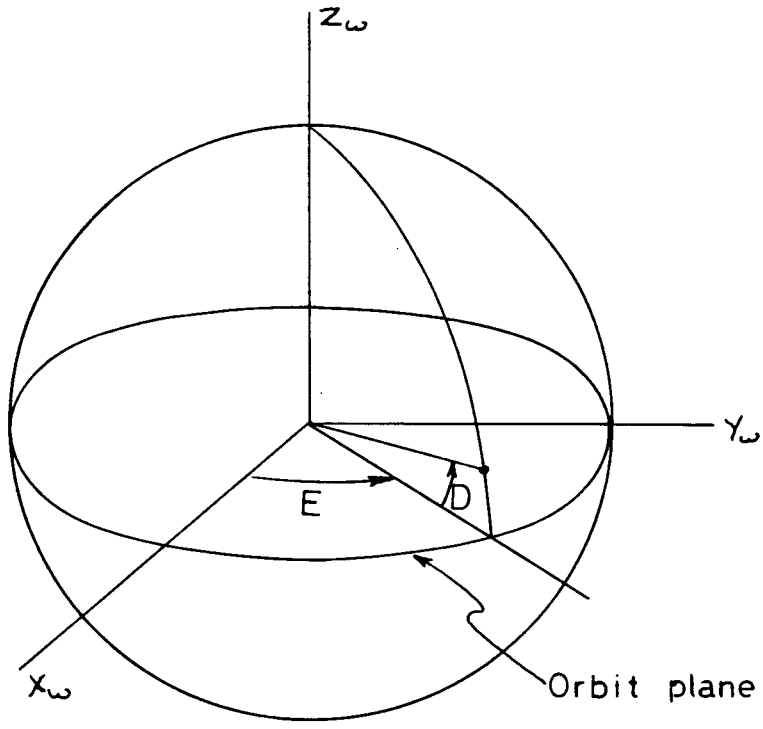

Orbital Plane Coordinate System Oblique View

Figure II.3

and Figure II.4. It is defined as the angle measured in the fundamental plane from the X axis to the point on a circle that circumscribes the actual ellipse of motion measured at the center of the circumscribed circle.

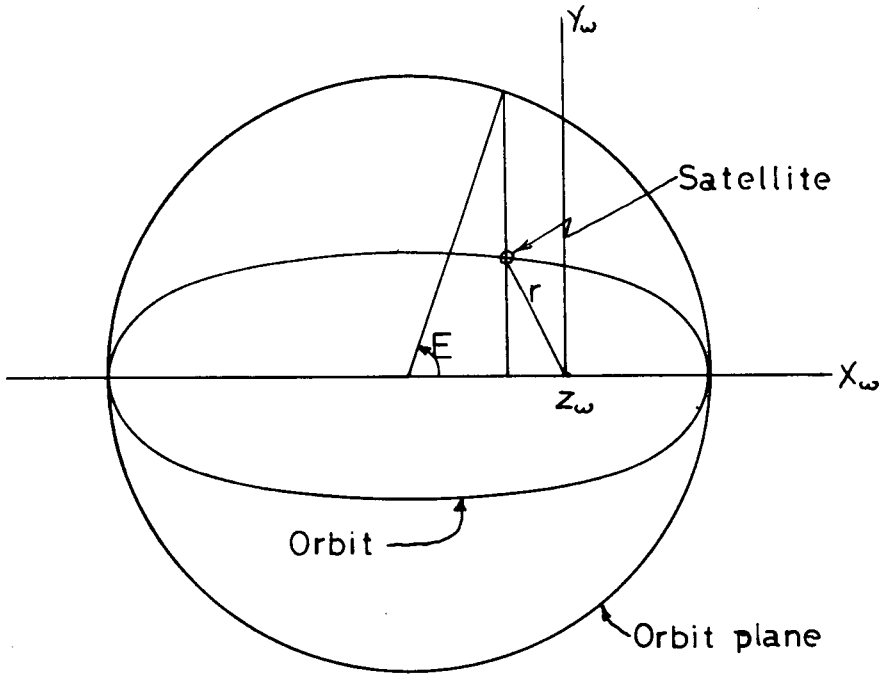

Orbital Plane Coordinate System Perpendicular View.

Figure II.4

4. State Model

The system model decided on has six states, three of position and three of velocity. A model based on these three states in an inertial reference frame was determined to be the simplest available. Attitude states etc. were neglected as irrelavant. The model is based solely on Newton's inverse square law. The satellite state vector X is defined as $(x_1, x_2, x_3, x_4, x_5, x_6)^T$ where:

x_1 is the velocity in the X direction

x_2 is the velocity in the Y direction

x_3 is the velocity in the Z direction

x_4 is the displacement in the X direction

x_5 is the displacement in the Y direction, and

x_6 is the displacement in the Z direction.

The state equation can be seen in Table II.1.

$$\begin{bmatrix} \dot{X}_1 \\ \dot{X}_2 \\ \dot{X}_3 \\ \dot{X}_4 \\ \dot{X}_5 \\ \dot{X}_6 \end{bmatrix} = \begin{bmatrix} \dfrac{-k\ X_4}{(X_4^2 + X_5^2 + X_6^2)^{3/2}} \\ \dfrac{-k\ X_5}{(X_4^2 + X_5^2 + X_6^2)^{3/2}} \\ \dfrac{-k\ X_6}{(X_4^2 + X_5^2 + X_6^2)^{3/2}} \\ X_1 \\ X_2 \\ X_3 \end{bmatrix}$$

State Equation.

Table II.1

5. Measurement Model

There are four types of measurements considered in this thesis. They are:

Range: The distance from the observing station to the satellite, obtained by measuring round trip signal times.

Range-Rate: The speed with which the satellite is approaching or receding along the line of sight, obtained by measuring the Doppler shift.

Azimuth: The azimuth angle to the satellite measured in the azimuth elevation coordinate system.

Elevation: The elevation angle to the satellite measured in the azimuth elevation coordinate system.

The equations for these measurements in terms of the system states can be found in Table II.2.

The noise present in the measurements was also modeled. Random numbers with a Gaussian distribution were added to the measurements before they were used. The standard deviations used were

Range..... 0.0001 E.R.

Range Rate..... 0.04 E.R./Day

Azimuth..... 0.01 radians

Elevation..... 0.01 radians.

It was felt that these values represented an easily achievable measurement accuracy.

Range $\lvert\rho\rvert$	$[(X_4 - S_4)^2 + (X_5 - S_5)^2 + (X_6 - S_6)^2]^{1/2}$
Range-Rate $\lvert\dot{\rho}\rvert$	$\dfrac{(X_4-S_4)(X_1-S_1)+(X_5-S_5)(X_2-S_2)+(X_6-S_6)(X_3-S_3)}{\lvert\rho\rvert}$
Elevation Angle (h)	$\sin^{-1}\left[\dfrac{\rho \cdot R}{\lvert\rho\rvert \lvert R\rvert}\right]$
Azimuth Angle (A)	$\cos^{-1}\left[\dfrac{\tilde{\rho} \cdot N}{\lvert\tilde{\rho}\rvert \lvert N\rvert}\right]$
symbol definitions	$S \triangleq$ Station State Vector S_1 X velocity S_2 Y velocity S_3 Z velocity S_4 X displacement S_5 Y displacement S_6 Z displacement $R \triangleq$ Station Position Vector R_1 through R_3 = S_4 through S_6 $N \triangleq$ Vector pointing due North in plane tangent to the earth at the station $\rho \triangleq$ Station to satellite position vector $\tilde{\rho} \triangleq$ Projection of ρ on plane tangent to the earth at station.

Measurement Equations.

Table II.2

CHAPTER III

KALMAN FILTERING AND SMOOTHING

1. Linear Kalman Filter

A filter, in the estimation sense of the word, is an algorithm which estimates the state vector at the current time based upon past measurements corrupted by noise. The linear Kalman filter is such an algorithm. It minimizes the estimation error in a well defined statistical sense. The linear Kalman filter equations are presented in Table III.1.

System Model	$X_k = \phi_{k-1} X_{k-1} + w_{k-1}, \quad w_k \sim N(0,Q)$
Measurement Model	$Z_k = H_k X_k + v_k, \quad v_k \sim N(0,R)$
State Estimate Extrapolation	$\hat{X}_k(-) = \phi_{k-1} \hat{X}_{k-1}(+)$
Error Covariance Extrapolation	$P_k(-) = \phi_{k-1} P_{k-1}(+) \phi_{k-1}^T + Q_{k-1}$
State Estimate Update	$\hat{X}_k(+) = \hat{X}_k(-) + K_k[Z_k - H_k \hat{X}_k(-)]$
Error Covariance Update	$P_k(-) = [I - K_k H_k] P_k(-)$
Kalman Gain Matrix	$K_k = P_k(-) H_k^T [H_k P_k(-) H_k^T + R_k]^{-1}$

Linear Kalman Filter Equations.

Table III.1

This filter is applicable only to linear systems but forms the basis of the extended Kalman filter.

2. Extended Kalman Filter

In order to be able to use the power of the Kalman filter on non linear state estimation problems, the Extended Kalman filter must be used. It is basically the same as the linear filter but with the state and measurement equations linearized about the current best estimate. The extended Kalman filter equations are presented in Table III.2. This filter forms the basis of our attack on the orbit observability problem.

System Model	$\dot{X}(t) = f(x(t),t) + w(t): \quad w(t) \sim N(0,Q(t))$
Measurement Model	$Z_k = h_k(X(t_k)) + v_k \qquad v_k \sim N(0,R_k)$
State Estimate Propagation	$\dot{\hat{X}}(t) = f(\hat{X}(t),t)$
Error Covariance Propagation	$\dot{P}(t) = F(\hat{X}(t),t)P(t) + P(t)F^T(\hat{X}(t),t) + Q(t)$
State Estimate Update	$\hat{X}_k(+) = \hat{X}_k(-) + K_k[Z_k - h_k(\hat{X}_k(-))]$
Error Covariance Update	$P_k(+) = [I - K_k H_k(\hat{X}_k(-))]P_k(-)$
Gain Matrix	$K_k = P_k(-)H_k^T(\hat{X}_k(-))[H_k(\hat{X}_k(-))P_k(-)H_k^T\hat{X}_k(-)) + R_k]^{-1}$
where	$F(\hat{X}(t),t) = \frac{\partial f(\hat{X}(t),t)}{\partial \hat{X}(t)}$,and $H_k(\hat{X}_k(-)) = \frac{\partial h_k(\hat{X}(t_k))}{\partial \hat{X}(t_k)}$

Extended Kalman Filter Equations.

Table III.2

3. Linearized Kalman Filter

If instead of linearizing about the best estimate as in the extended Kalman filter, the state is linearized about some known

trajectory the filter becomes what is known as the linearized Kalman filter. This filter works well in reducing error due to small perturbation in the state vector. The linearized Kalman filter equations are presented in Table III.3.

System Model	$\dot{X}(t) = f(X(t),) + w(t)$: $w(t) \sim N(0, Q(t))$
Measurement Model	$Z_k = h_k(X(t_k)) + v_k$: $v_k \sim N(0, R_k)$
State Estimate Propagation	$\dot{\hat{X}}(t) = f(\bar{X}(t),t) + F(\bar{X}(t),t)[\hat{X}(t) - \bar{X}(t)]$
State Estimate Update	$\hat{X}_k(+) = \hat{X}_k(-) + K_k[Z_k - h_k(\bar{X}(t_k)) - H_k(\bar{X}(t_k))[\hat{X}_k(-) - \bar{X}(t_k)]]$
Error Covariance Propogation	$\dot{P}(t) = F(\bar{X}(t),t)P(t) + P(t)F^T(\bar{X}(t),t) + Q(t)$
Error Covariance Update	$P_k(+) = [I - K_k H_k(\bar{X}(t_k))]P_k(-)$
Gain Matrix	$K_k = P_k(-)H_k^T(\bar{X}(t_k))[H_k(\bar{X}(t_k))P_k(-) H_k^T(\bar{X}(t_k)) + R_k]^{-1}$
where	$F(\bar{X}(t),t) = \frac{\partial f(\bar{X}(t),t)}{\partial \bar{X}(t)}$, and $H_k(\bar{X}(t_k)) = \frac{\partial h_k(\bar{X}(t_k))}{\partial \bar{X}(t_k)}$

Linearized Kalman Filter Equations.

Table III.3

4. Smoothing

Smoothing differs from filtering in that it it uses all the measurements from an entire pass to estimate the state at some time "t" during the pass. In the linear case it can be shown [2] that the optimal smoother is a linear combination of two Kalman filters, one filtering the data in the forward direction to time "t", and the other filtering backwards to "t". The equations for this smoother are

$$\hat{x}(t|T)=P(t|T)[P^{-1}(t)\hat{x}(t)+P_b^{-1}(t)\ \hat{x}_b(t)]$$

$$P^{-1}(t|T)=P^{-1}(t)+P_b^{-1}(t)$$

where the subscript b indicates the backwards estimate. If we are only interested in the initial state, ie. t=0, and we assume that our initial error covariance is very large with respect to the error covariance after the data has been processed, then the initial state is a function only of the backwards filter.

If we assume that the nonlinear smoother is also a linear combination of the forward and backward filters, then the same equations hold true in the non-linear case.

CHAPTER IV

SIMULATION PROCEDURES

1. Generating The Measurement Data

1.1 Algorithm Used To Generate Data

Actual tracking data was impossible to obtain due to the many different types of measurement and orbit required. Simulated measurement data was therefore used. This data was obtained by assuming an orbit and using the algorithm which follows to calculate the satellite position and velocity at appropriate measurement intervals. From this known position and velocity, measurements as they would have appeared to an earth tracking station were calculated. The equations for this algorithm are listed in Table IV.1 and Table II.2.

Step 1: The desired orbital parameters are read into the computer. They are:

Orbital Inclination i

Longitude of the Ascending Node ...L

Argument of the Perigee.....p

Eccentricity.....e

Semi-major axis.....a

Time of Perifocal passage.....T_p

Step 2: Calculate the direction cosines for converting from the orbital plane coordinate system to the ascension declination

Direction Cosines	$P_x = \cos(p)\cos(L) - \sin(p)\sin(L)\cos(i)$ $P_y = \cos(p)\sin(L) + \sin(p)\cos(L)\cos(i)$ $P_z = \sin(p)\sin(i)$ $Q_x = -\sin(p)\cos(L) - \cos(p)\sin(L)\cos(i)$ $Q_y = -\sin(p)\sin(L) + \cos(p)\cos(L)\cos(i)$ $Q_z = \cos(p)\sin(i)$
Mean Motion	$n = ku^{1/2}/a^{3/2}$
Mean Anomaly	$M = n(t-T_p)$
Eccentric Anomaly	$E = M + 2\sum_{m=1}^{\infty} \frac{1}{m} J_m(me)\sin(mM)$
State in Orbital plane coordinates	$\dot{E} = \frac{1}{r}\sqrt{\frac{u}{a}}$ $X_\omega = a(\cos(E) - e)$ $Y_\omega = a(1 - e^2)^{1/2}\sin(E)$ $\dot{X}_\omega = -aE\sin(E)$ $\dot{Y}_\omega = aE(1 - e^2)^{1/2}\cos(E)$
State in Right Asc. Dec. Cords.	$\rho = X \cdot P + Y \cdot Q$ $\begin{bmatrix} \dot{X} \\ \dot{Y} \\ \dot{Z} \end{bmatrix} \begin{bmatrix} P_x & Q_x \\ P_y & Q_y \\ P_z & Q_z \end{bmatrix} \begin{bmatrix} X_\omega \\ Y_\omega \end{bmatrix}$

Satellite State Calculation

Table IV.1

system.

Step 3: Compute time since perifocal passage.

Step 4: Compute mean anomaly.

Step 5: Compute Eccentric anomaly.

Step 6: Calculate coordinates of the satellite in the orbital plane coordinate system.

Step 7: Calculate coordinates in right ascension declination system.

Step 8: Calculate velocities in orbital plane coordinate system.

Step 9: Calculate velocities in the right ascension declination system.

Step 10: Calculate range, range-rate, azimuth, and elevation from ground station to satellite.

Step 11: If elevation angle is greater than one degree (ie. if the satellite is not hidden behind earth) store the measurements calculated and the satellite state.

Step 12: Increment current time.

Step 13: Go to step 3.

The earth station coordinates used are those of the Hector MacLeod building at the University of British Columbia and are listed in Table IV.2. Typical measurement curves can be seen in Figure IV.1 .

1.2 Types of Orbit

In order to account for possible orbit type dependancy by the smoothing algorithms, a set of standard orbits was developed which cover the many different types of orbit currently in use. Table IV.3 lists

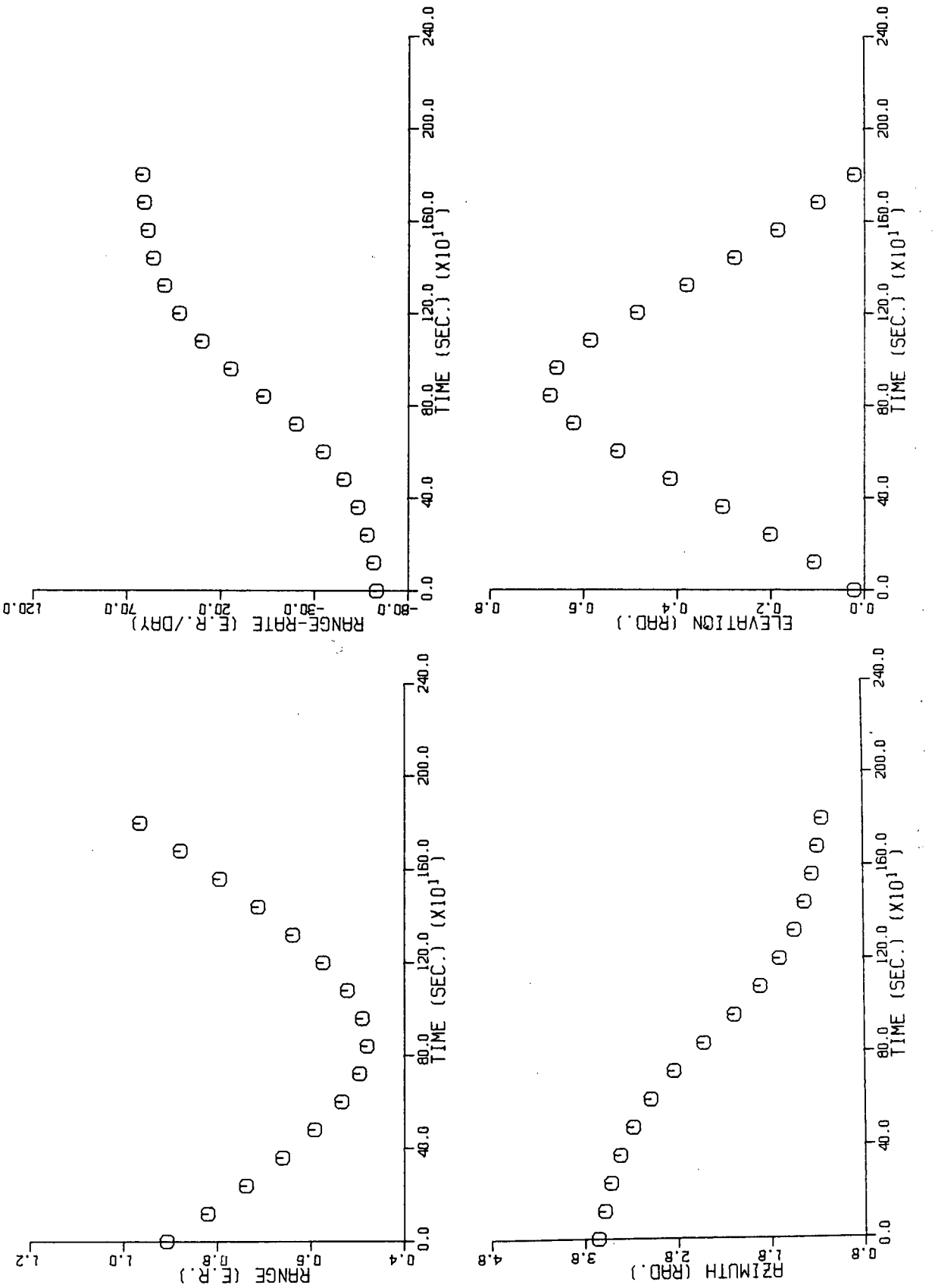

Typical Measurements (Orbit.1) Figure iv.1

East Longitude	236.75^{o}
Latitude	49^{o} 15' 45"
Altitude	310 feet

Coordinates of Hector McLeod Bldg.

Table IV.2

the orbits used and assigns to each a reference number. This reference number will appear on many figures to follow. For instance "ORBIT.3" will indicate that orbital data for the orbit with reference number 3 was used.

Among the orbits in Table IV.3 are circular orbits, eccentric orbits, polar orbits, close orbits, and distant orbits. These represent a good cross-section of the infinite number of orbital possibilities.

Orbits Used in Study

Table IV.3

No.	Inclination	Ascending node	Argument of perigee	Semi-major axis	Eccentricity	Time of Peri-focal passage
1	45°	45°	45°	1.5	0.1	2345345.329167
2	90°	0°	0°	1.05	0.	2444055.5
3	90°	0°	0°	1.5	0.	2444055.5
4	90°	0°	0°	1.5	0.2	2444055.5
5*	0°	90°	0°	6.6227	0.	2444055.5
6	45°	0°	0°	1.5	0.	2444055.5

* geosynchronous orbit.

2. Simulation Algorithm

In this study we wish to arrive at a good state estimate at some epoch time. This estimate could then be used for future orbit prediction. For our purposes, the epoch time was chosen to be the time of the first measurement (t=0). Due to the non-linear nature of the problem, an optimal estimate cannot be computed directly. A repetitive algorithm can, however, be used. It will be shown in the simulation results that the estimate at t=0 can be made to approach the correct estimate by repetitive filtering.

The principal result obtained from the simulation runs described in the next chapter are the computer produced plots of the error in the state estimate calculated by the smoother. These show the magnitudes of the error in the position estimates and the velocity estimates plotted against time. These errors could be calculated because when the simulated measurement data was generated and saved, the satellite state vector was also saved. These states were then read by the simulation program together with the measurement data and compared with the smoother's estimates.

Due to the state initialization procedure described in the next section, the time of closest satellite approach to the earth station is used for the initial guess. The smoother, therefore, normally starts somewhere in the middle of the measurement data. From this point the filter sweeps foreward in time using the extended Kalman filter algorithm. When the final measurement is reached, the final state estimate becomes the initial state estimate, the direction of sweep is reversed, and the error covariance is re-initialized. The filter then sweeps backwards in time to the first measurement using the same data.

This procedure repeats itself for two more sweeps of the data.

The arrows present on most of the following graphs indicate the direction of sweep when the curve nearest to the arrow was calculated. During all these sweeps the estimated state and the true state are compared and their difference computed. Two error magnitudes are computed, the position error which is the square root of the sum of the squares of the three position state errors; and the speed error which is the square root of the sum of the squares of the three velocity state errors. These error quantities are then plotted on two separate graphs, and a performance measure of the smoothing algorithm results. It should be noted that the abscissa is always the time since the first measurement of the pass.

The algorithm used in the simulation runs is described in somewhat more detail in Table IV.4. The step numbers correspond to the circled numbers on the typical result shown in Figure IV.2 .

1	Initialize Kalman Filter at Minimum Range Time (T_m) using computed initial guess (X_{init}) and Initial Error Covariance (P_{init}). $X_o = X_{init}$ $P_o = P_{init}$
2	Use Extended Kalman Filter on data between T_m and Final Measurement Time (T_f).
3	Re-initialize Kalman Filter at T_f using final state estimate ($X(T_f)$) and Initial Error Covariance. $X_o = X(T_f)$ $P_o = P_{init}$
4	Use Extended Kalman Filter backwards in time on data between T_f and First Measurement Time (T_s).
5	Re-initialize Kalman Filter at T_s using final state estimate of backward sweep ($X(T_s)$) and Initial Error Covariance. $X_o = X(T_s)$ $P_o = P_{init}$
6	Use Extended Kalman Filter forward in time on data between T_s and T_f.
7	Re-initialize Kalman Filter at T_f using latest state estimate at T_f and Initial Error Covariance. $X_o = X(T_f)$ $P_o = P_{init}$

Simulation Algorithm (Continued next page)

8	Use Extended Kalman Filter backwards in time on data between T_f and T_s.
9	Final Estimate Error at T_s. State Estimate at T_s can be used for future orbit prediction.

Simulation Algorithm (Continued from previous page)

Table IV.2

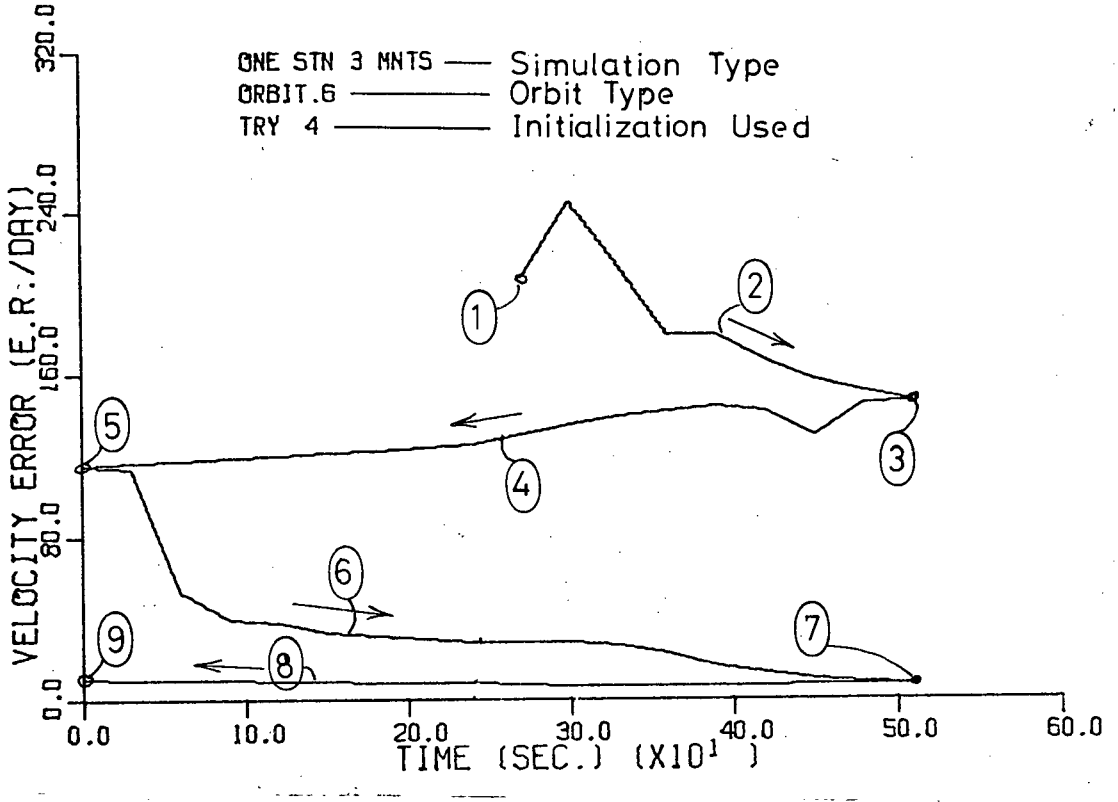

Typical Simulation Run Result

Figure IV.2

3. Initialization

The initialization of the smoothing algorithms turned out to be an important consideration. Near the beginning of the study the initial state estimate was made quite arbitrarily, however it soon became apparent that the this guess was in some cases critical due to the fact that the extended Kalman filter initially uses approximations of the state and measurement functions linearized about this first guess. The validity of these approximations therefore depended on the accuracy of this guess. The following algorithm was developed to calculate four different initial guesses one of which was close enough to the correct initial state to allow the smoother to converge.

Step 1: Range data was scanned and the minimum range found.

Step 2: This minimum range was used as an altitude to position the satellite directly above the measuring earth station. The time at which the minimum range measurement was made was used as the initial time.

Step 3: Velocities were computed which would put the satellite into a circular orbit in one of four directions. In figures to follow this initial direction will be indicated by the "TRY" number.

TRY 1 is due North

TRY 2 is due South

TRY 3 is due East

TRY 4 is due West

This algorithm was used to initialize all the smoothing algorithms except the linearized smoother.

The initial value of the error covariance was arrived at by trial

and error, but once a reasonable value had been found it was used throughout all the simulation runs. It was also found necessary to reinitialize the error covariance after each sweep within a run because the error covariance became so small after one or two sweeps that convergence became very slow. The initial error covariance was set to 0.1 for the variance of the position states and to 100.0 for the velocity state variances. All other covariances were set to zero.

CHAPTER V

SIMULATION RESULTS

The plots to follow represent the results of this simulation study. The reader is referred to the previous chapter for an explanation of format and titles.

1. Range and Range-rate From One Station

An Extended Kalman filter based smoother was written which was to calculate a preliminary orbit estimate using only range and range rate data from one station. As previously stated, if feasible, such a program would greatly reduce the cost of tracking equipment. Even a simple dipole antenna could be used if signal strengths were sufficient. This would do away with the need for large steerable dish antennas or large phased arrays, at least at lower frequencies. Also no optical equipment would be needed. The required equipment would consist of an accurate timer for measuring round trip travel time of a signal to and from the satellite, and an accurate frequency counter for measuring doppler shift.

As can be seen from Figure V.1 and Figure V.2 the smoother did not converge for any set of initial conditions. Typically the position error would increase linearily with time from the point of nearest approach. Such behavior can be understood by assuming the filter to have little or no effect on the error in the initial guess. In such a case the distance between the assumed position of the satellite and the true position would be least when they were nearest to the station and would increase approximately linearly as they diverged. Such behavior

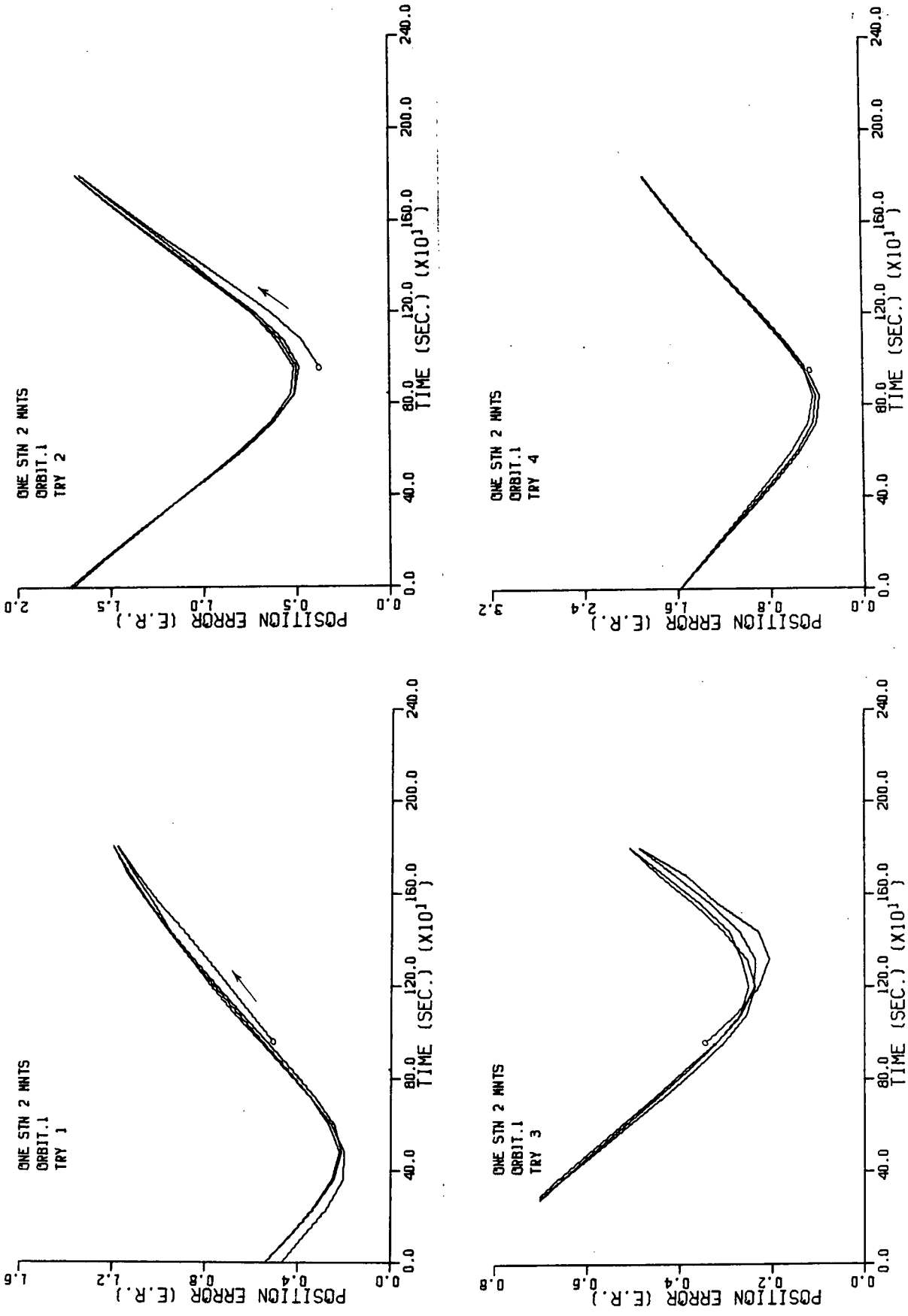

Position Error with Range and Range - Rate Figure V.1

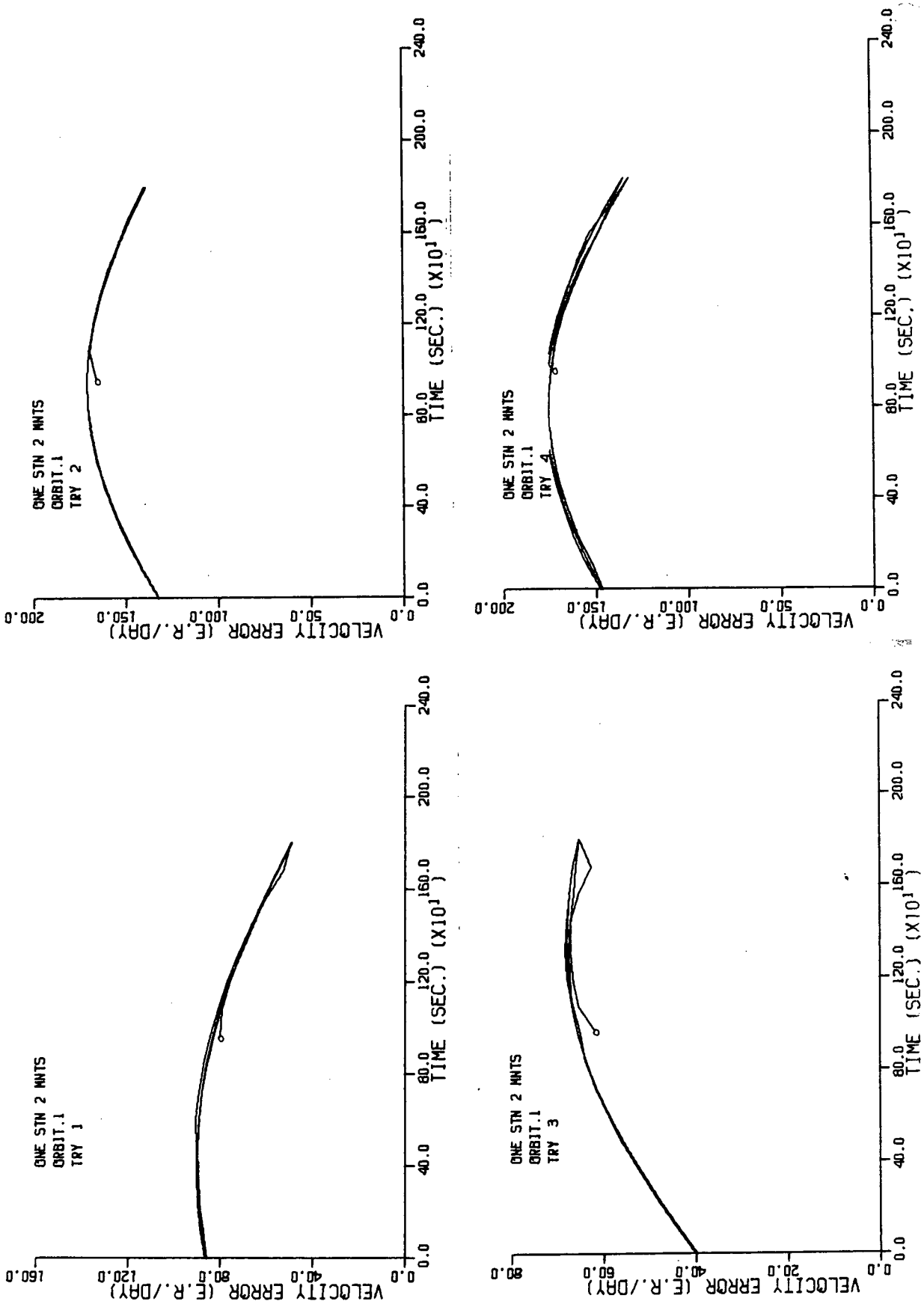

Velocity Error with Range and Range-Rate Figure V.2

by the filter can be assumed to indicate that the system is unobservable.

Other types of orbit were tried with the same result.

2. Range, Range-Rate and Azimuth from One Station

The dimension of the measurement vector must be increased from two if the system is to be made observable. There are two ways of increasing the measurement vector dimension. The first is to add an additional measurement of a different type from the same station. The second is to use the same type of measurements but add a second station. This section deals with the first of these possibilities, the other is dealt with in section 4.

The smoothing algorithm was modified to accept a third measurement. Azimuth angle was chosen but elevation angle was tried and would have worked equally well. Simulation runs were made using all the orbits of Table IV.3. Figure V.3 and Figure V.4 show the results of the Orbit 1 simulation. Every initialization converged in this case, a rare occurrence during this study due, as will be discussed later, to the algorithm's sensitivity to initialization. Figure V.5 and Figure V.6 show the results for Orbit 2. Only initialization Try 2 converged in this case. Figure V.7 and Figure V.8 show the results for Orbit 3, where Try 4 was the only initialization to converge. With Orbit 4 two initializations worked, Try 2 and Try 4 as shown in Figure V.9 and Figure V.10 . Orbit 5, the geosynchronous orbit proved to be unobservable. (See Figure V.11 and Figure V.12) It will be shown, in the next two sections, that the addition of an elevation angle measurement or a second station was required to obtain convergence with

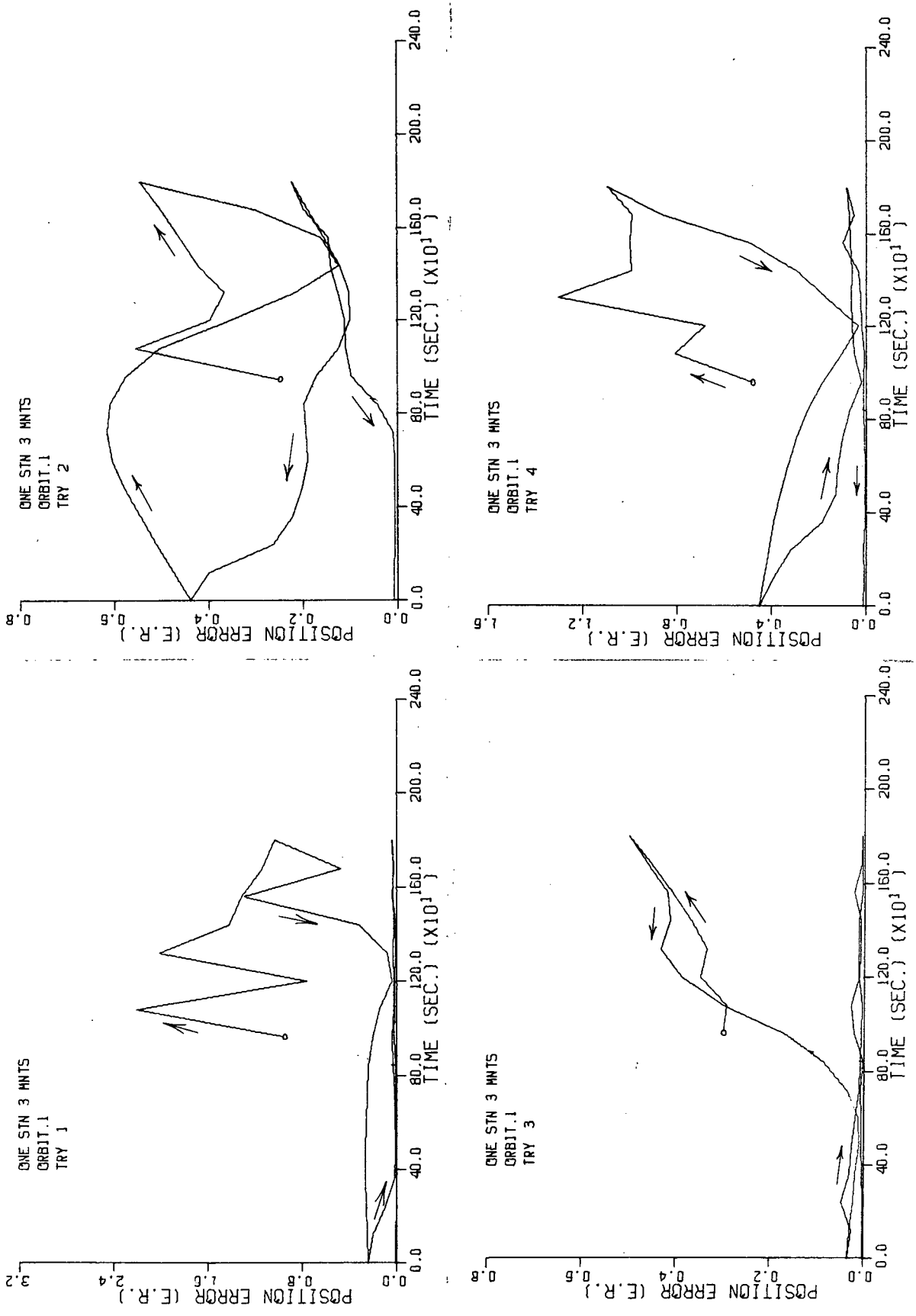

Orbit 1 Position Error with 3 Measurements Figure V.3

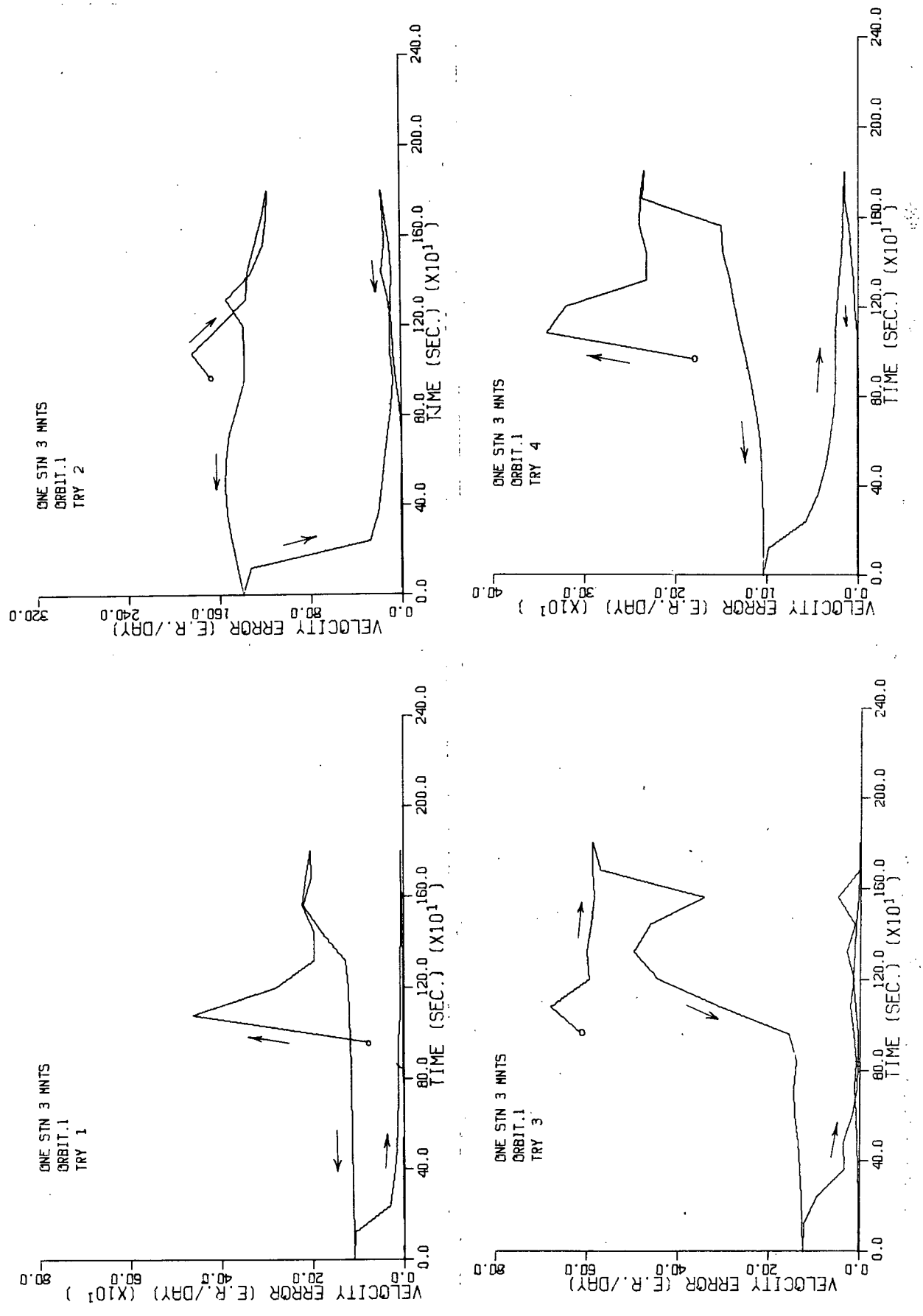

Orbit 1 Velocity Error with 3 Measurements Figure V.4

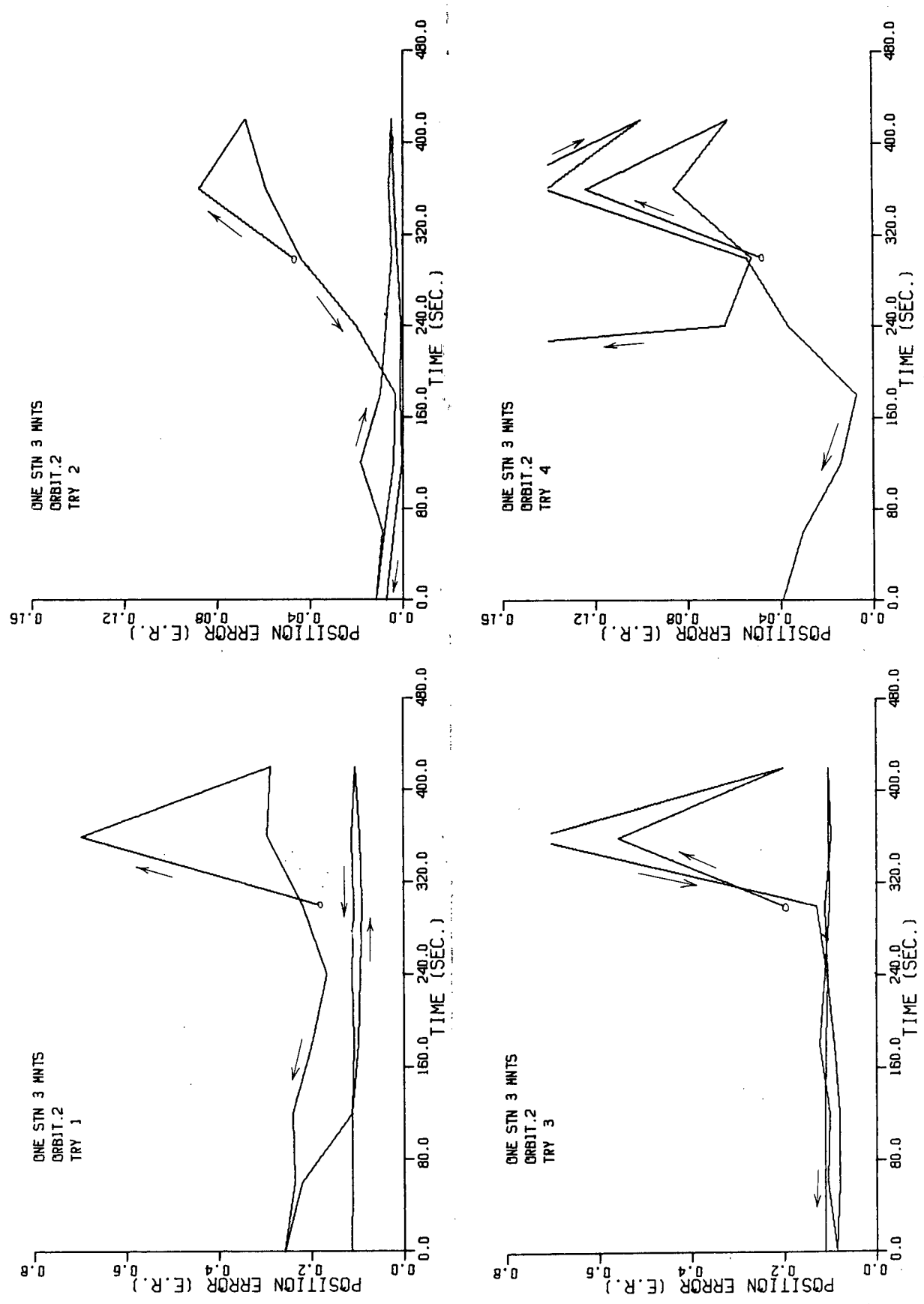

Orbit 2 Position Error with 3 Measurements Figure V.5

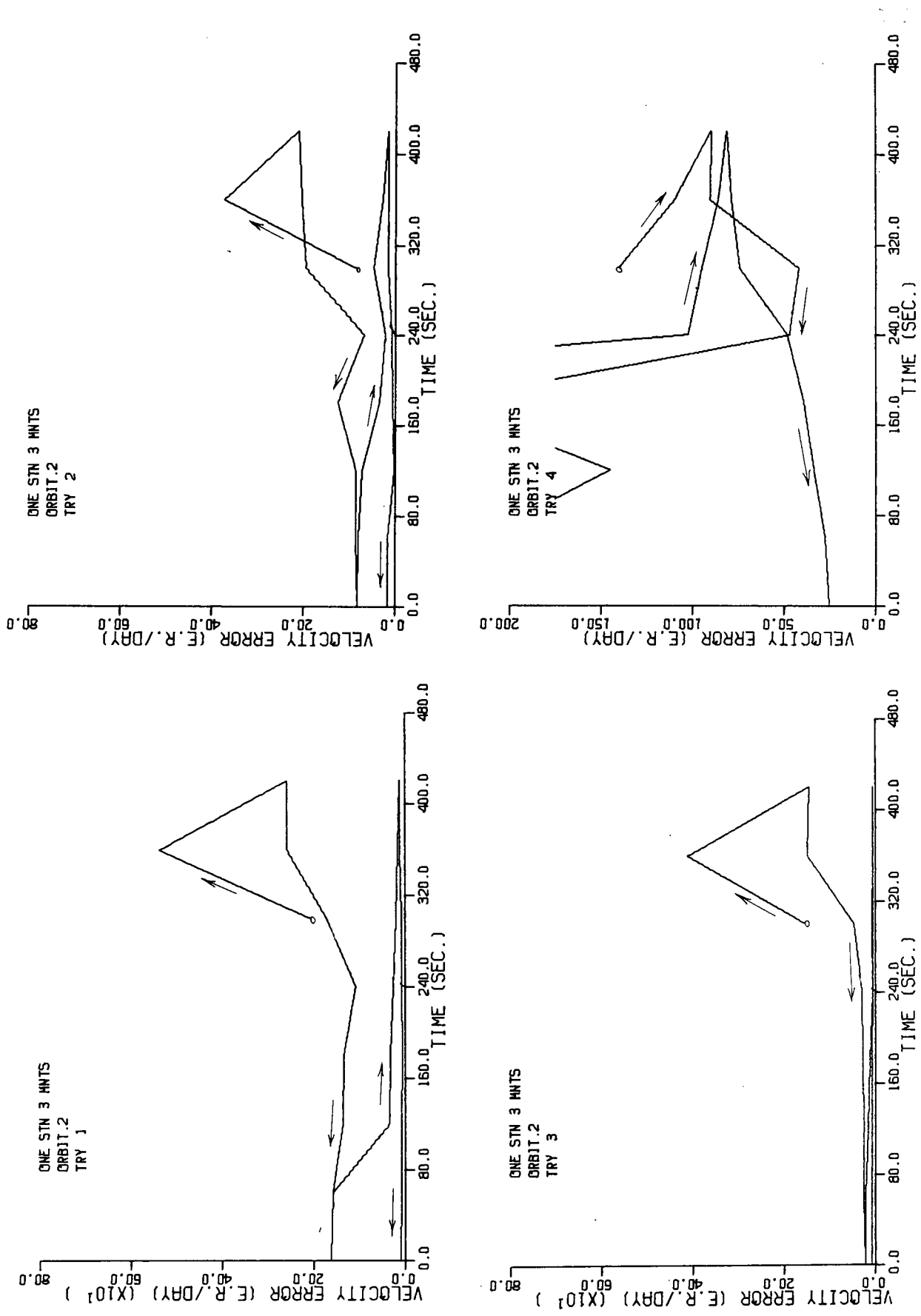

Orbit 2 Velocity Error with 3 Measurements Figure V.6

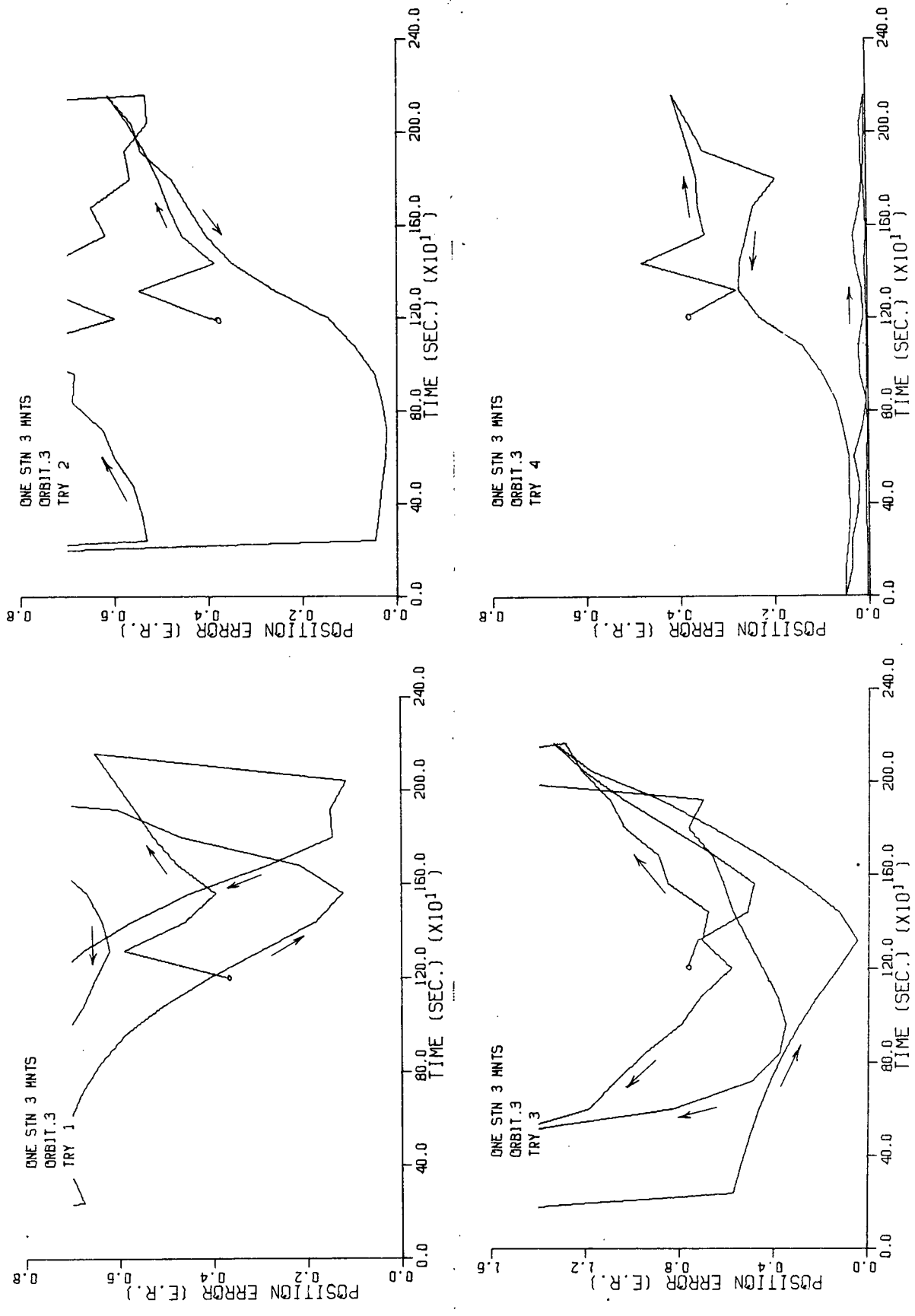

Orbit 3 Position Errorm with 3 Measurements Figure V.7

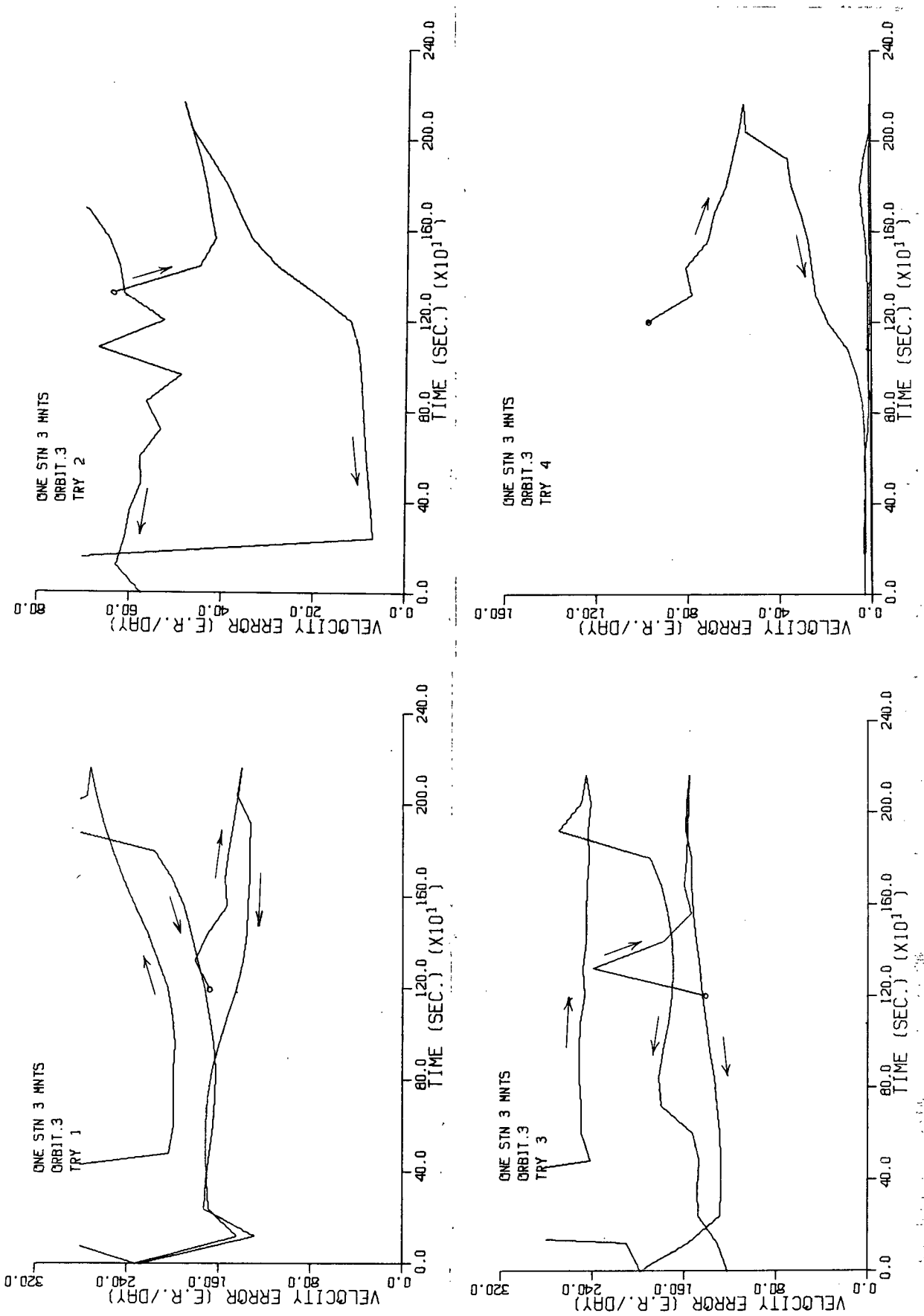

Orbit 3 Velocity Error with 3 Measurements Figure V.8

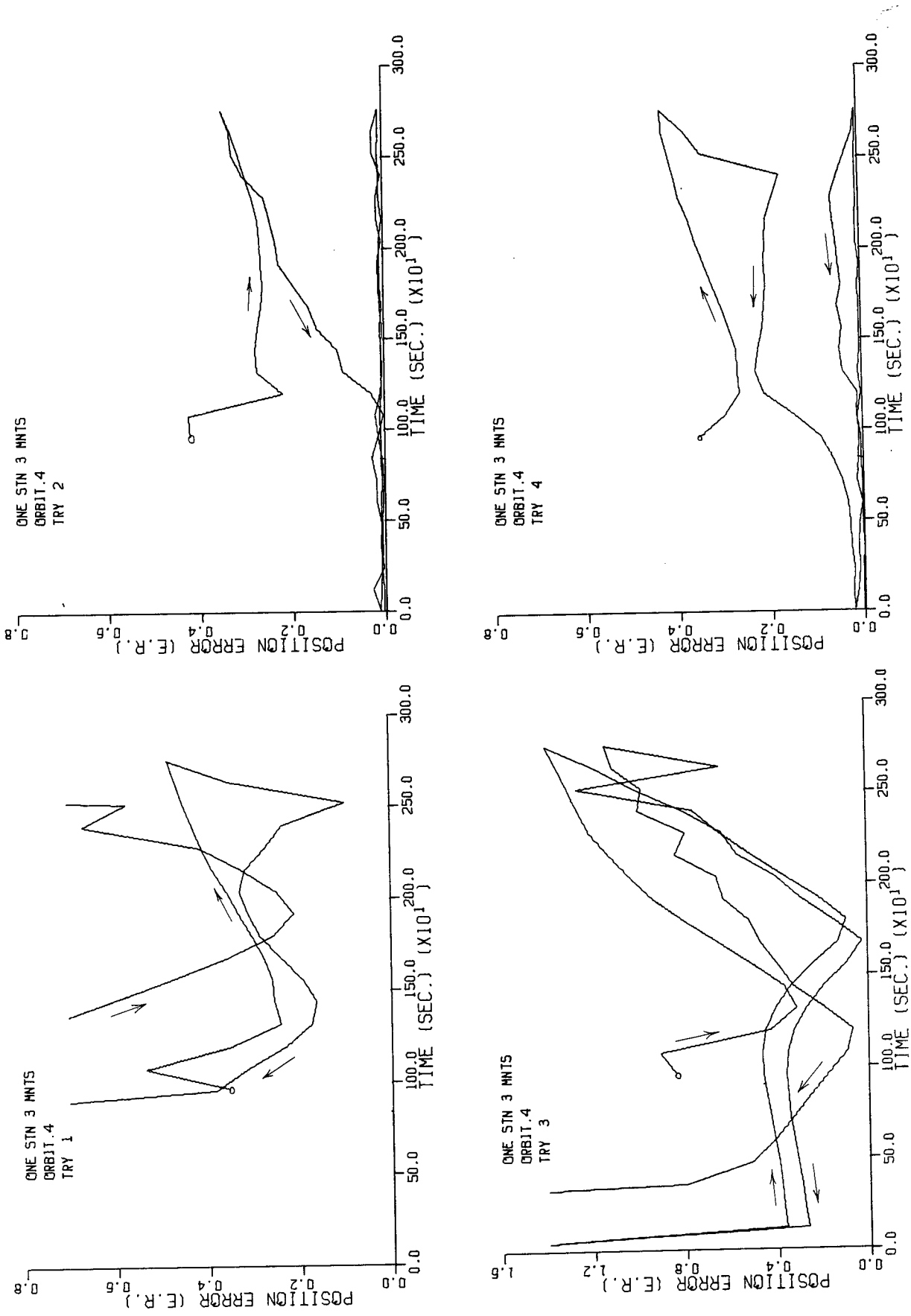

Orbit.4 Position Error with 3 Measurements Figure V.9

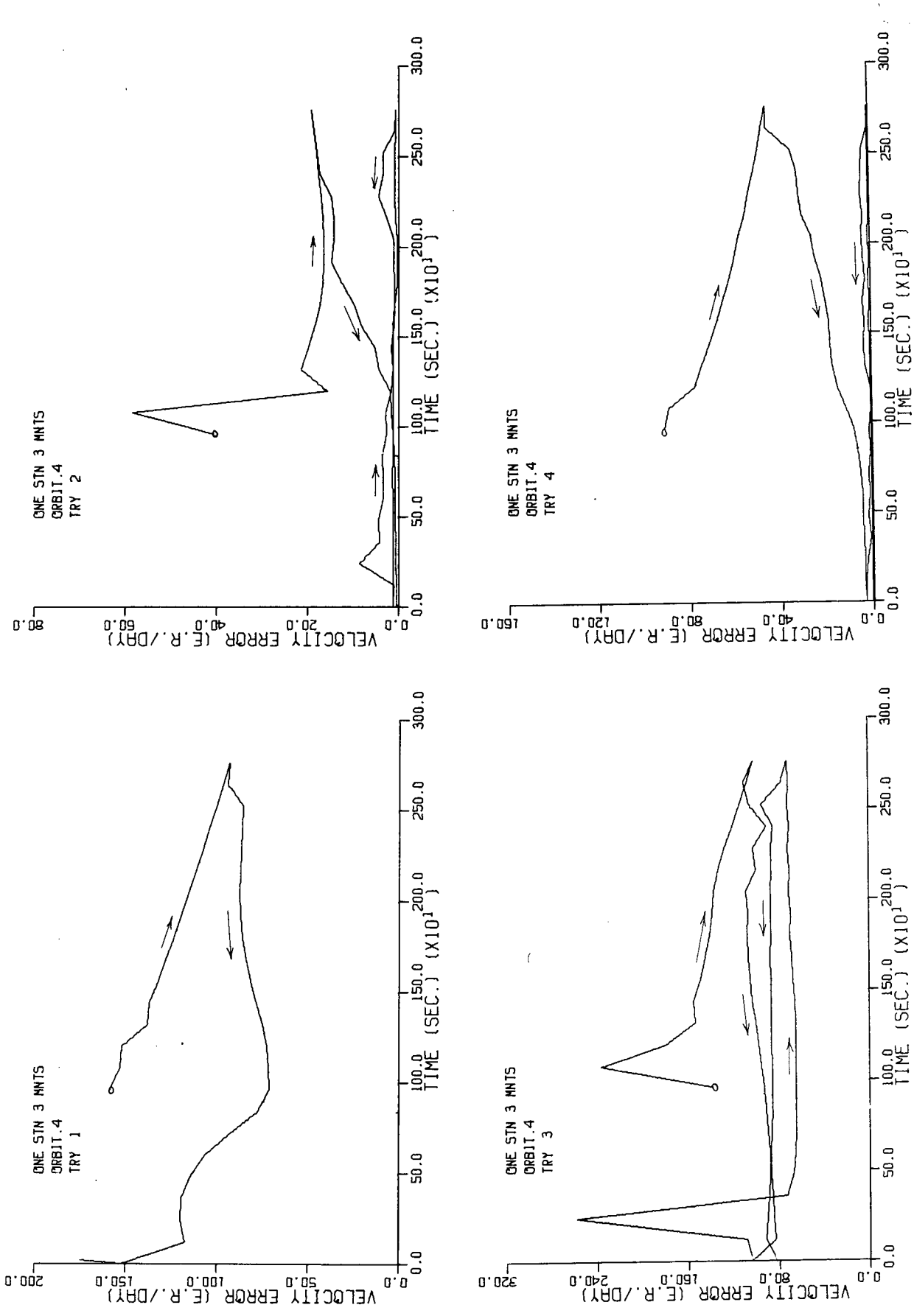

Orbit 4 Velocity Error with 3 Measurements Figure V.10

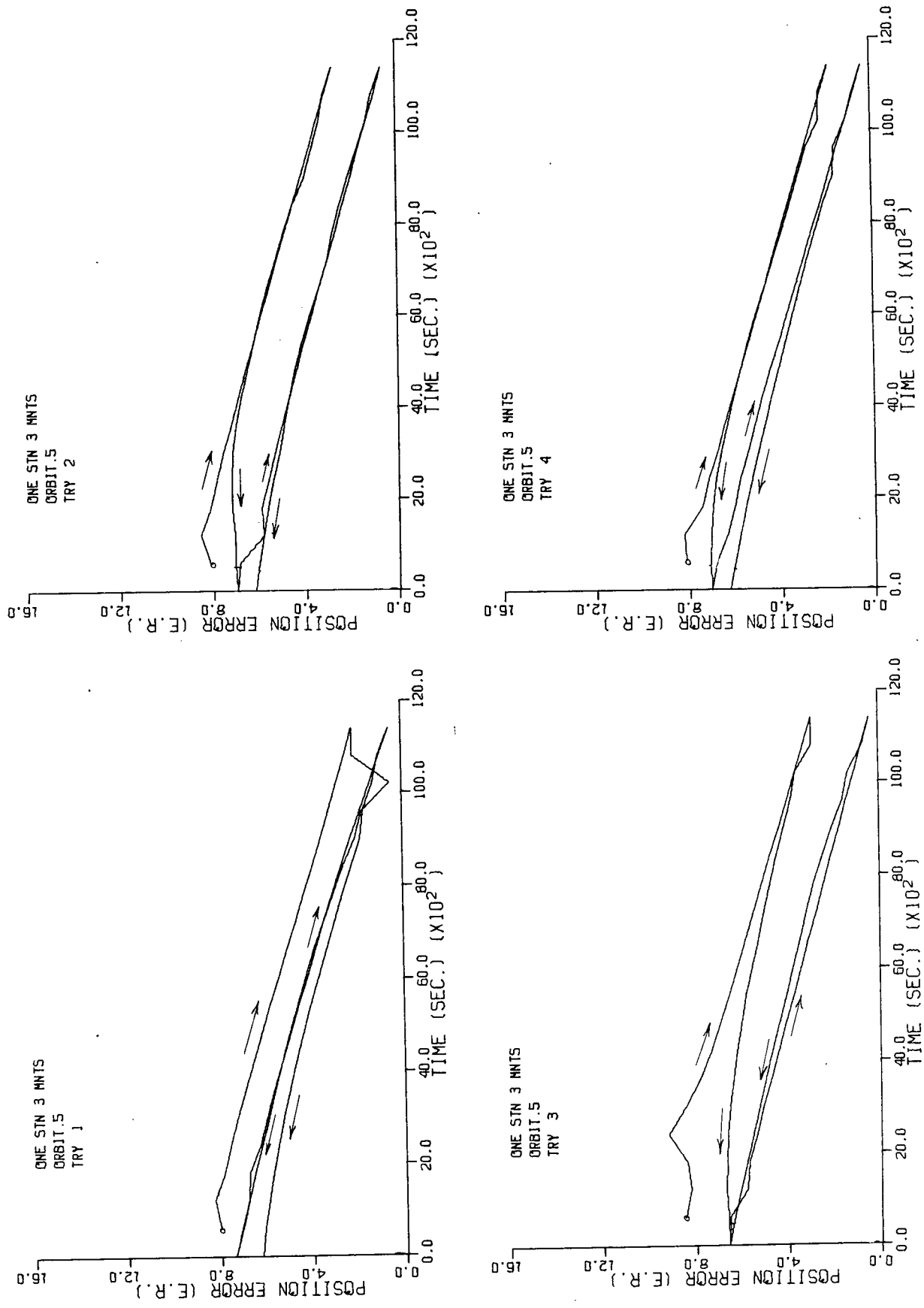

Orbit 5 Position Error with 3 Measurements Figure V.11

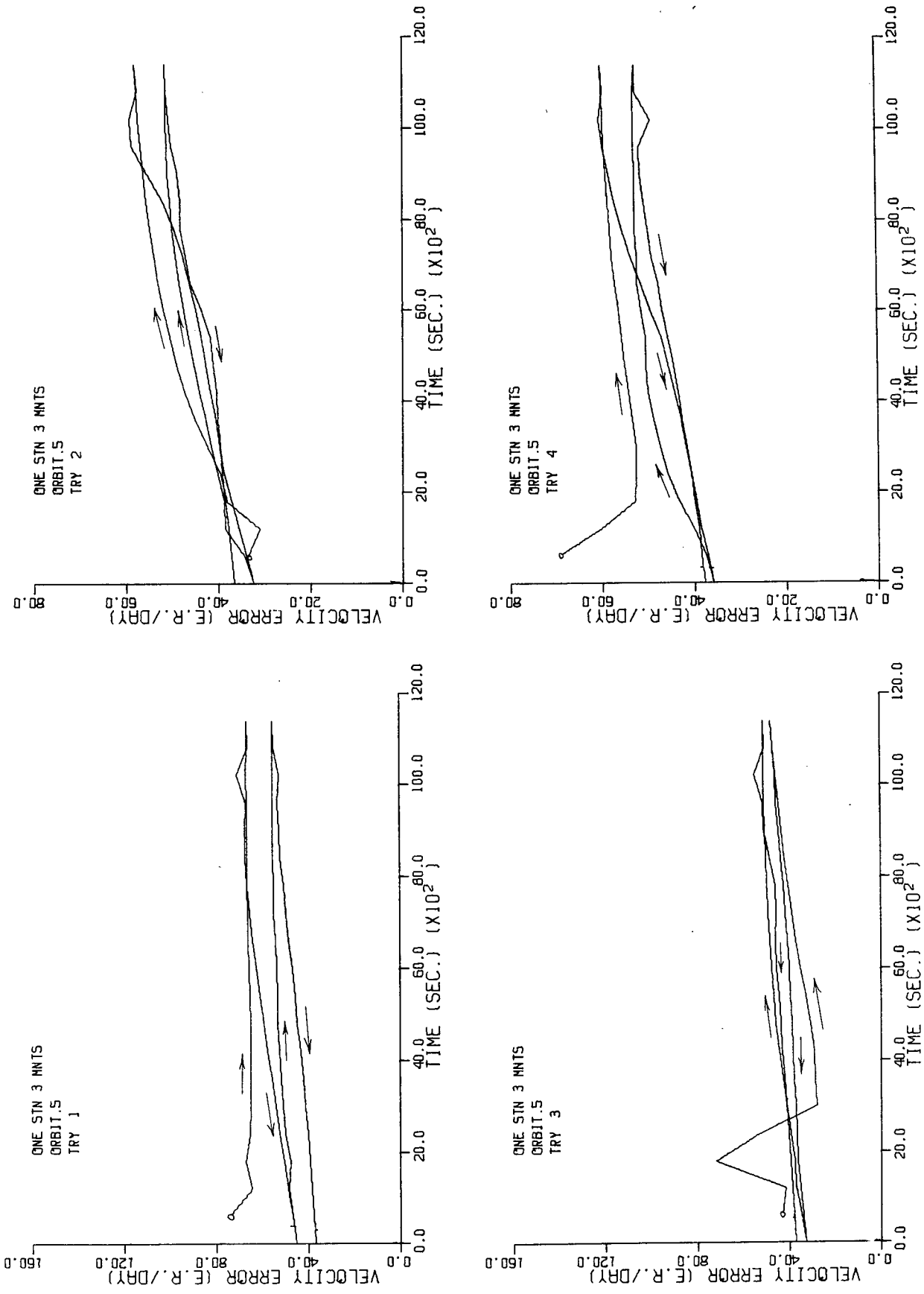

Orbit 5 Velocity Error with 3 Measurements Figure V.12

this orbit. Finally, the results with Orbit 6 are shown in Figure V.13 and Figure V.14 .

As can be seen from all these figures, the smoother required a number of sweeps to converge and the rate of convergence varied with the orbit and the initialization used. The number of sweeps was fixed at 4 in the belief if convergence had not occurred by then, the observability was not satisfactory. For non-linear systems observability seems to be a matter of degree reather than a yes or no choice as with linear systems. The rate of convergence of these figures gives a crude measure of the degree of observability.

In practice if one were using a smoothing algorithm of this sort to track a satellite, one would need some method of selecting the initialization to use. In the presence of no prior information at all, the choice can only be made after all have been tried. The differences between the estimated measurements and the actual ones (the residuals), provide a basis for an intelligent choice. Table V.1 , Table V.2 , Table V.3 , and Table V.4 list the residuals for the four initialization tries of Orbit 2. The residuals of Try 2 are somewhat smaller than those of the other initializations, indicating that Try 2's state estimate should be used.

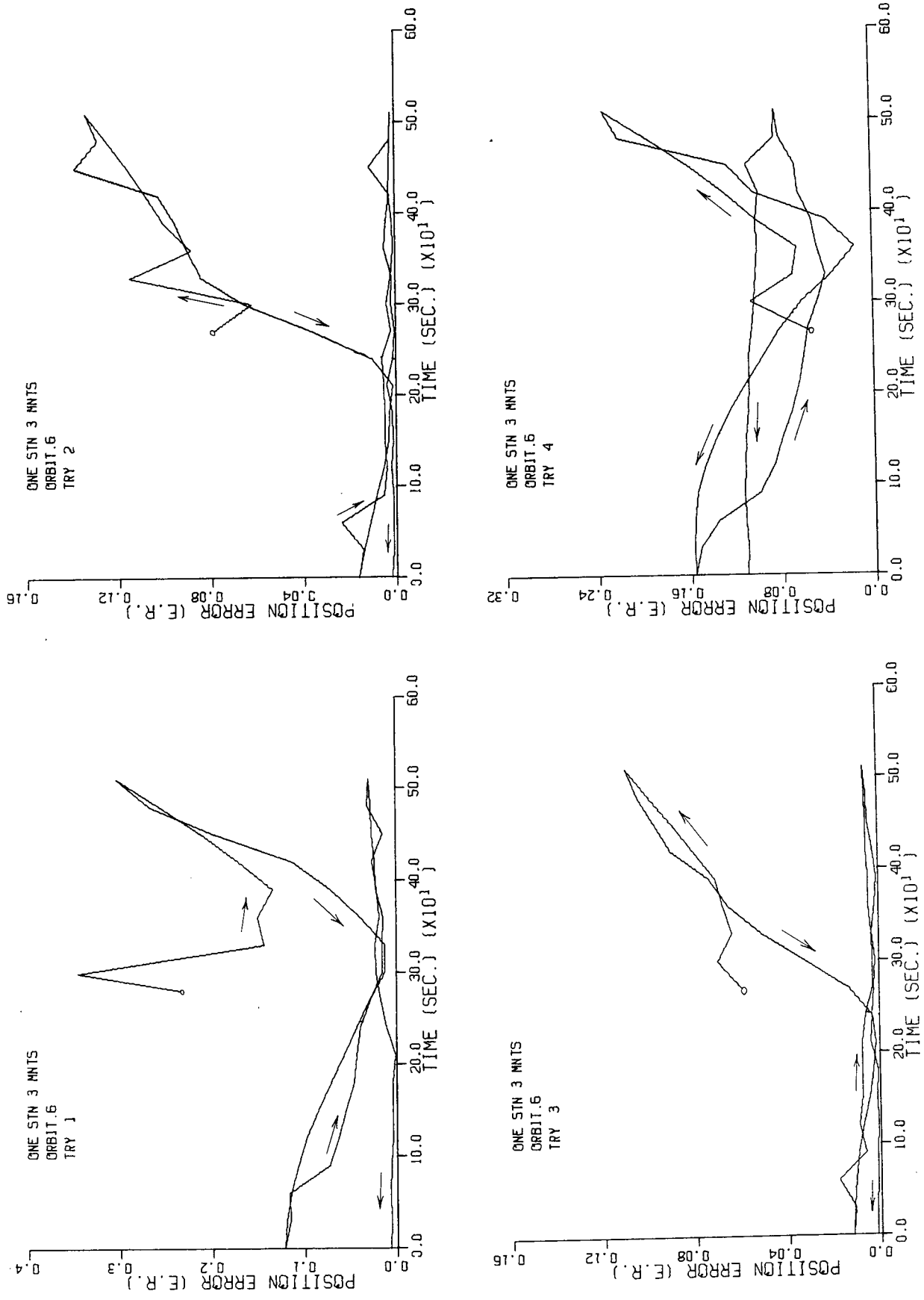

Orbit 6 Position Error with 3 Measurements Figure V.13

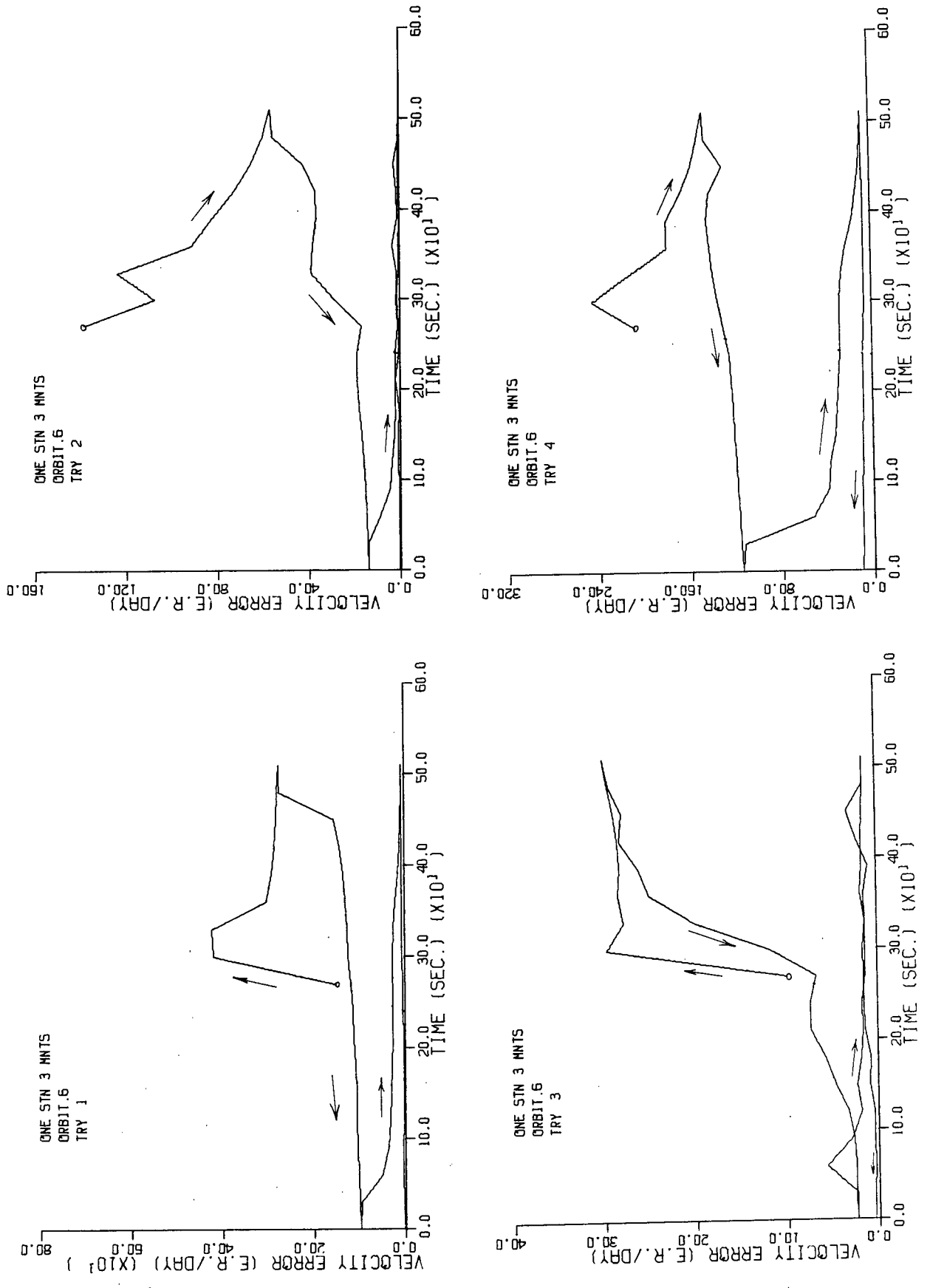

Orbit 6 Velocity Error with 3 Measurements Figure V.14

Range	Range-Rate	Azimuth
-.8381E+00	-.3392E+03	-.4433E+00
-.1307E+00	-.9203E+02	-.2465E+00
-.2586E+00	0.1826E+03	0.1101E+01
-.2416E+00	0.1772E+03	-.2970E+00
-.4715E-01	0.2386E+02	0.3150E+01
-.3801E-01	0.3641E+02	0.1301E+01
-.2996E-01	0.4186E+02	0.3966E+00
-.2395E-01	0.1821E+02	0.8938E-01
-.2865E-01	-.6040E+02	0.3589E+00
-.4230E-01	-.5620E+02	0.9020E-01
0.1549E-02	0.4509E+01	-.1848E-01
0.1087E-02	0.4037E+01	-.1108E+00
0.3077E-03	0.5349E+01	-.1324E+00
0.4264E-03	0.4489E+01	-.7383E-01
0.1085E-03	0.2085E+01	-.2640E-01
0.1417E-04	-.1507E+01	0.1789E-01
-.5115E-04	-.2568E+00	0.4123E-01
-.1020E-02	0.1424E+01	0.2616E-02
-.4421E-03	0.7822E+00	-.8096E-01
-.8899E-03	0.6302E+00	-.7399E-02
-.3457E-03	0.6076E+00	0.1353E-01
0.5664E-04	0.2649E+00	-.1442E-01

ORBIT 2 Residuals TRY 1

Table V.1

Range	Range-Rate	Azimuth
-.1140E-01	-.3845E+01	-.3849E-01
-.2196E-02	-.1052E+01	0.3125E-01
-.1321E-02	0.4325E+01	-.2515E-01
-.1291E-02	0.2932E+01	-.2887E+00
-.2651E-02	0.2207E+00	-.1529E+00
-.3584E-02	0.3131E+01	0.3009E-01
-.7135E-03	0.1499E+01	-.9842E-02
-.5560E-03	0.1103E+01	0.7740E-02
-.1650E-03	-.1209E+01	0.1940E-01
-.6281E-03	-.9997E+00	-.1839E-01
-.1056E-02	-.3440E+00	-.9710E-02
-.1800E-03	0.1137E+01	-.7980E-01
-.1100E-02	-.2760E-01	0.6004E-01
-.1069E-02	-.1314E+01	0.3871E-02
-.1540E-03	-.5402E+00	-.1847E-01
-.9338E-04	0.1679E+00	-.2359E-02
-.3574E-03	0.1502E+00	-.3136E-02
0.2282E-03	-.1033E+00	0.9054E-02
-.1222E-04	-.2392E+00	0.1408E-02
0.1975E-03	-.8041E-01	-.7714E-02
-.1593E-03	0.2514E-01	-.2481E-01
0.1338E-04	0.2932E+00	-.1415E-01

ORBIT 2 Residuals TRY 2

Table V.2

Range	Range-Rate	Azimuth
-.6224E+00	-.2423E+03	-.2953E-01
-.1044E+00	-.1114E+03	0.6841E-01
-.6729E+00	0.1362E+03	0.3769E-01
-.6471E-01	0.1434E+02	0.1522E+00
-.6395E-02	-.3907E+01	0.8628E-01
0.1994E-02	-.5798E+01	0.1038E+00
0.1118E-02	-.4745E+01	0.4725E-01
0.6013E-03	-.2817E+01	0.4790E-01
-.3729E-03	0.1578E+01	-.2231E-01
-.2616E-03	-.8364E+00	-.9740E-01
-.4843E-02	-.8827E+01	-.1529E-01
-.3760E-03	0.1217E+01	0.1386E+00
-.1141E-02	-.7937E+00	0.8082E-01
-.1053E-02	-.3459E+00	-.2295E-01
0.8400E-04	-.1448E+00	0.4786E-02
-.7330E-04	0.7654E-01	0.1570E-01
-.1714E-03	-.2121E+00	-.1897E-01
-.2312E-02	0.3295E+01	-.2960E-01
-.9902E-03	0.9765E+00	-.2760E-02
-.3928E-03	0.1101E+01	-.2289E-01
-.3831E-03	0.8845E+00	-.5726E-02
-.8311E-04	0.4567E+00	0.7893E-02

ORBIT 2 Residuals TRY 3

Table V.3

Range	Range-Rate	Azimuth
-.8889E-01	-.5327E+02	-.1297E+00
-.2735E-01	-.2061E+02	0.7395E-01
-.3638E-01	0.4473E+02	0.6343E+00
-.2051E-01	0.8351E+01	0.2925E+00
-.5617E-03	-.2068E+00	0.5272E+01
-.3280E+00	0.1188E+03	0.4274E+01
-.3662E+00	-.6786E+02	0.3332E+01
-.4257E-01	0.7297E+01	0.3313E+01
-.2076E+00	-.1252E+03	0.2214E+01
-.1486E+01	-.8053E+02	0.7935E+00
-.1354E+01	-.5313E+03	-.4740E+00
-.4716E+00	-.4272E+03	0.3740E+01
-.8421E-01	-.1687E+02	0.1944E+01
-.1945E+00	0.4245E+02	0.6598E+00
-.6867E-01	-.1672E+02	0.4191E+00
-.3197E-01	0.2982E+02	0.4007E-01
-.3238E-01	0.2354E+02	-.7951E-01
-.1511E-01	0.1269E+02	0.3247E+00
-.7205E-02	-.6797E+01	0.2604E+00
-.2075E-03	-.7731E+01	-.2234E-01
-.3088E-03	-.3620E+01	-.1230E-01
0.6582E-03	-.1663E+01	-.2828E-01

ORBIT 2 Residuals TRY 4

Table V.4

3. Range, Range-Rate, Azimuth, and Elevation

The smoothing algorithm was modified to expand the measurement vector once again. This time elevation angle was added. This was done to see if any significant improvement occurred and also to observe if Orbit 5 converged with four measurements. Figure V.15 and Figure V.16 show the results obtained with Orbit 1. These can be compared with Figure V.3 and Figure V.4 which showed the results with three measurements. Some improvement in convergence speed can be seen but not enough to justify the extra expense. Figure V.17 and Figure V.18 show that with 4 types of measurement Orbit 5 can be made observable.

4. Range and Range-Rate from Two Stations

The satellite-observer system has been shown to be unobservable using range and range-rate from one station. The addition of a second station some distance from the first, also supplying range and range-rate information, might make this system observable. To check this situation, the smoother used in previous sections was modified, and simulation runs made using two stations. The primary station remained the Hector McLeod Building, while the second was located from 0.1 to 20 degrees due East or North. Results indicated that orbit determination could be accomplished if the stations were far enough apart.

4.1 Orbit 2 Results

Initially the second station was placed 1/2 degree latitude away from the primary station, and Orbit 2, the close polar orbit, was used as the orbit under observation. Figure V.19 and Figure V.20 show encouraging but unsatisfactory behavior for Try 1 initialization. Doubling the separation to 1 degree, Figure V.21 and Figure V.22 ,

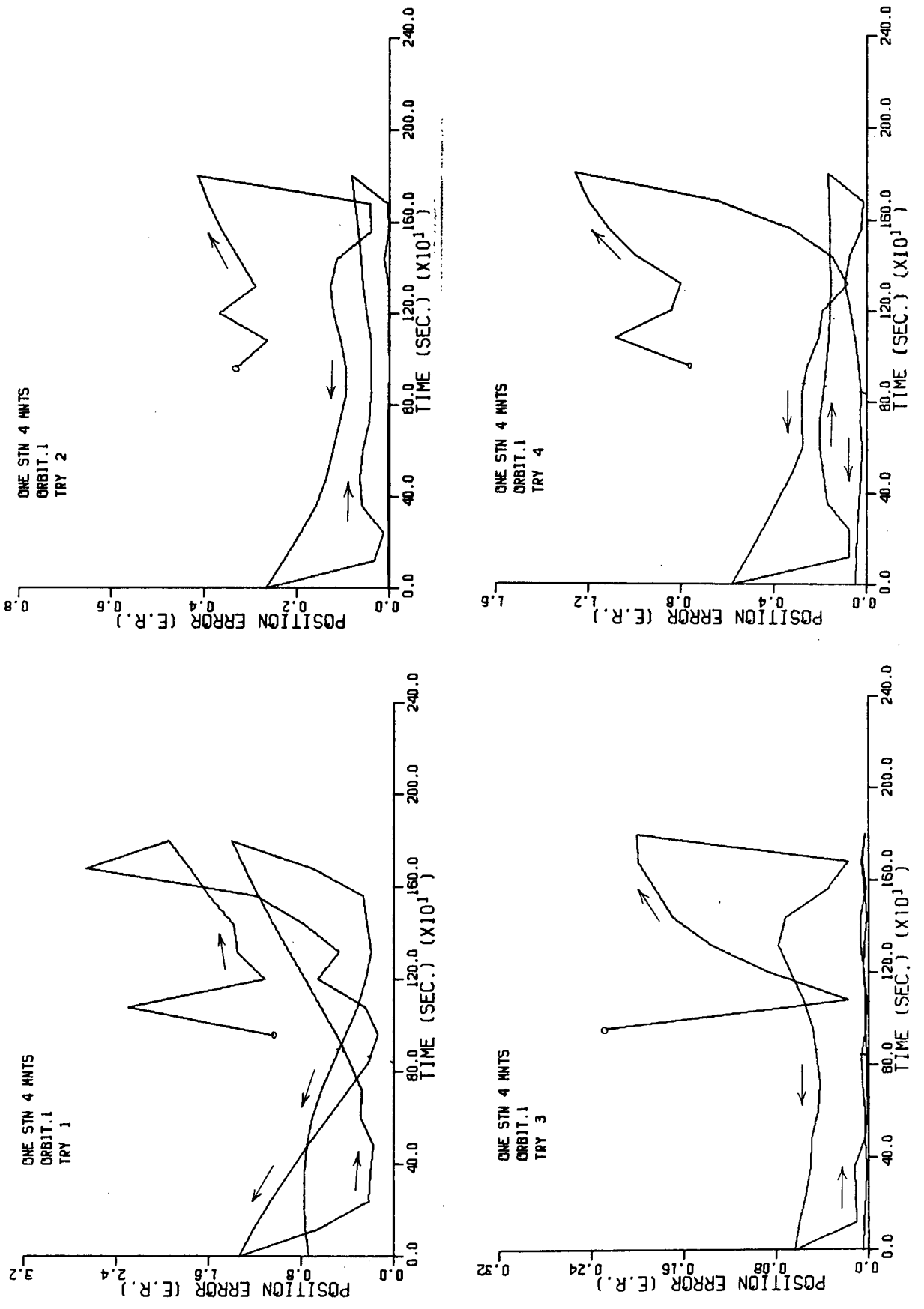

Orbit 1 Position Error with 4 Measurements Figure V.15

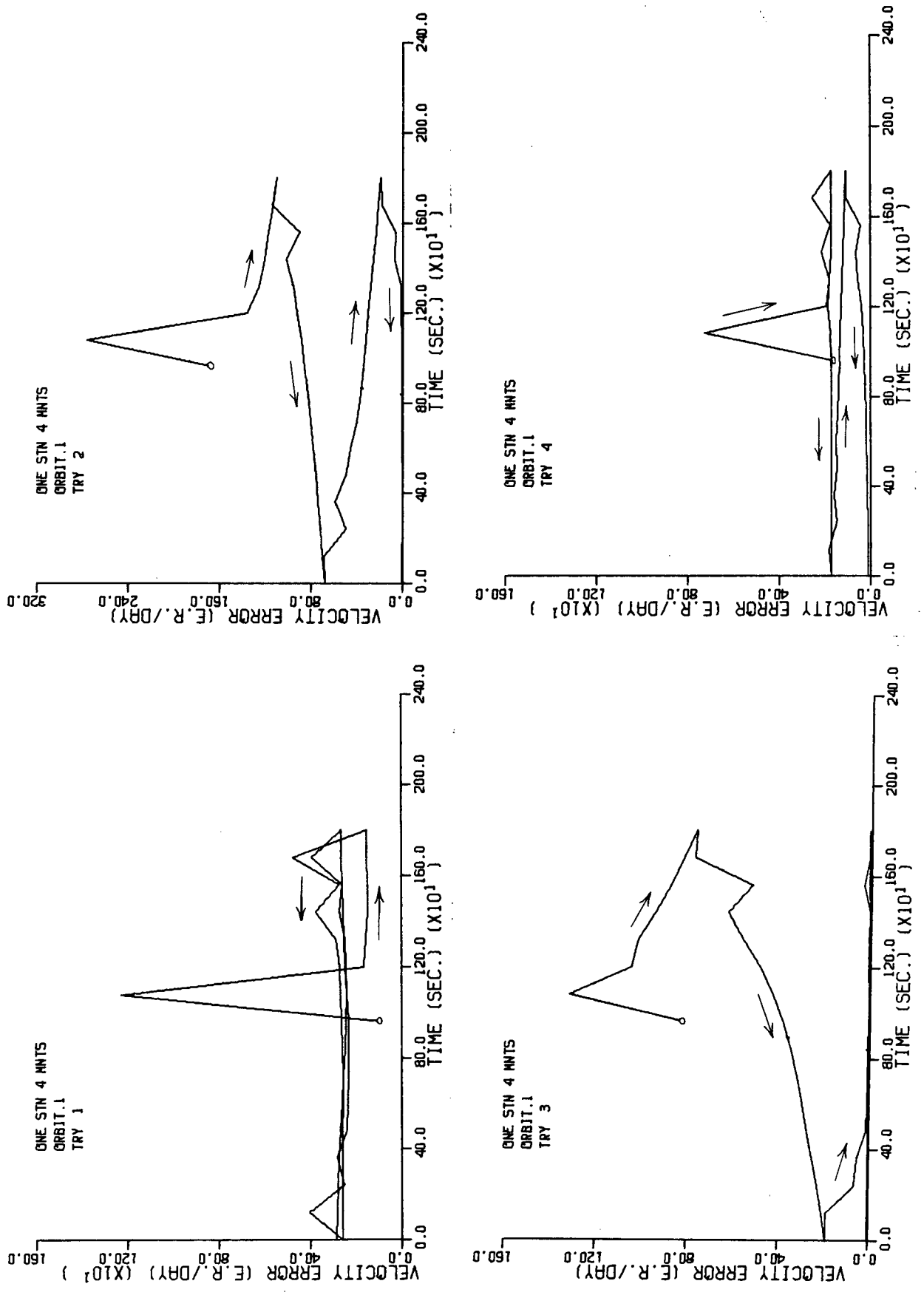

Orbit 1 Velocity Error with 4 Measurements Figure V.16

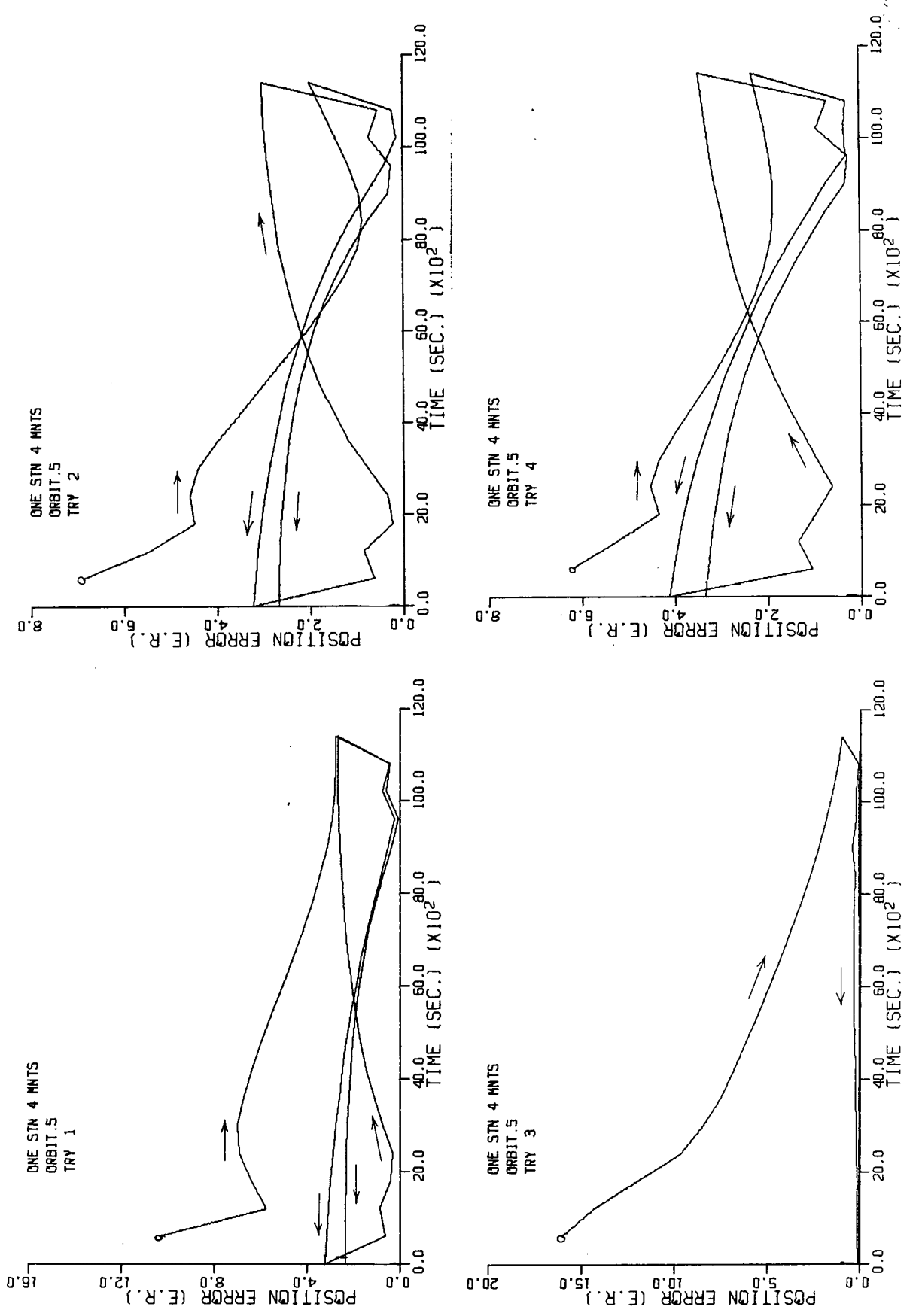

Orbit 5 Position Error with 4 Measurements Figure V.17

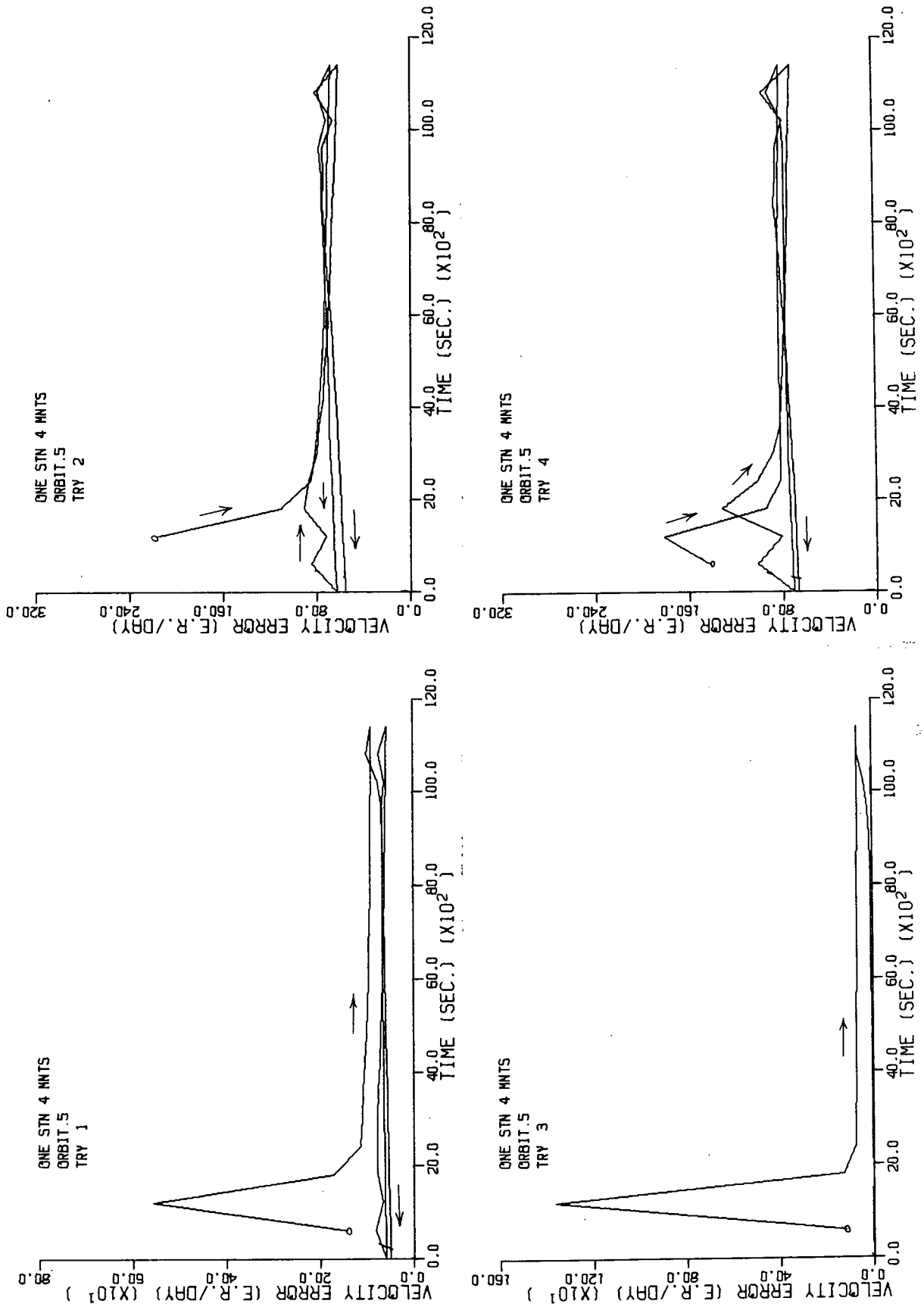

Orbit 5 Velocity Error with 4 Measurements , Figure V.18

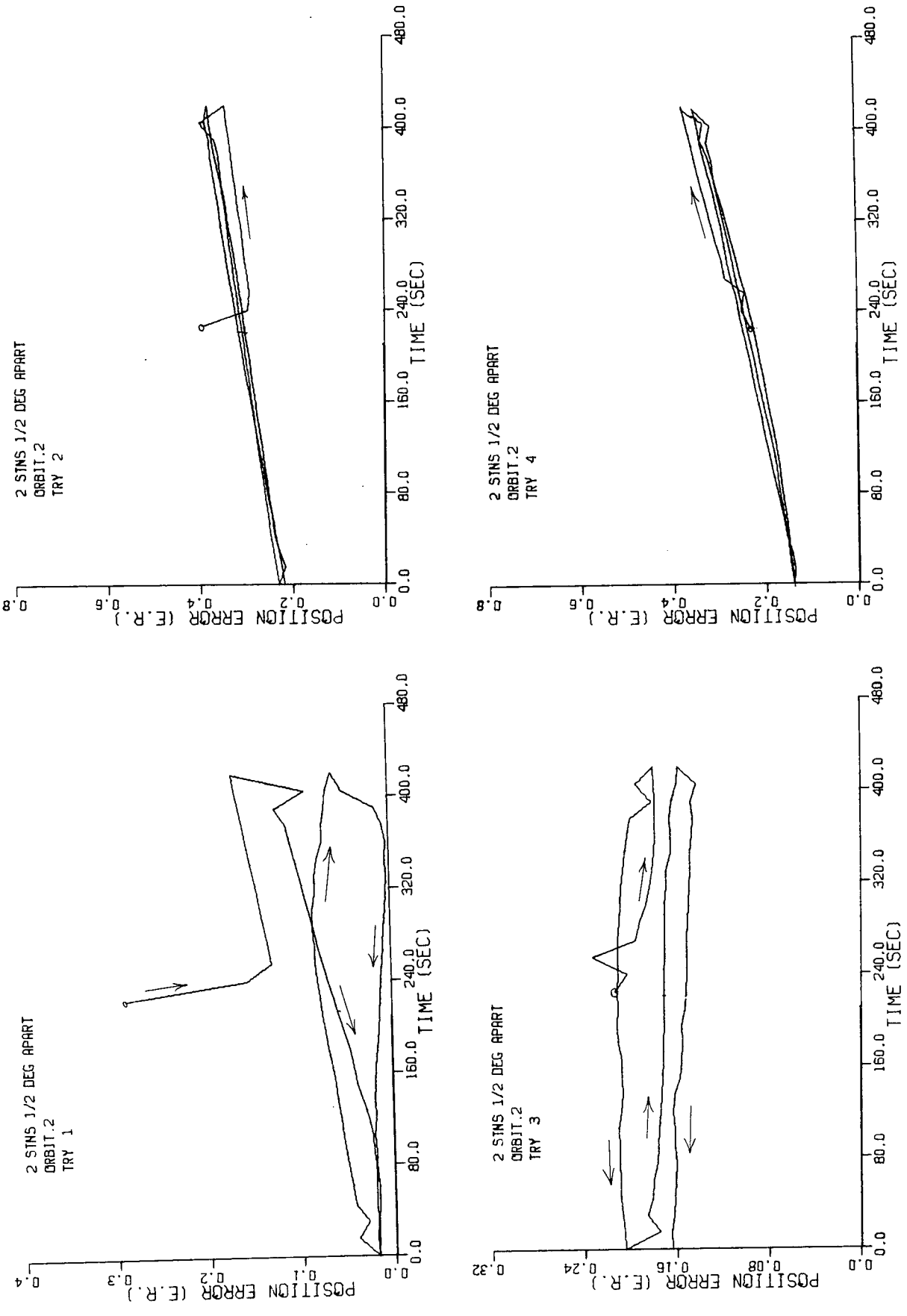

Orbit 2 Position Error $1/2^{o}$ Latitude Separation Figure V.19

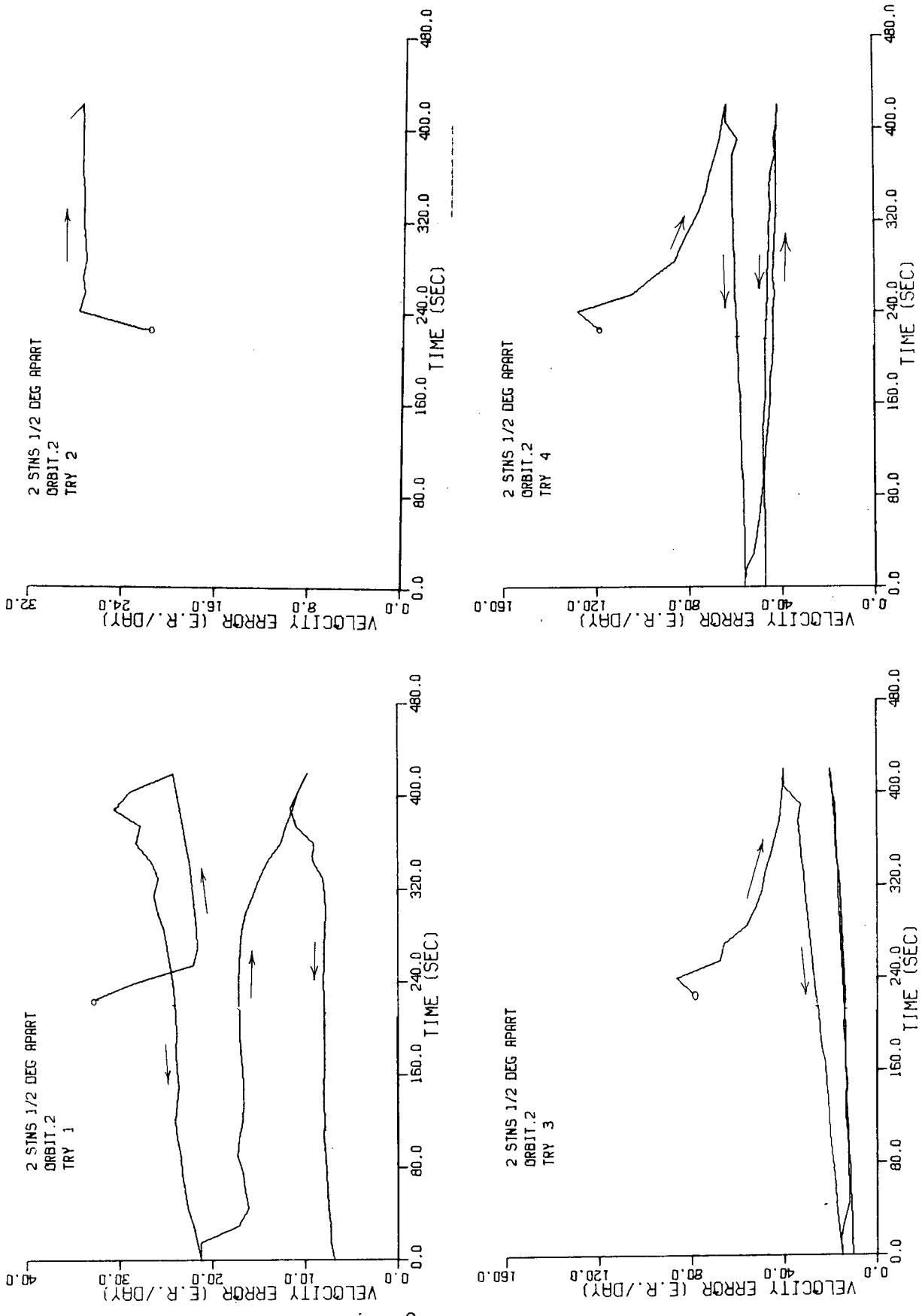

Orbit 2 Velocity Error $1/2^{o}$ Latitude Separation Figure V.20

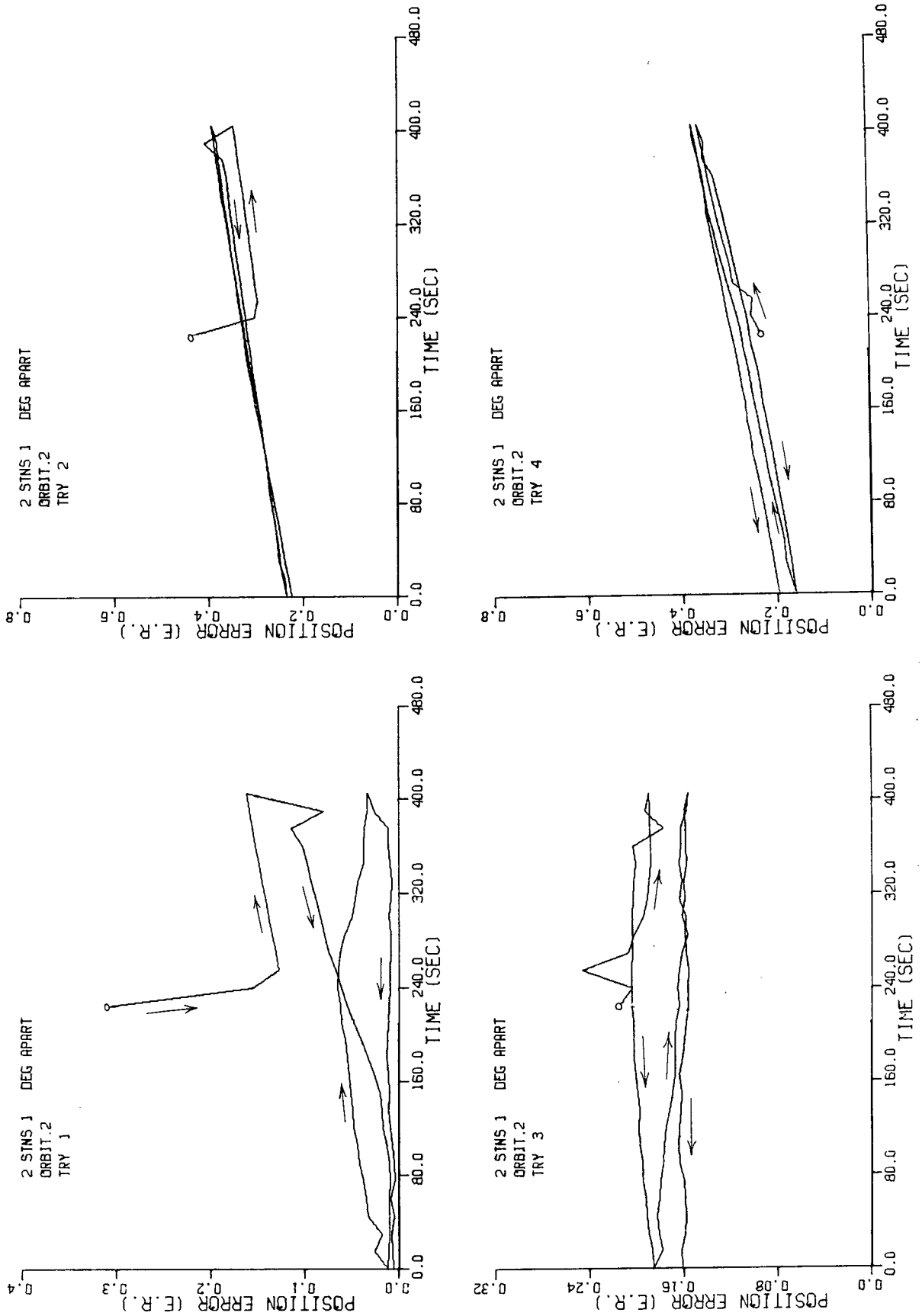

Orbit 2 Position Error 1^{o} Latitude Separation Figure V.21

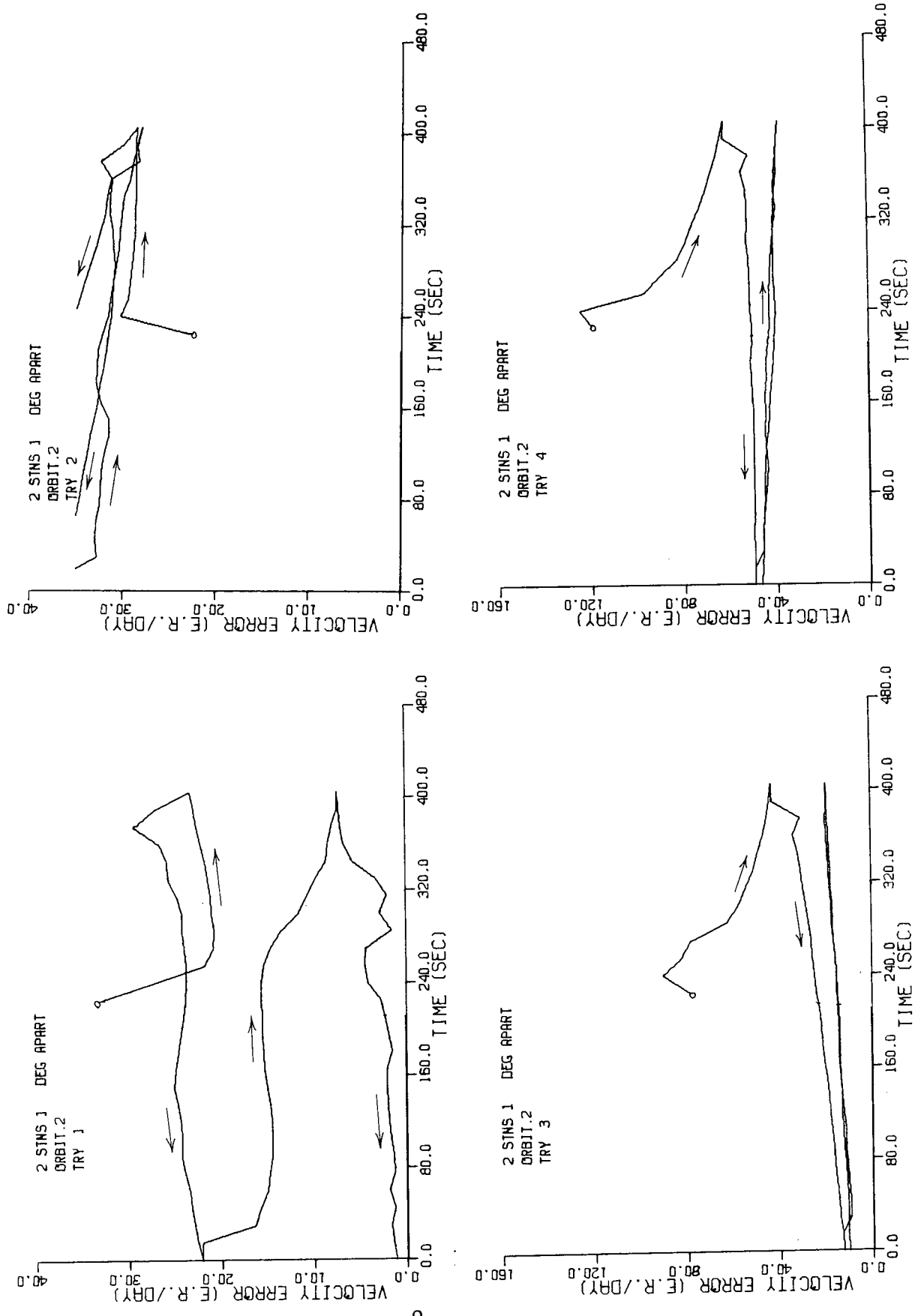

Orbit 2 Velocity Error 1^{o} Latitude Separation Figure V.22

approximately halved the final state estimate error but was still unsatisfactory. It was not until the separation was increased to 5 degrees latitude, Figure V.23 and Figure V.24 , that satisfactory convergence was obtained.

In order to determine if the direction of station separation had any effect, the stations were repositioned 1/2 degree longitude apart. The results shown in Figure V.25 and Figure V.26 demonstrate a marked improvement over the 1/2 degree latitude separation, an improvement equivalent to the 5 degree latitude case. Intuitively one could expect that a satellite with a ground track perpendicular to a line drawn between the two earth stations could be better observed than a satellite with a parallel ground track. This turned out to be the case. Also, the best initialization is no longer Try 1 as with 5 degree latitude, but Try 2 and Try 3. This phenomena of the best initialization changing with the separation was observed frequently.

Longitudinal separation had to be decreased to 0.1 degree, Figure V.27 and Figure V.28 , before convergence ceased, and when increased to 3 degrees, Figure V.29 and Figure V.30 , Try 3 initialization no longer converged while Try 4 improved markedly.

Convergence seems to gradually slow with decreasing station separation until, in the limit, the system becomes totally unobservable as shown in section 2. The station separation required for observability is a function of the direction of separation and, as will be shown next, the type of orbit.

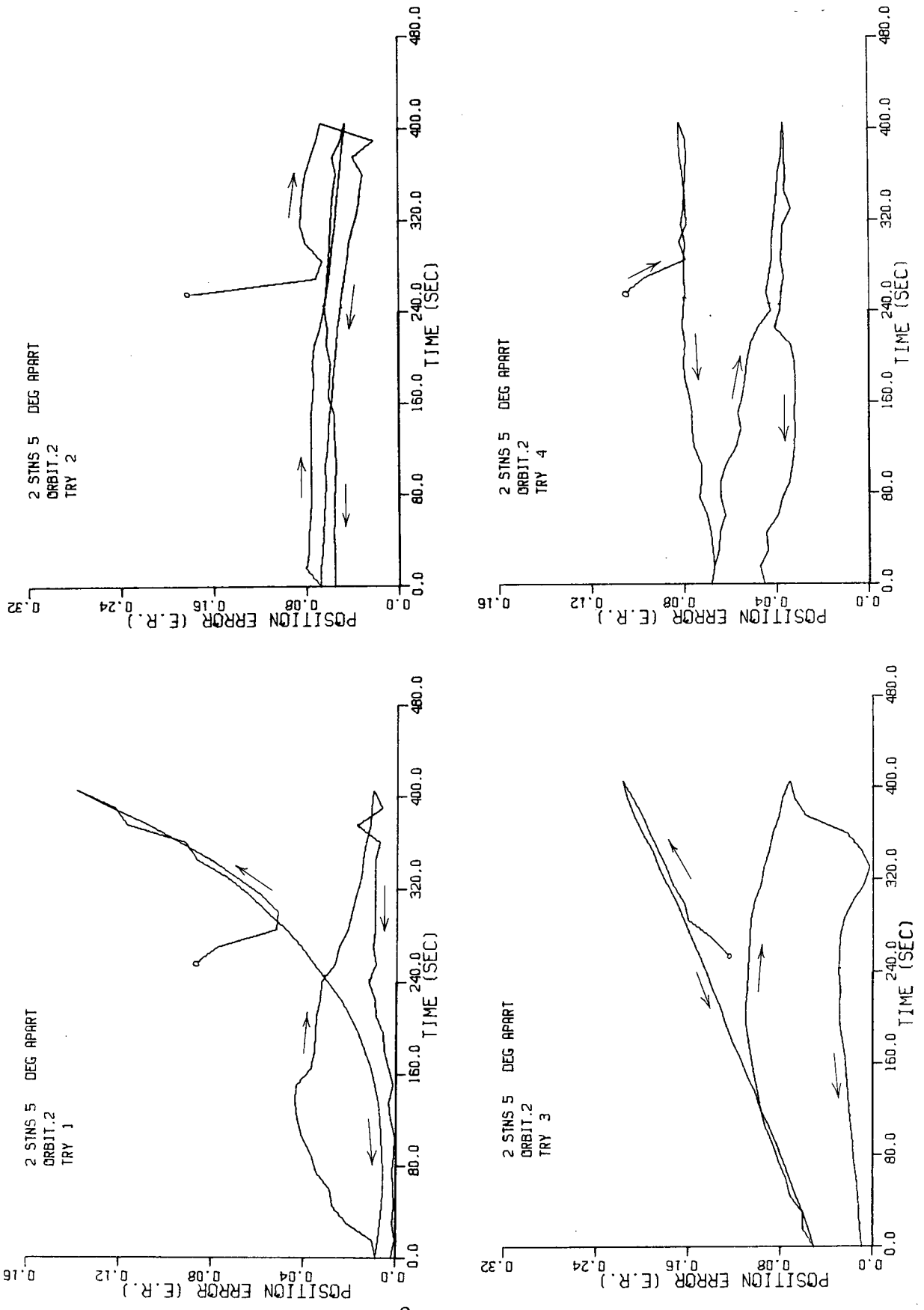

Orbit 2 Position Error 5^{o} Latitude Separation Figure V.23

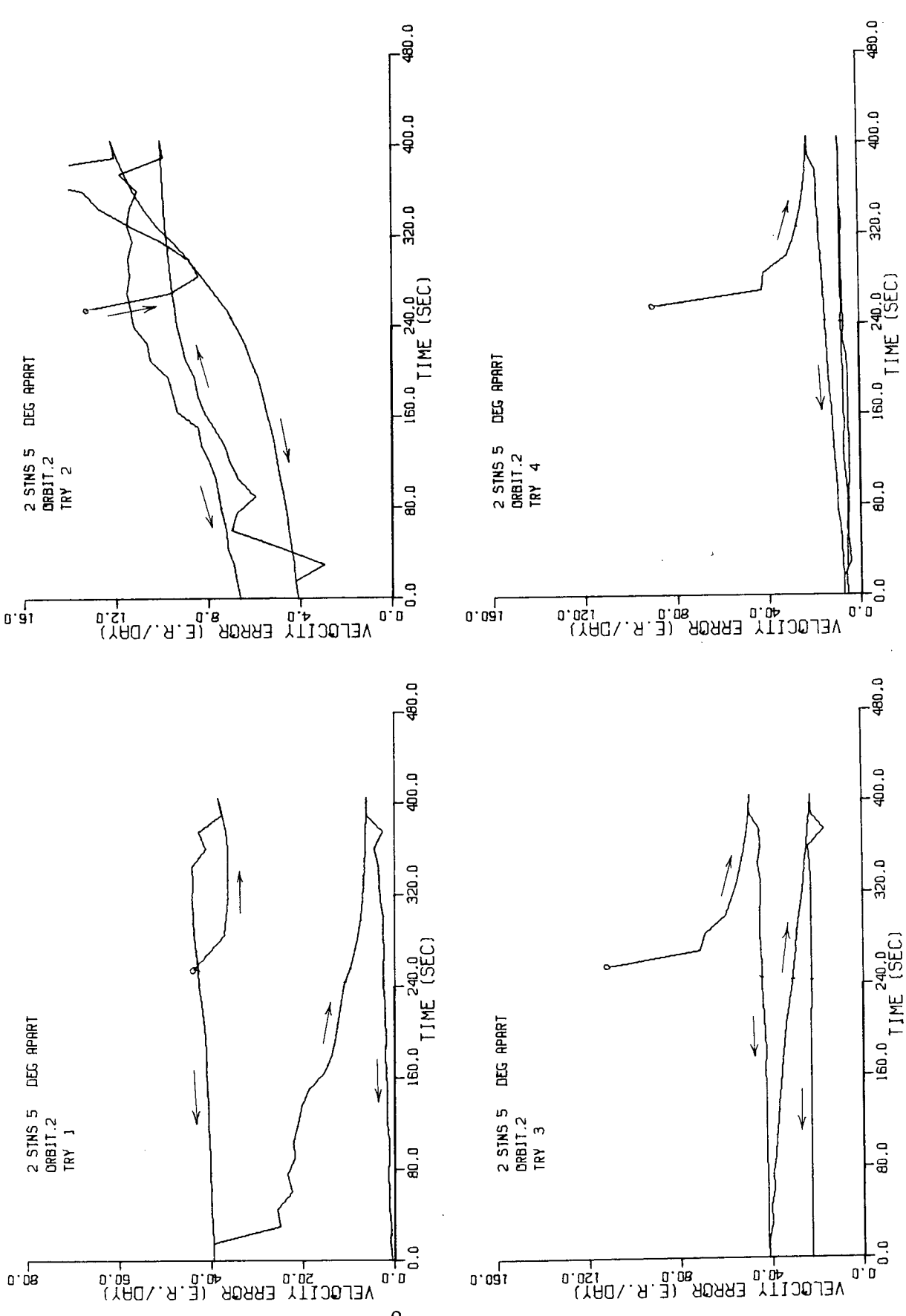

Orbit 2 Velocity Error 5^{o} Latitude Separation Figure V.24

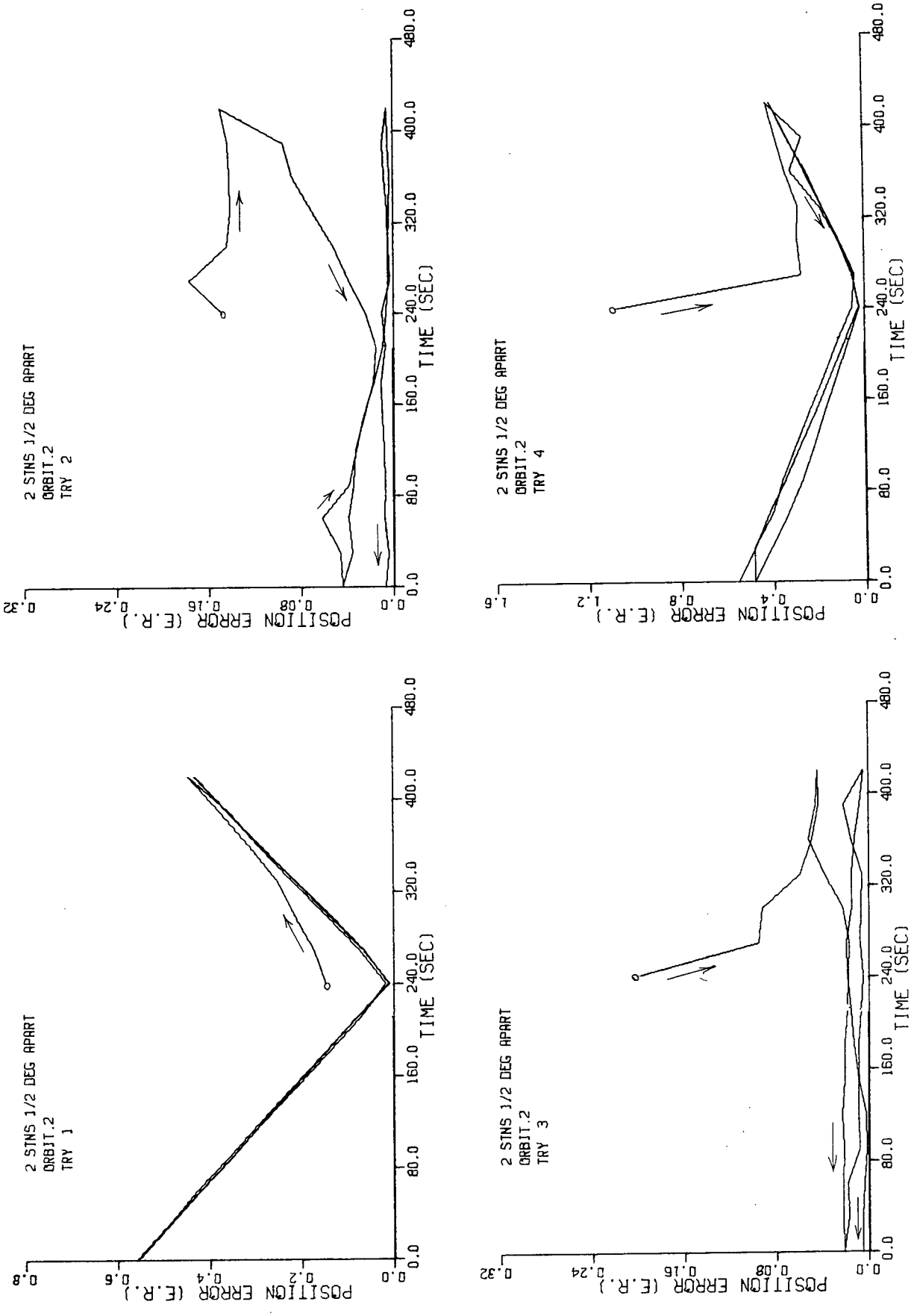

Orbit 2 Position Error $1/2^{o}$ Longitude Separation Figure V.25

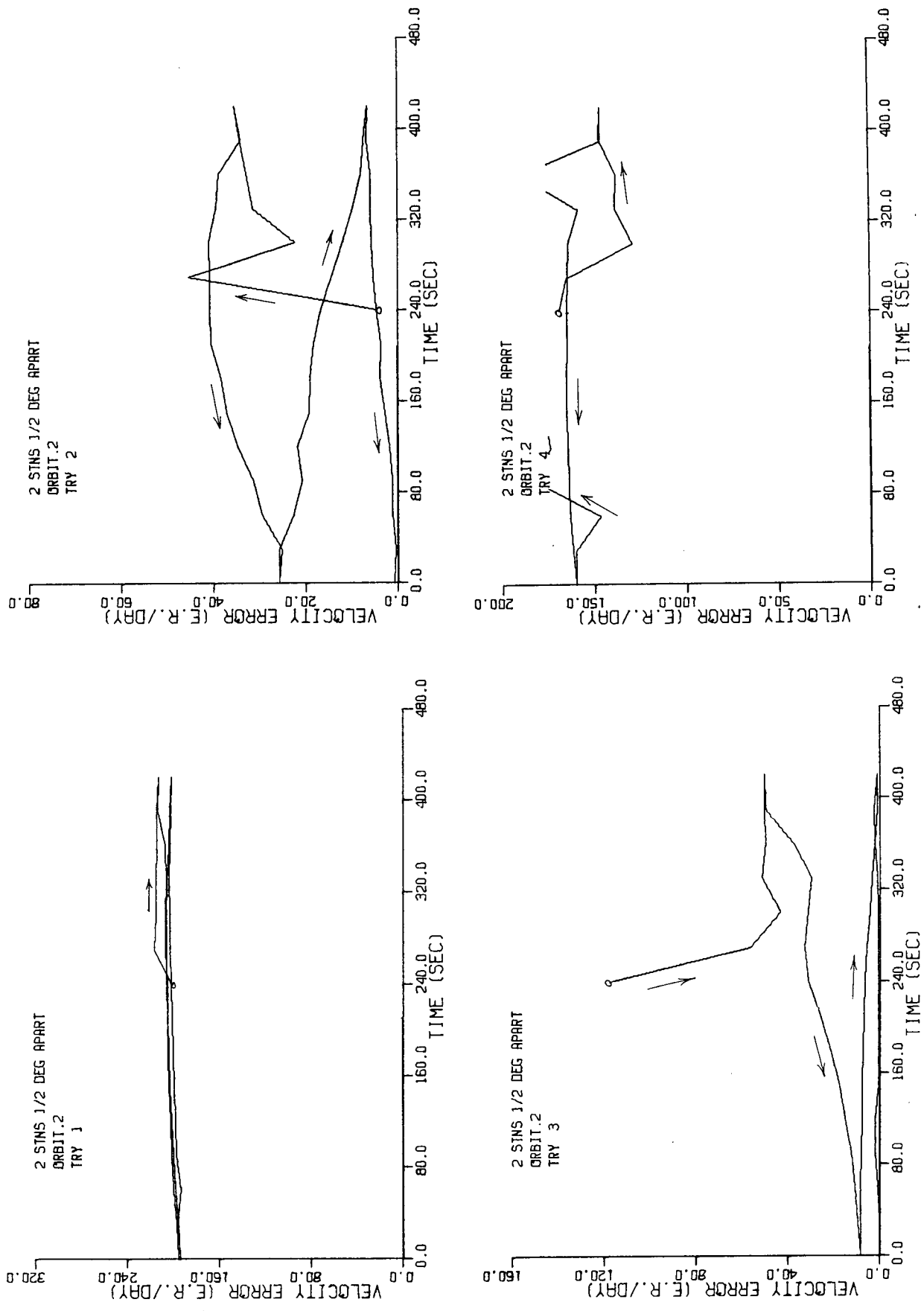

Orbit 2 Velocity Error $1/2^{o}$ Longitude Separation Figure V.26

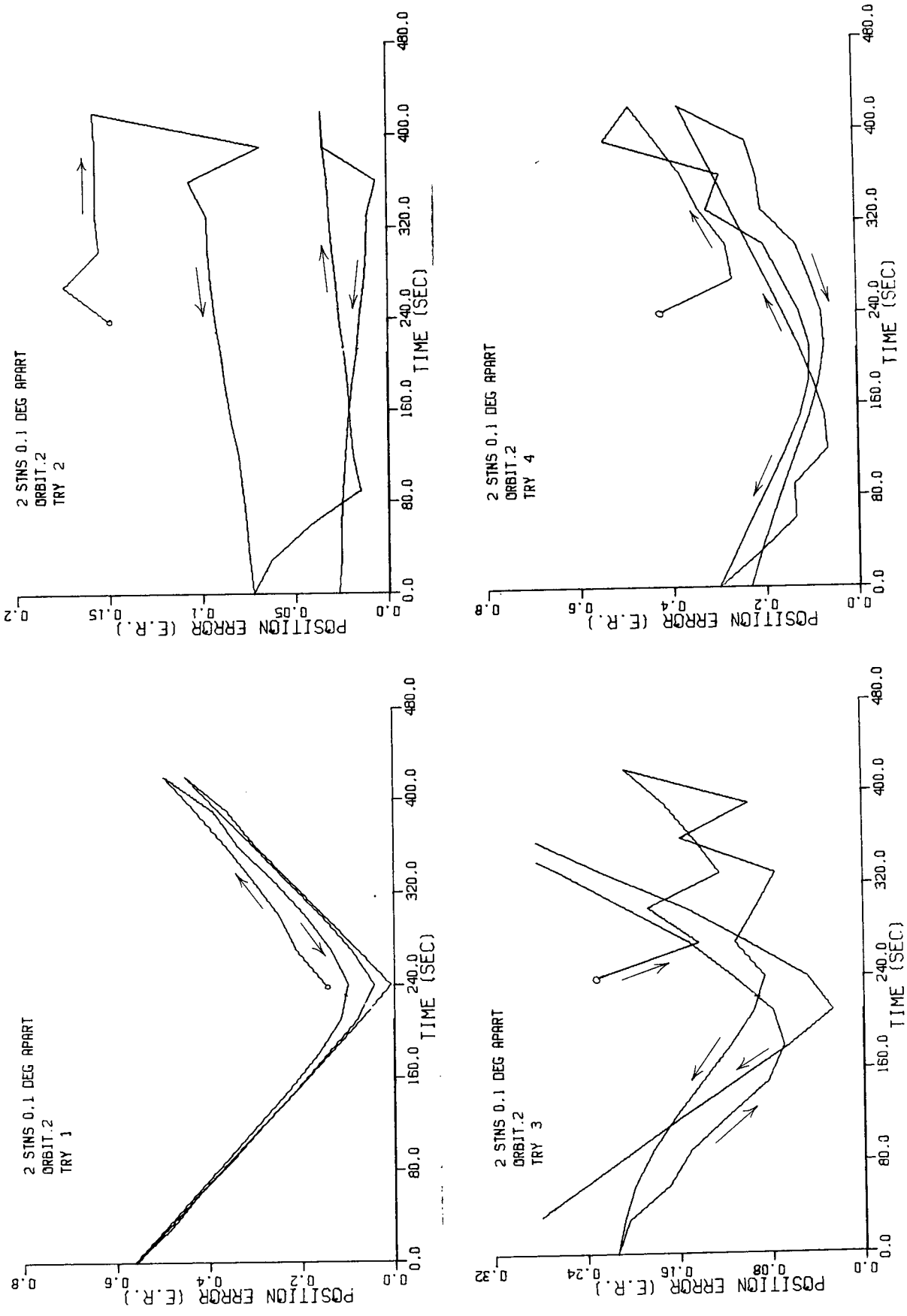

Orbit 2 Position Error 0.1° Longitude Separation Figure V.27

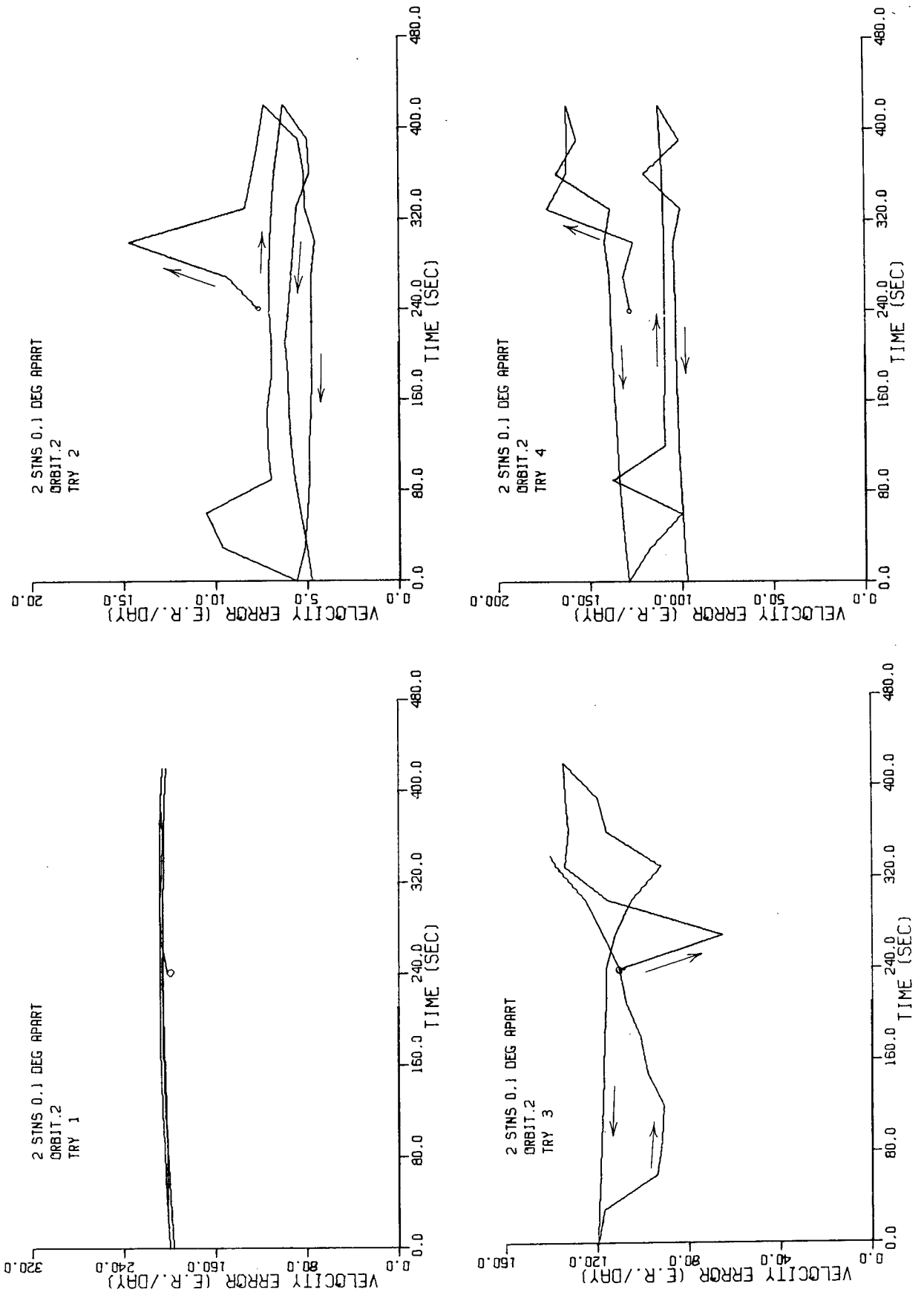

Orbit 2 Velocity Error 0.1° Longitude Separation Figure V.28

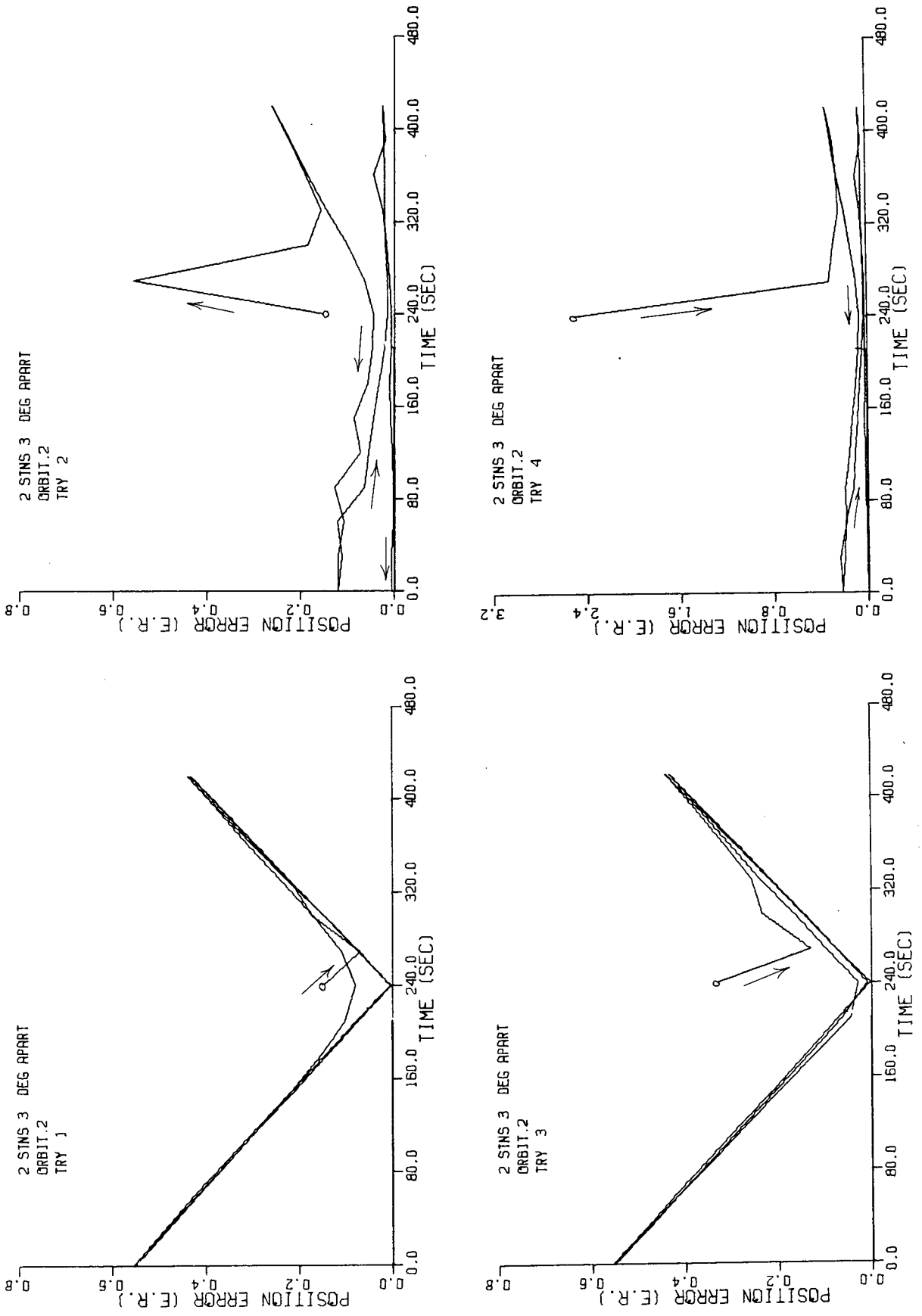

Orbit 2 Position Error 3^{o} Longitude Separation

Figure V.29

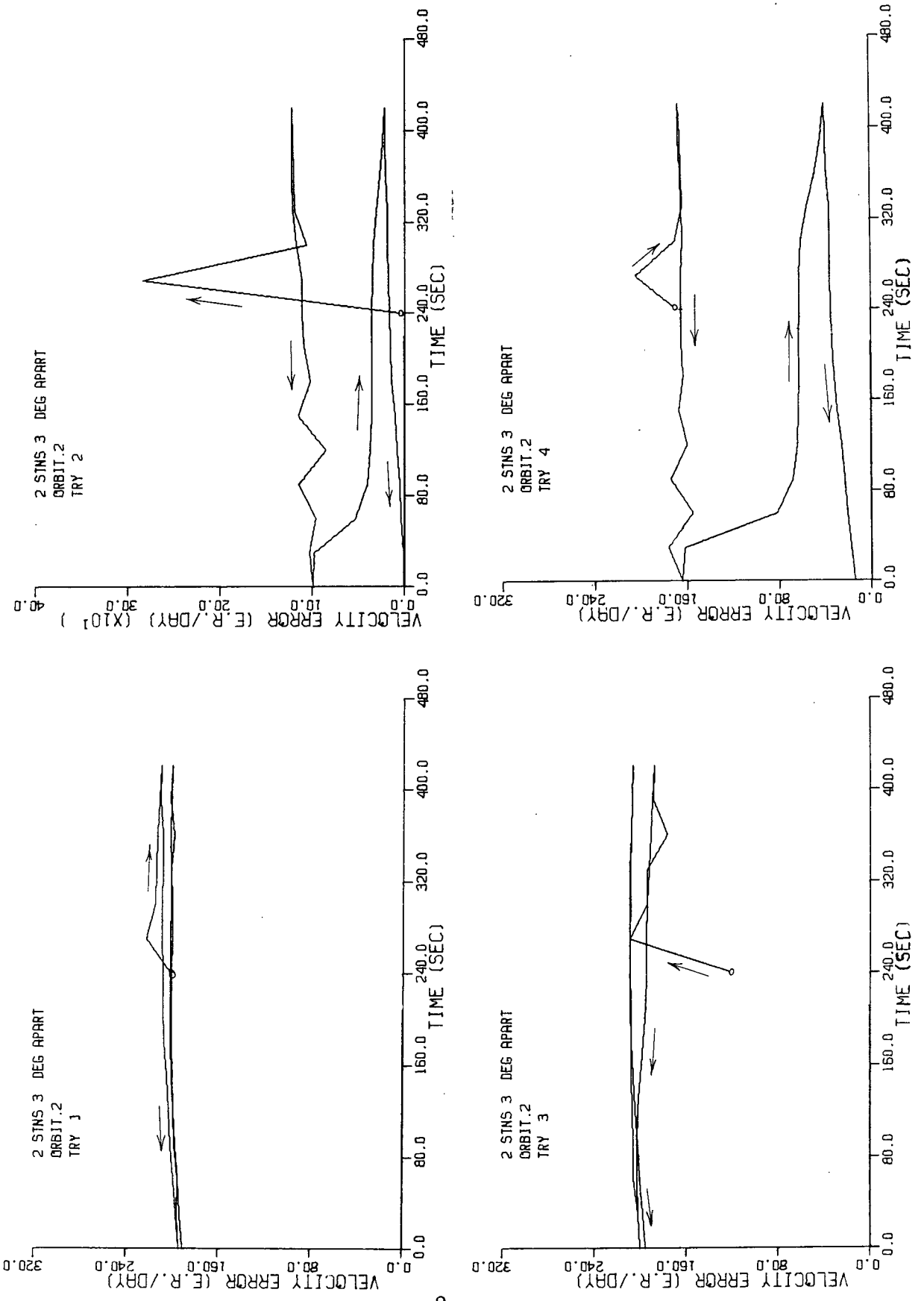

Orbit 2 Velocity Error 3° Longitude Separation

Figure V.30

4.2 Orbit 1 Results

When Orbit 1, the inclined eccentric orbit, was used as the orbit under observation, a separation of even 2 degrees longitude was insufficient as shown in Figure V.31 and Figure V.32 . However, a separation of 2 degrees latitude showed good convergence. (See Figure V.33 and Figure V.34) Longitudinal separation had to be increased to 3 degrees, Figure V.35 and Figure V.36 , before convergence became satisfactory. This can be explained by the fact that at 50 degrees latitude, stations one degree apart in longitude are about three fifths as distant as stations one degree apart in latitude due to the convergence of the lines of longitude towards the poles. Reducing the latitudinal separation to 1 degree caused no discernable decrease in performance. In fact, as can be seen from Figure V.37 and Figure V.38 , the reduction caused the Try 1 initialization to converge, which it had not done for the 2 degree separation.

The ideal separation direction changes with the type of orbit and in some cases from pass to pass of the same orbit. The erratic behavior of the different initialization tries underscores this algorithm's sensitivity to initialization. If we envisage a six dimensional initialization space, discontinuous regions exist from which convergence is possible. As the stations are separated by increasing distances, the measurement equations change, shifting these regions of convergence. A given initialization can therefore pass in and out of convergence. A theoretical explanation of why and how the changing measurement equations shift these regions is beyond the scope of this thesis. It can be said, however, that in general the larger the separation the better the observability. Increasing station separation must be traded

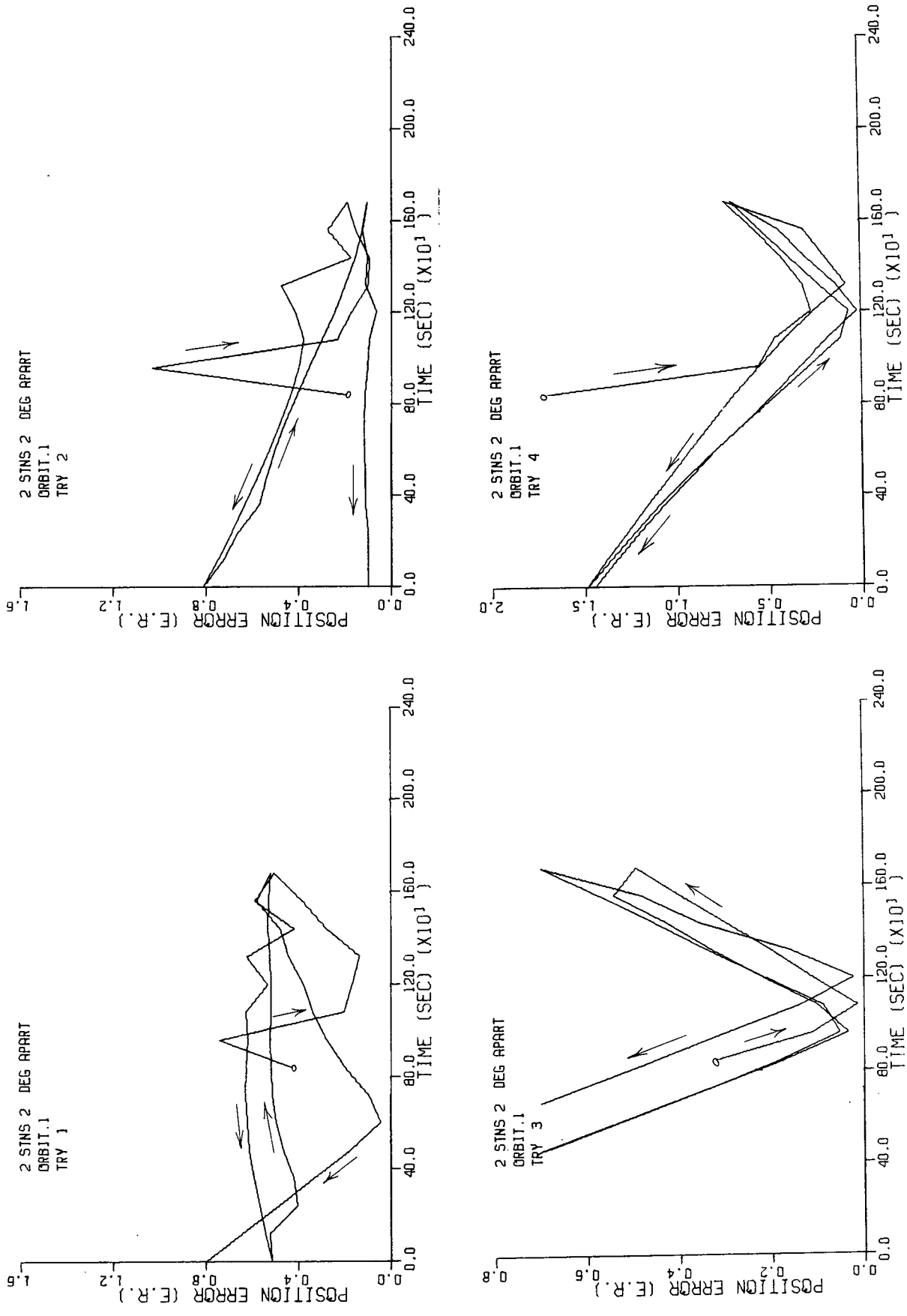

Orbit 1 Position Error 2^{o} Longitude Separation Figure V.31

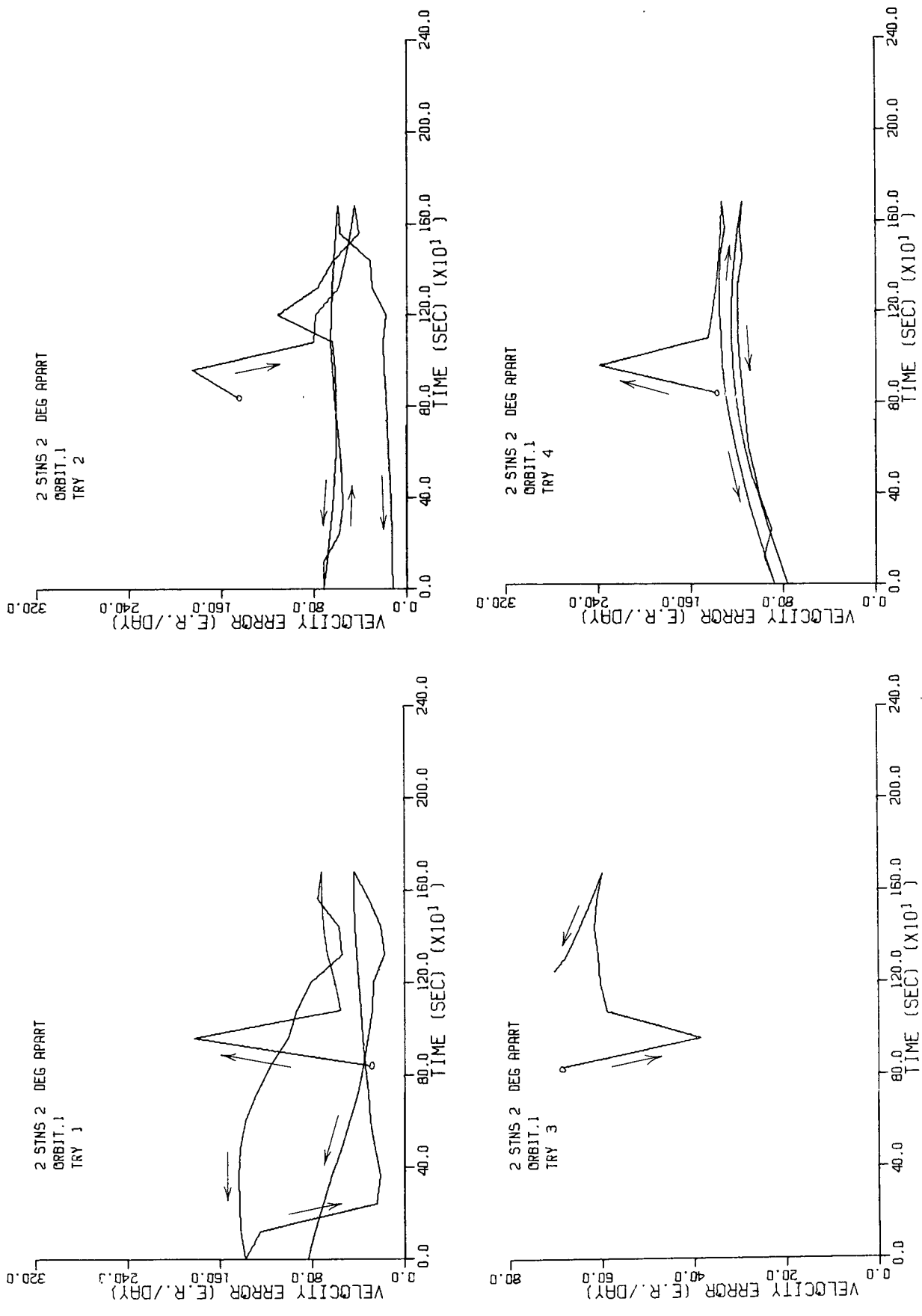

Orbit 1 Velocity Error 2^{o} Longitude Separation Figure V.32

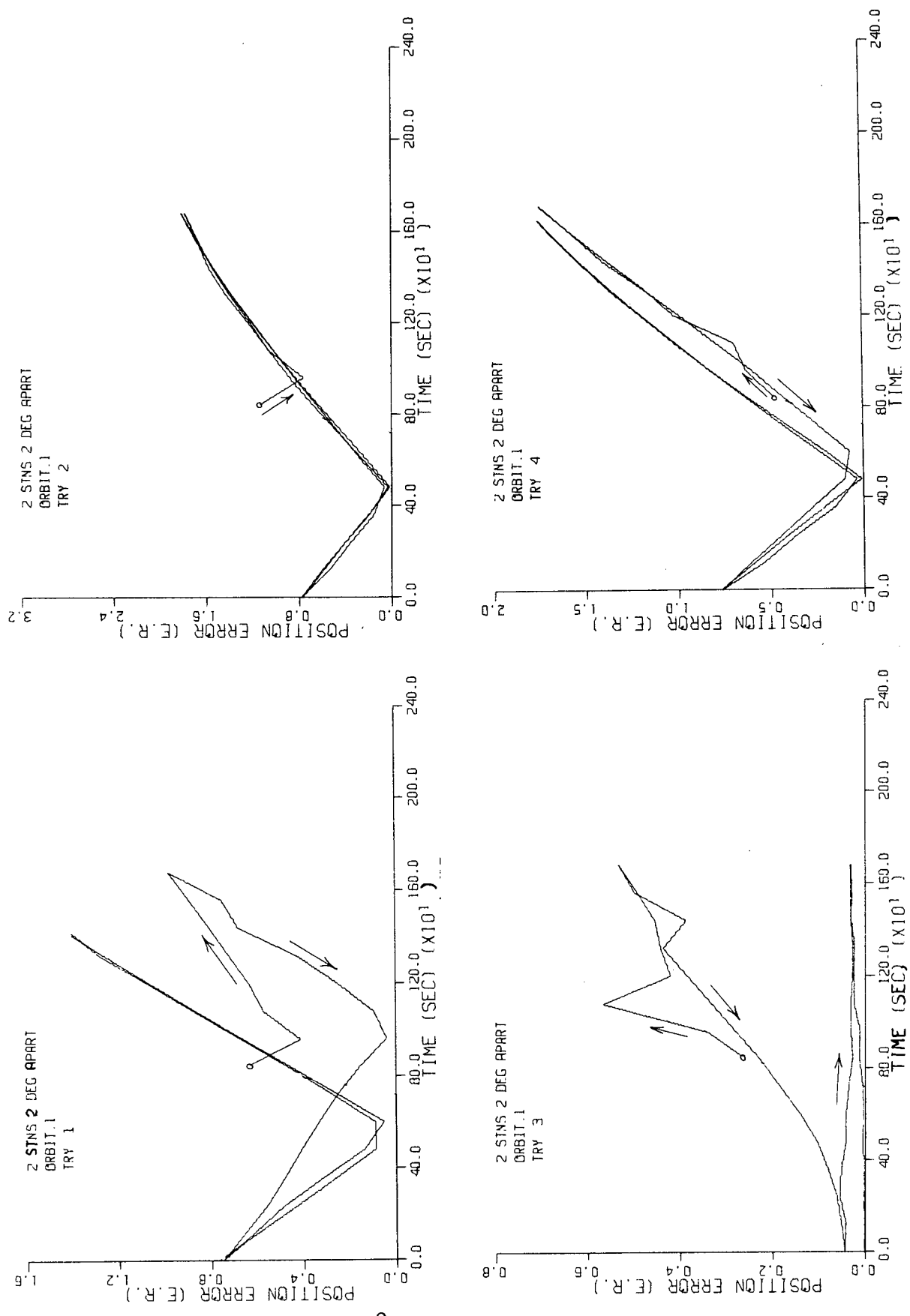

Orbit 1 Position Error 2^{o} Latitude Separation Figure V.33

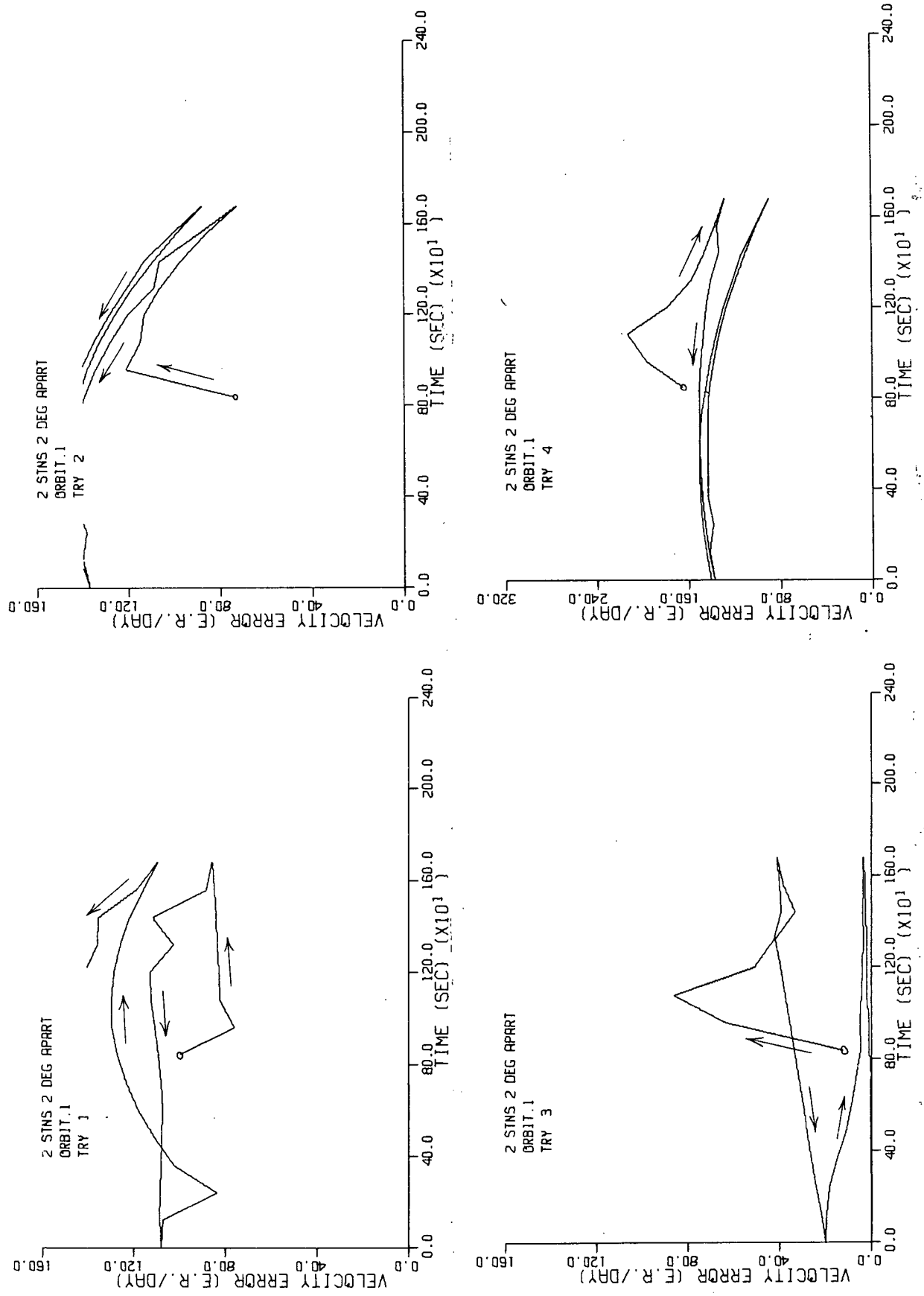

Orbit 1 Velocity Error 2^{o} Latitude Separation Figure V.34

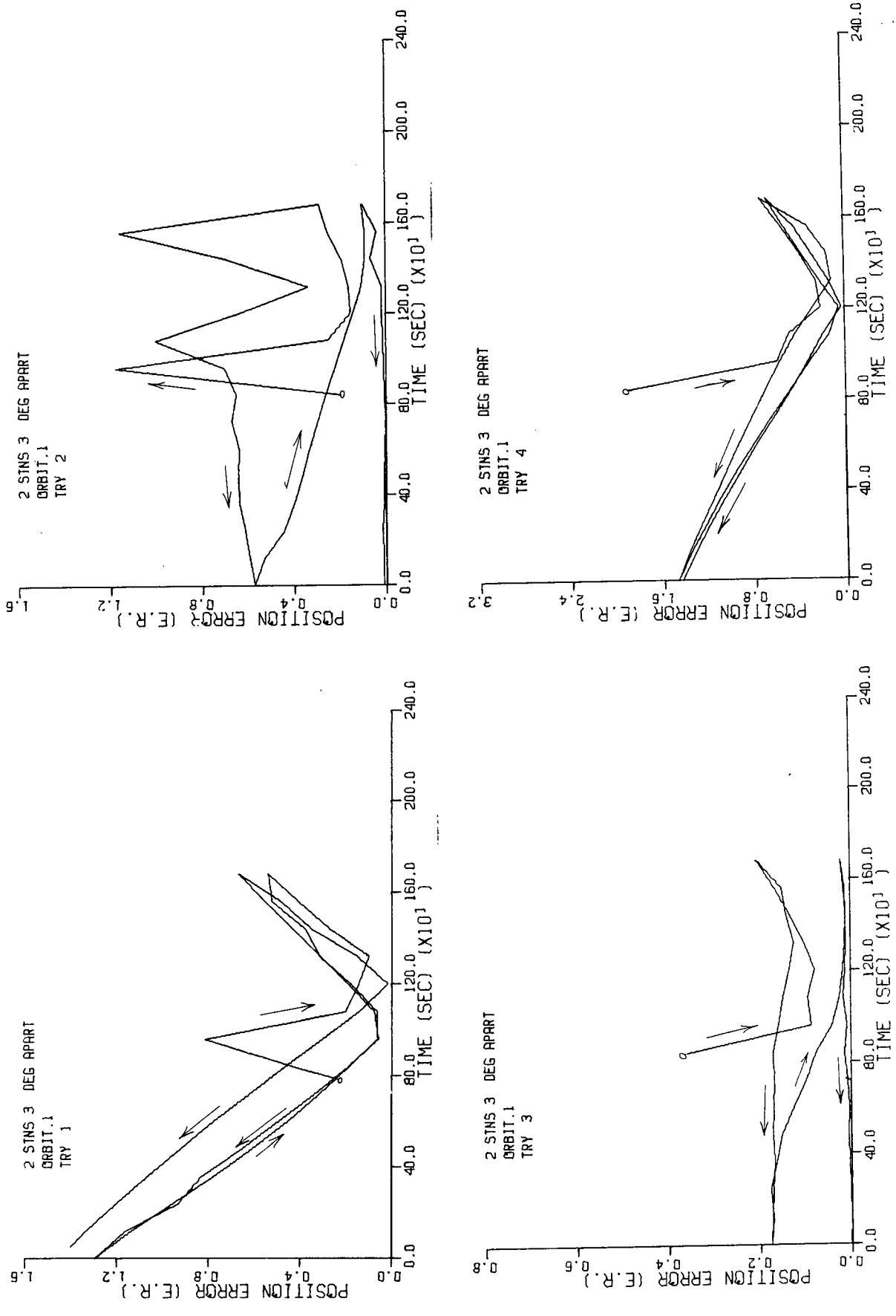

Orbit 1 Position Error 3^{o} Longitude Separation Figure V.35

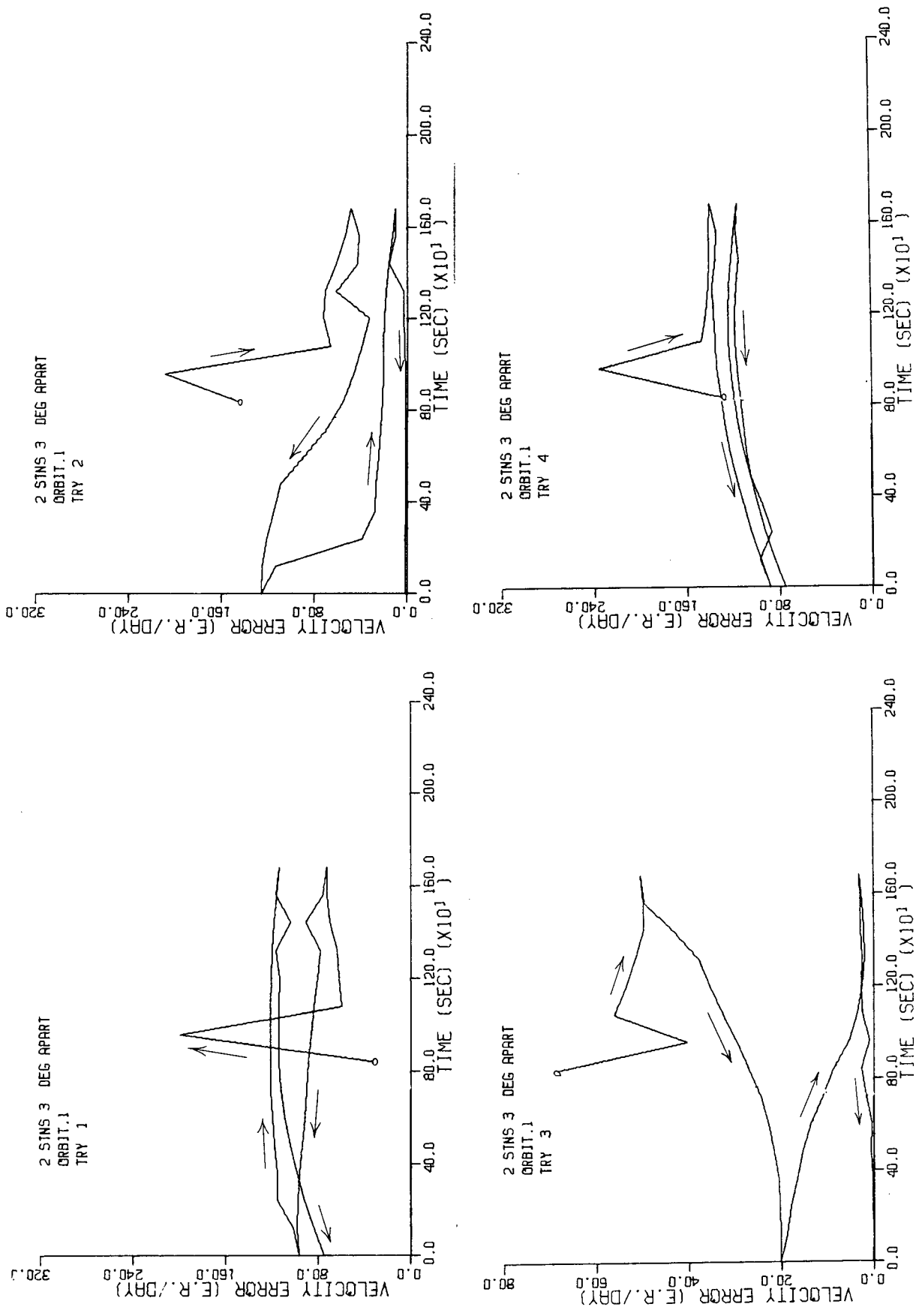

Orbit 1 Velocity Error 3^{o} Longitude Separation Figure V.36

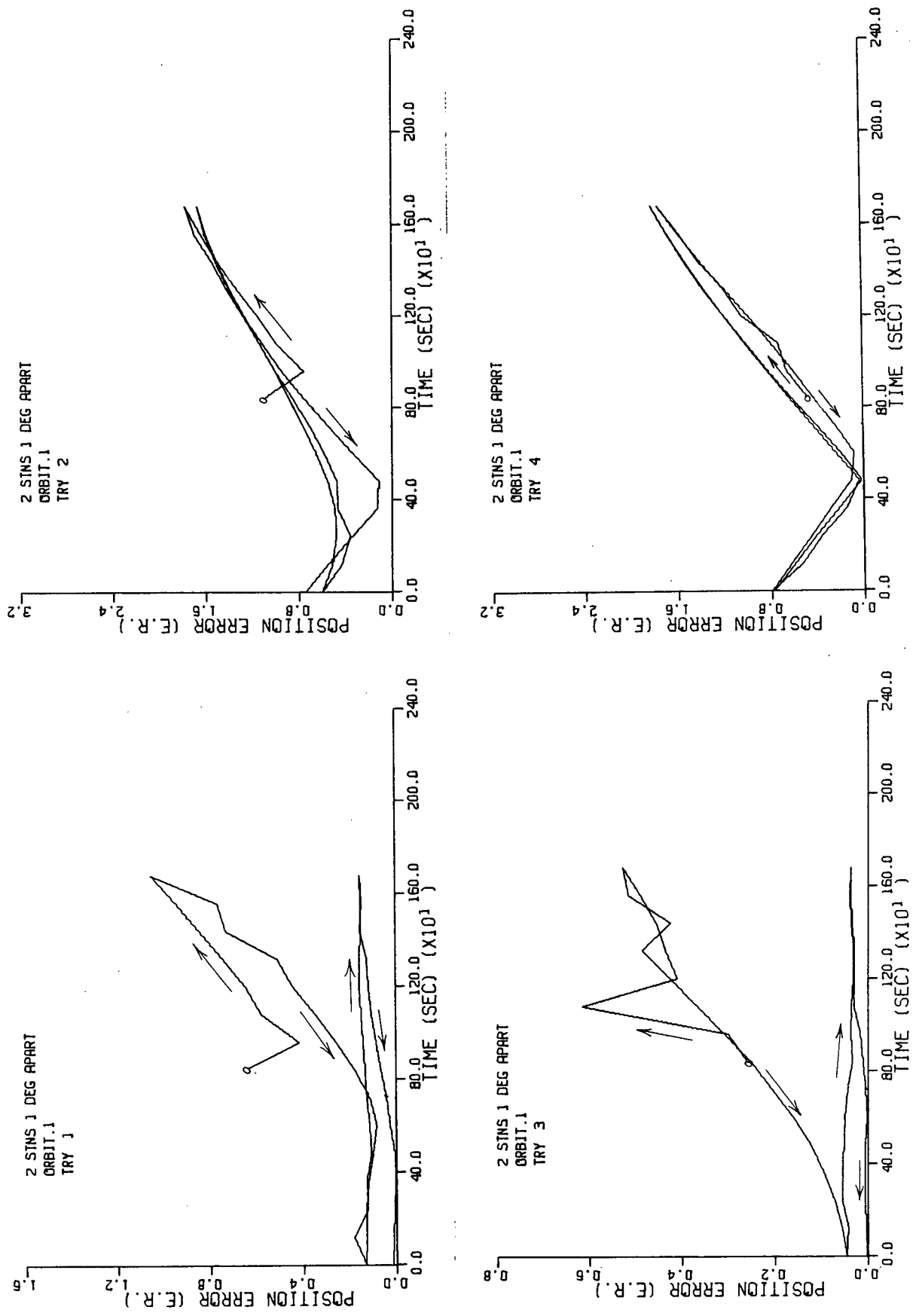

Orbit 1 Position Error 1^{o} Latitude Separation Figure V.37

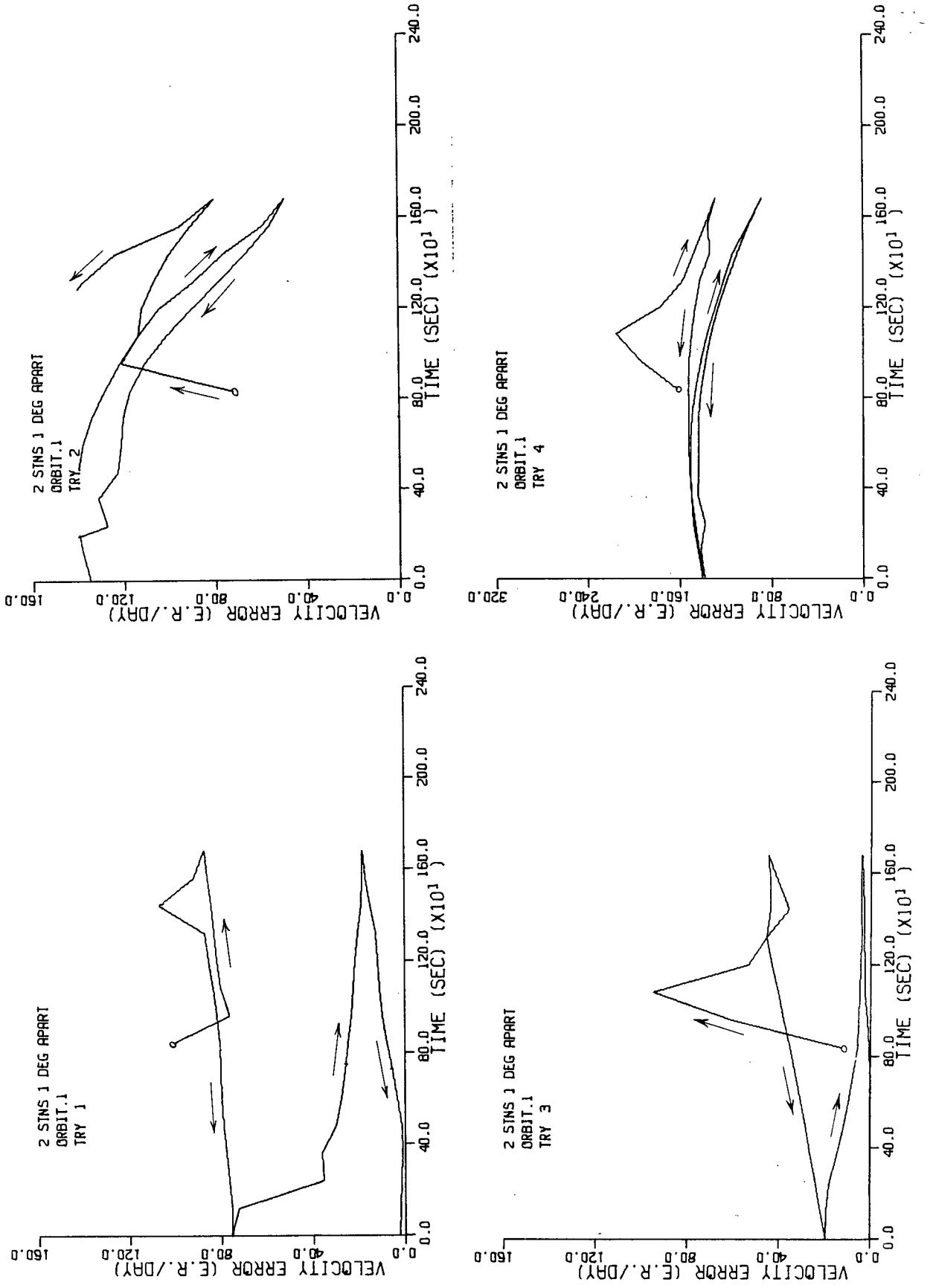

Orbit 1 Velocity Error 1^{o} Latitude Separation

Figure V.38

off against a reduced measurement time during which the satellite is visible to both stations.

4.3 Other Orbits' Results

Simulation runs were made using the other orbits of Table IV.3. All were found to converge if station separation was sufficient. Figure V.39 and Figure V.40 show the results obtained with Orbit 3 and a 2 degree longitude station separation. Figure V.41 and Figure V.42 show Orbit 4's results also with a 2 degree longitude separation. Orbit 5, the geosynchronous orbit, required a 20 degree separation in longitude to achieve the results shown in Figure V.43 and Figure V.44 . Finally, the results using Orbit 6 and a 2 degree latitude separation are shown in Figure V.45 and Figure V.46 .

5. Known Orbit Improvement

As previously shown, it is not possible to accomplish preliminary orbit determination using only range and range-rate measurements from one station. The question then arose as to how much information could be extracted from these two simple measurements. Was it possible, for instance, to correct for small perturbations from an orbit which was fairly well known "a priori"? If so, how large an error could be corrected or improved upon? The linearized Kalman filter was idealy suited to answer these questions as it assumes a known state trajectory.

Simulation runs were made to answer these questions. These runs were similar to the runs already described in the previous sections with the following important differences. The initial state estimate was not calculated using the algorithm described in section IV.3 but was set equal to the initially assumed orbit. A fifth trace was added to the

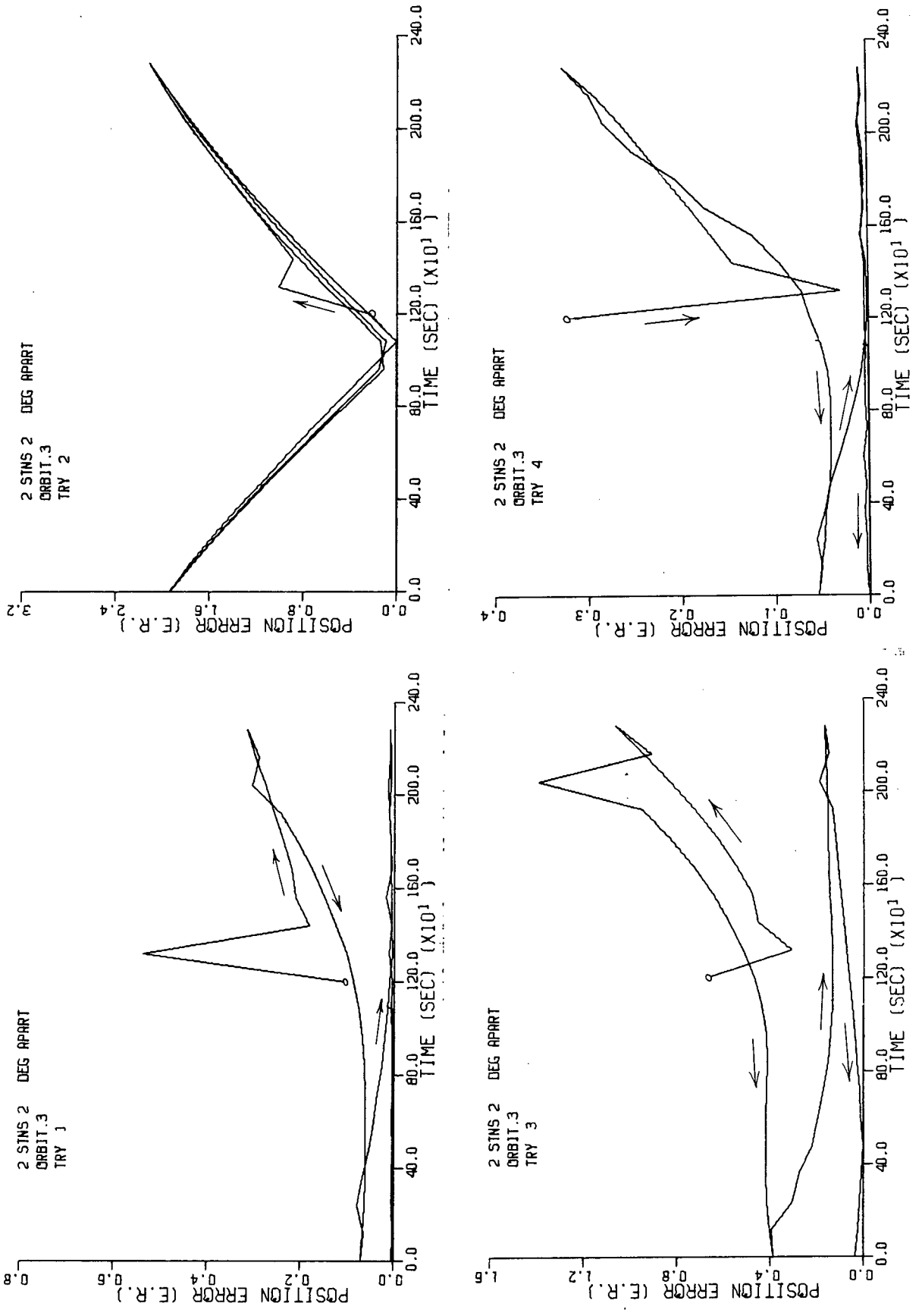

Orbit 3 Position Error 2^{o} Longitude Separation Figure V.39

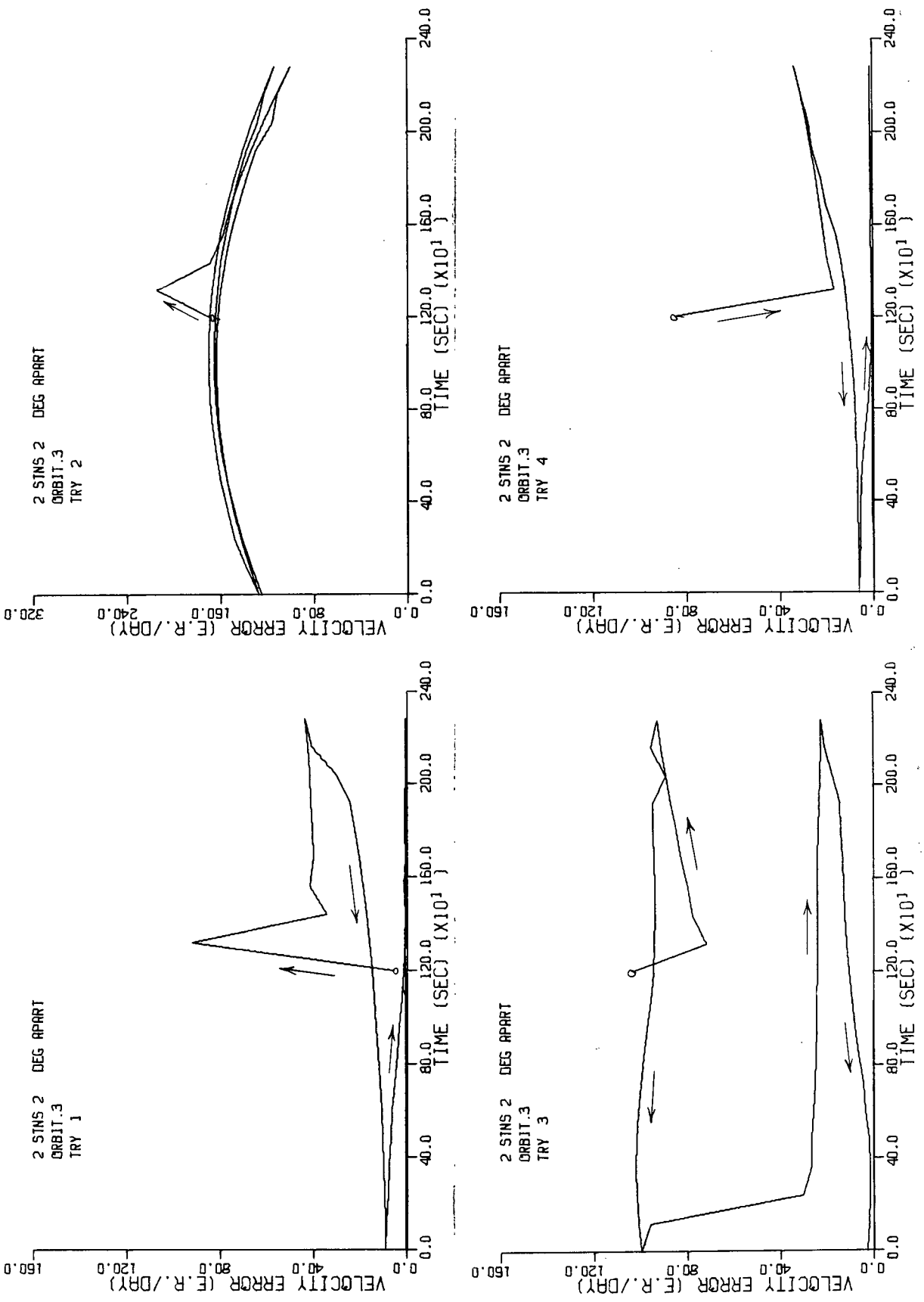

Orbit 3 Velocity Error 12° Longitude Separation

Figure V.40

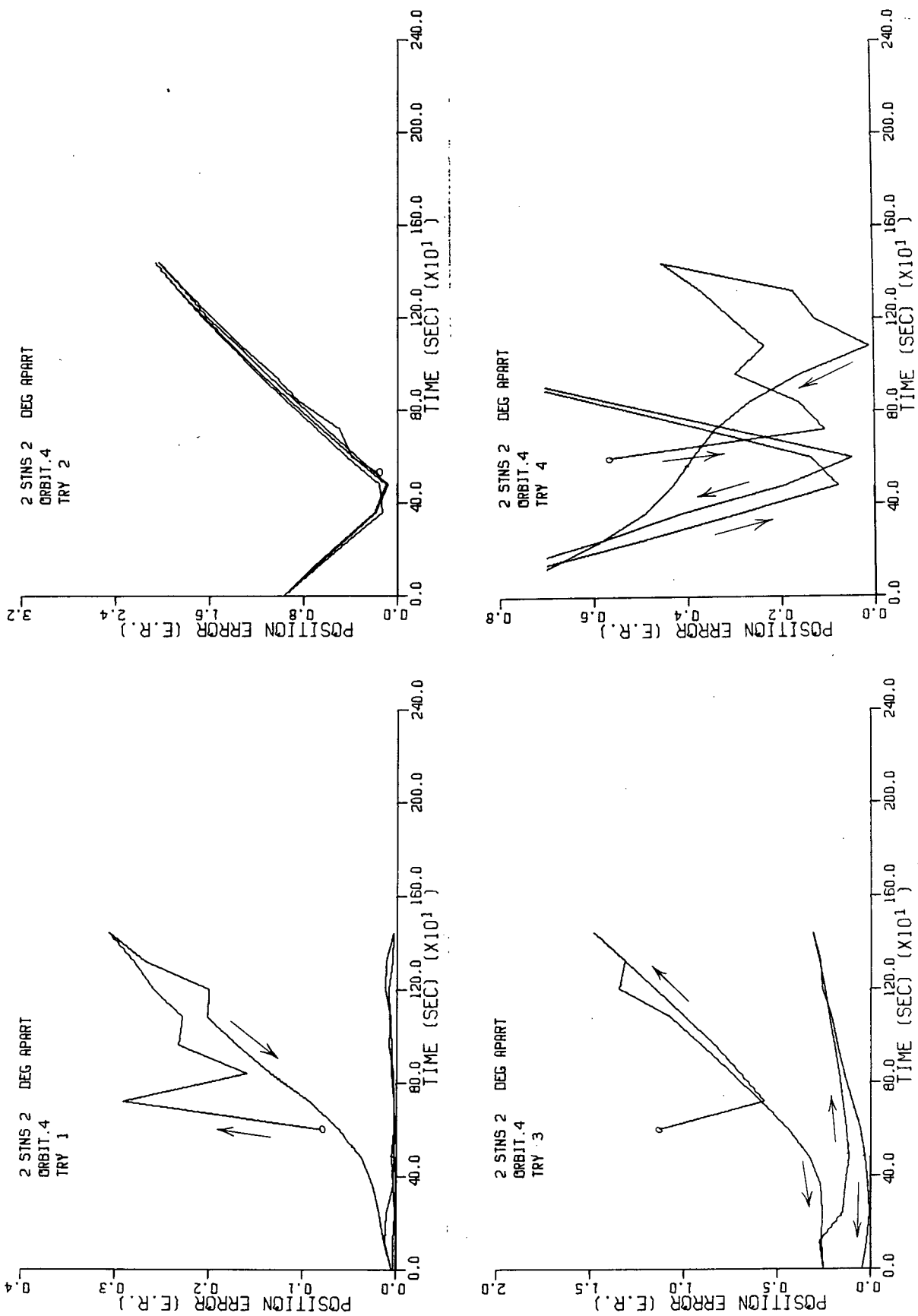

Orbit 4 Position Error 2^{o} Longitude Separation

Figure V.41

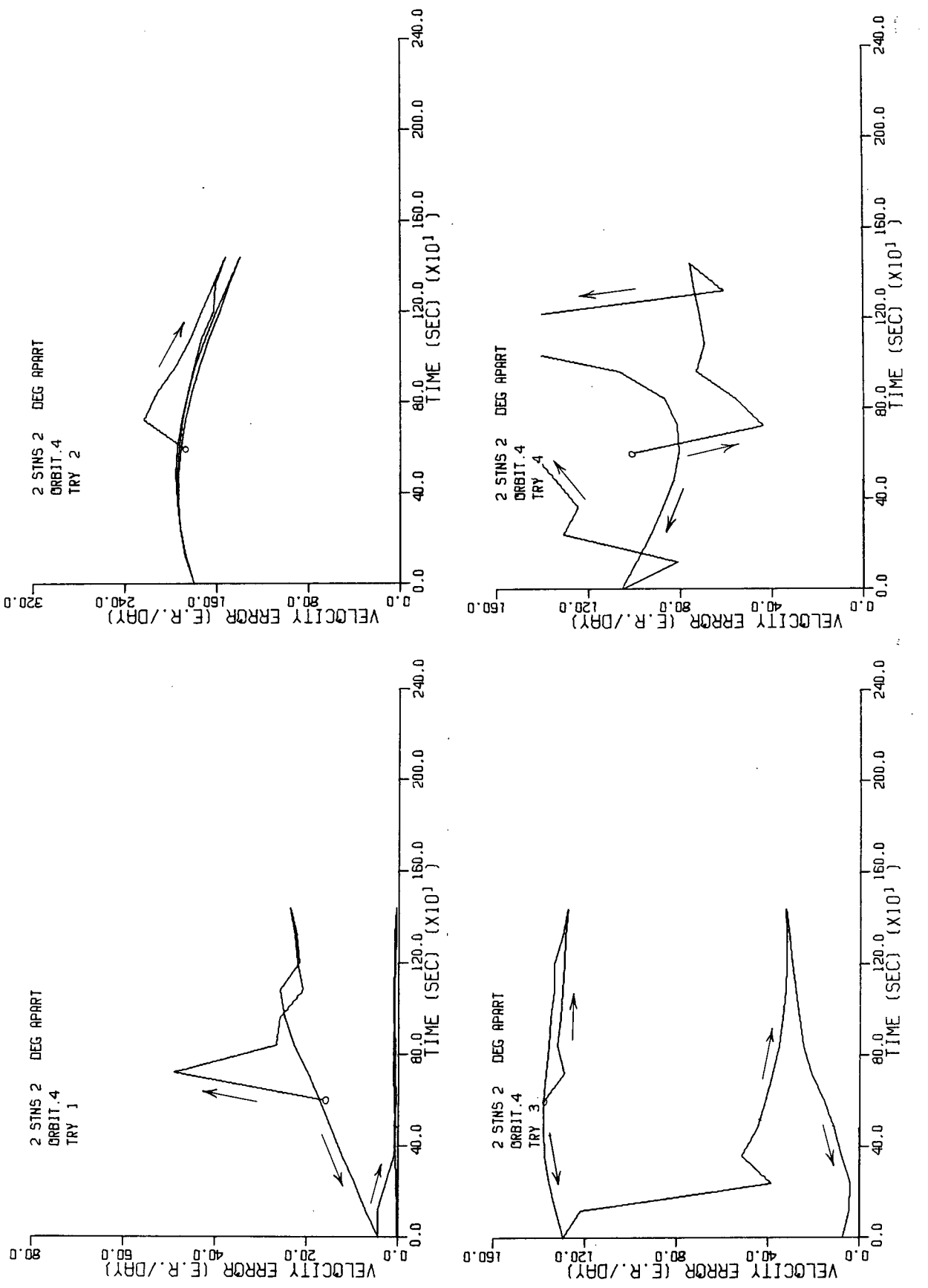

Orbit 4 Velocity Error 2^{o} Longitude Separation

Figure V.42

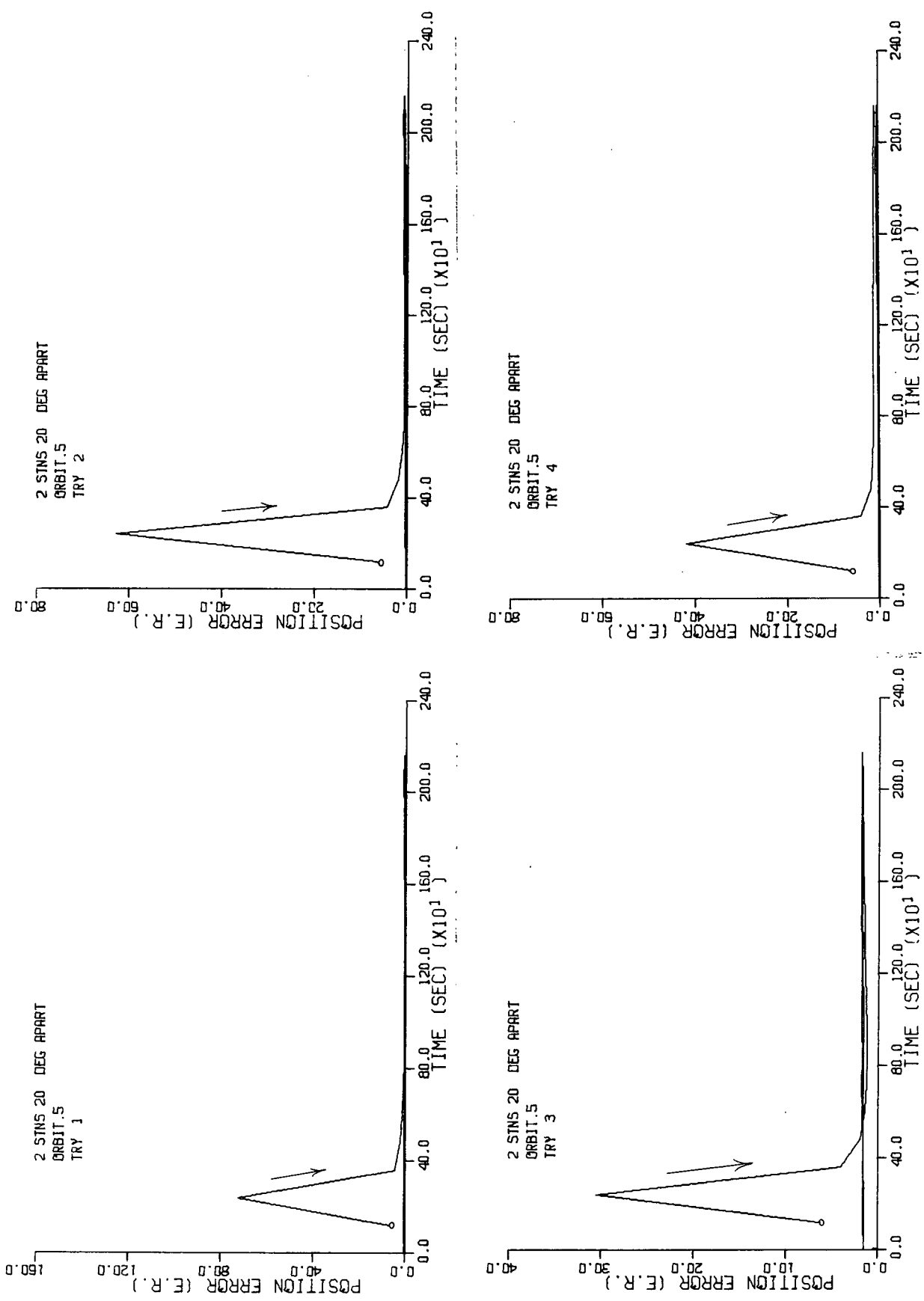

Orbit 5 Position Error 20° longitude Separation Figure V.43

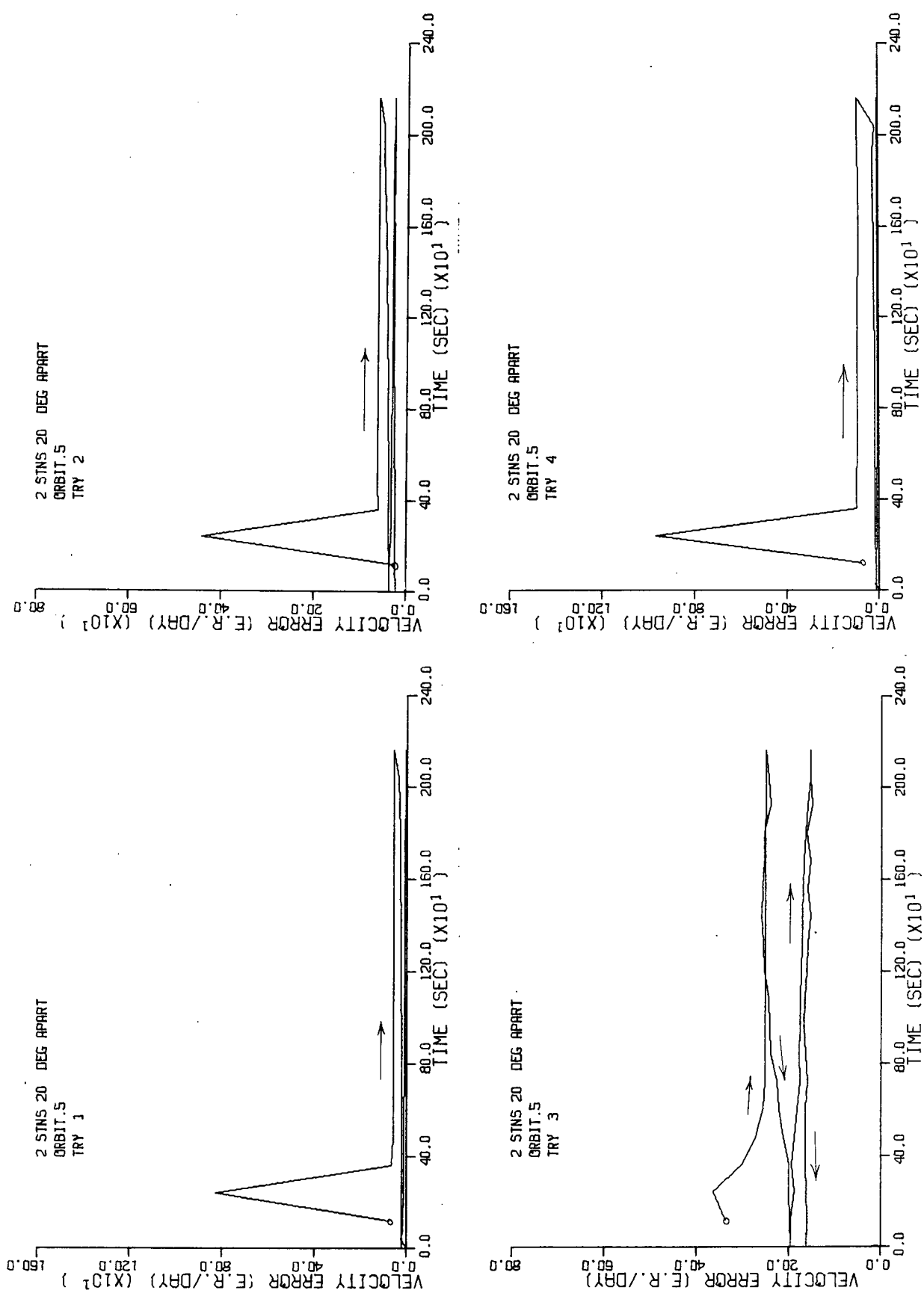

Orbit 5 Velocity Error 20° Longitude Separation Figure V.44

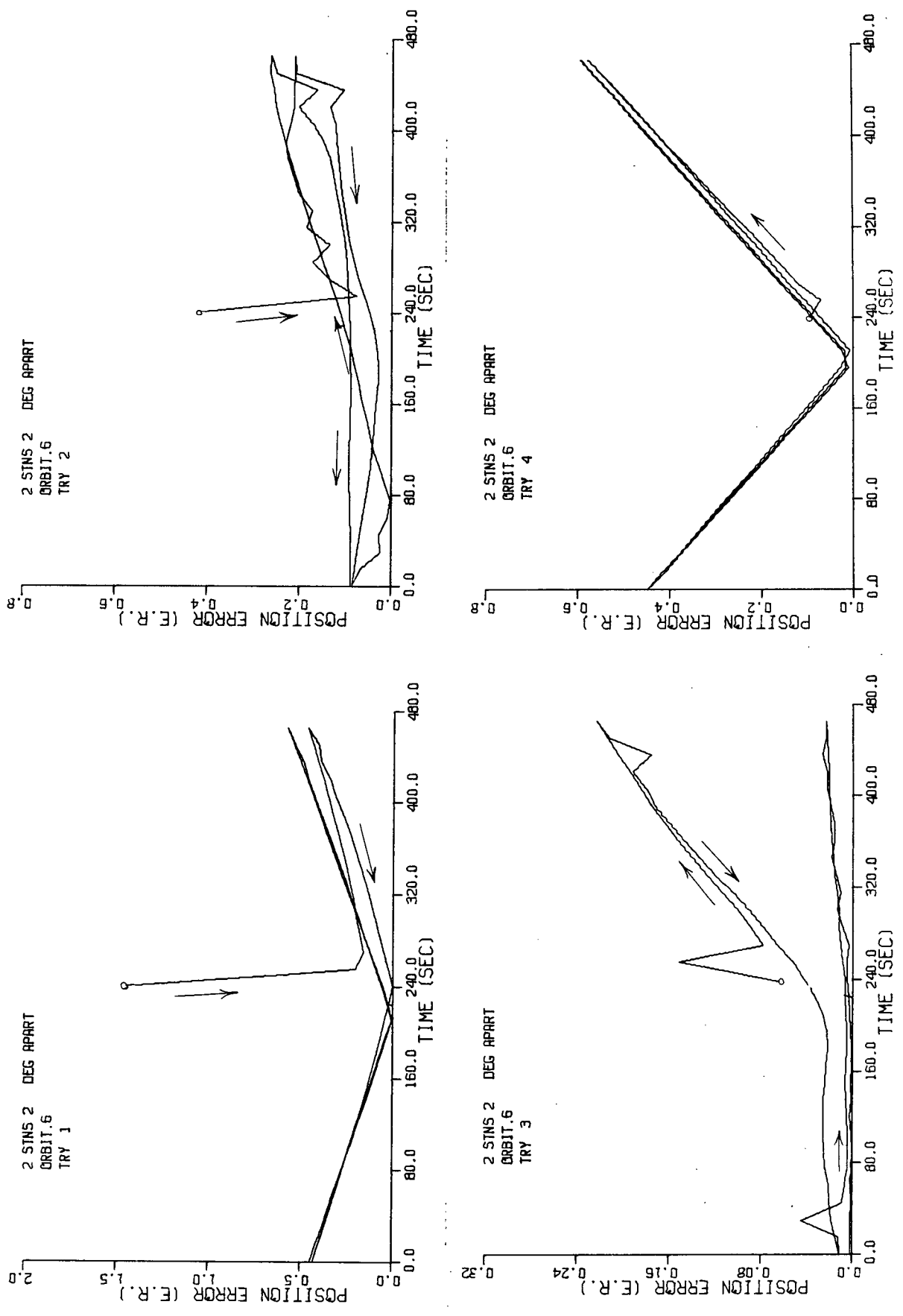

Orbit 6 Position Error 2^{o} Latitude Separation Figure V.45

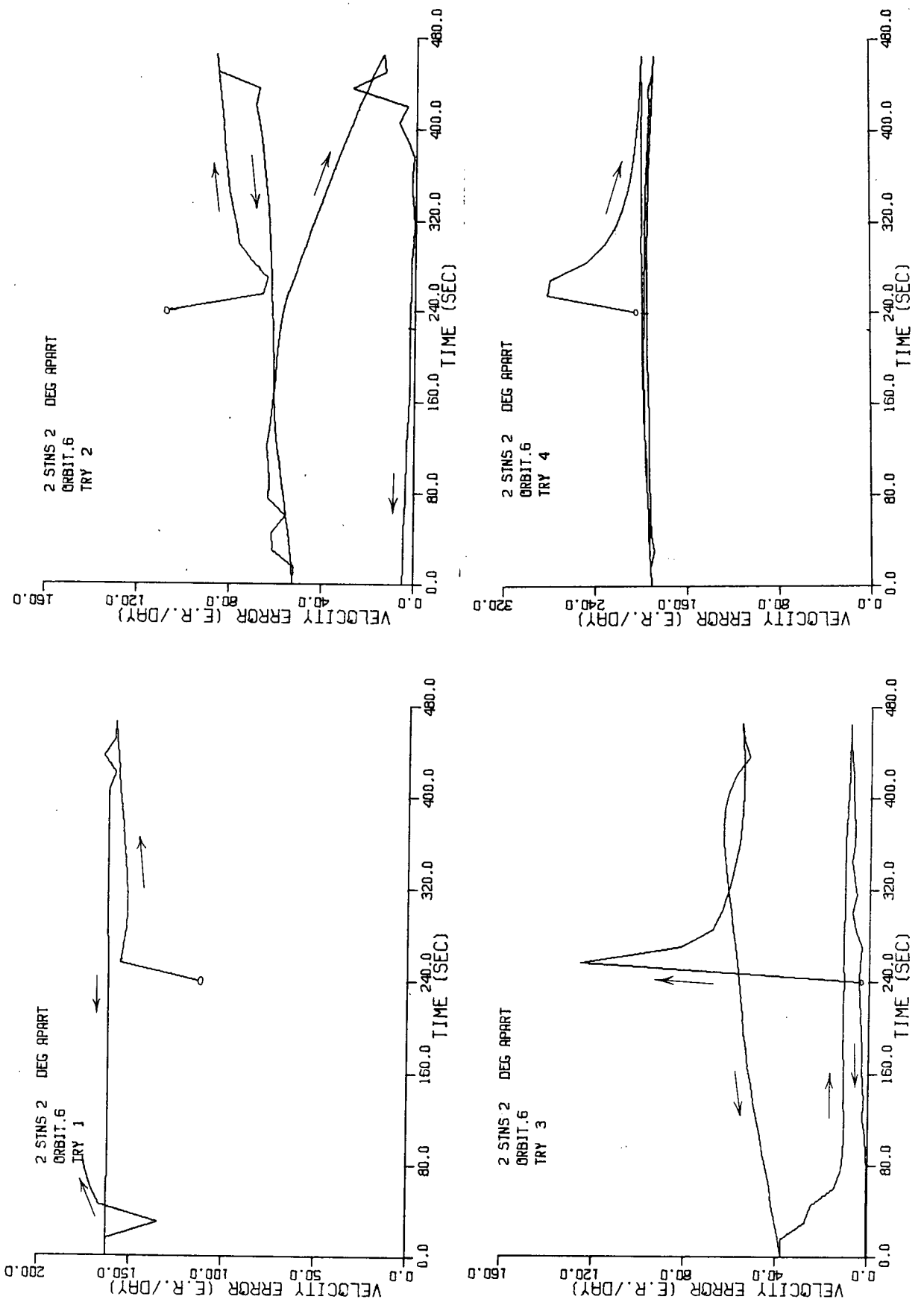

Orbit 6 Velocity Error 2^{o} Lattitude Separation Figure V.46

plots produced. This trace, which is the relatively straight line without kinks, represents the error in the initially assumed uncorrected orbit. Four sweeps were made of the data and the trajectory about which linearization occurs was updated to the best estimate after each sweep.

The results obtained indicated that the range and range-rate measurements could be used to improve the orbital estimates, at least in some cases. They did, however, demonstrate a high degree of dependance on the orbital geometry. Figure V.47 shows the results obtained when an error of 0.05 E.R. is assumed in the semi-major axis of orbit 1. All other parameters are assumed error free. As can be seen a definite improvement in the magnitude of the error occurs. The position error is decreased from approximately 0.4 E.R. to 0.2 E.R.. Similarly the velocity error decreases from about 24 E.R./day to 8 E.R./day. This is accomplished over four sweeps of the data. In some cases all four sweeps were not necessary, the best estimate having been calculated after one sweep. Figure V.48 shows the results of a one degree error in the assumed ascending node. The velocity error is actually greater than the uncorrected estimate for half the first sweep and the position error for parts of the second sweep. However, the third sweep brings a definite improvement in both velocity and position. Figure V.49 shows the improvement when the argument of the perigee is in error by one degree. Figure V.50 and Figure V.51 show improved results for similar errors in orbits 3 and 4.

As an example of the poor results obtained when the observation period was too brief or the number of measurements too few, Figure V.52 shows a simulation result when a one degree error in inclination was assumed in orbit 2, the close polar orbit.

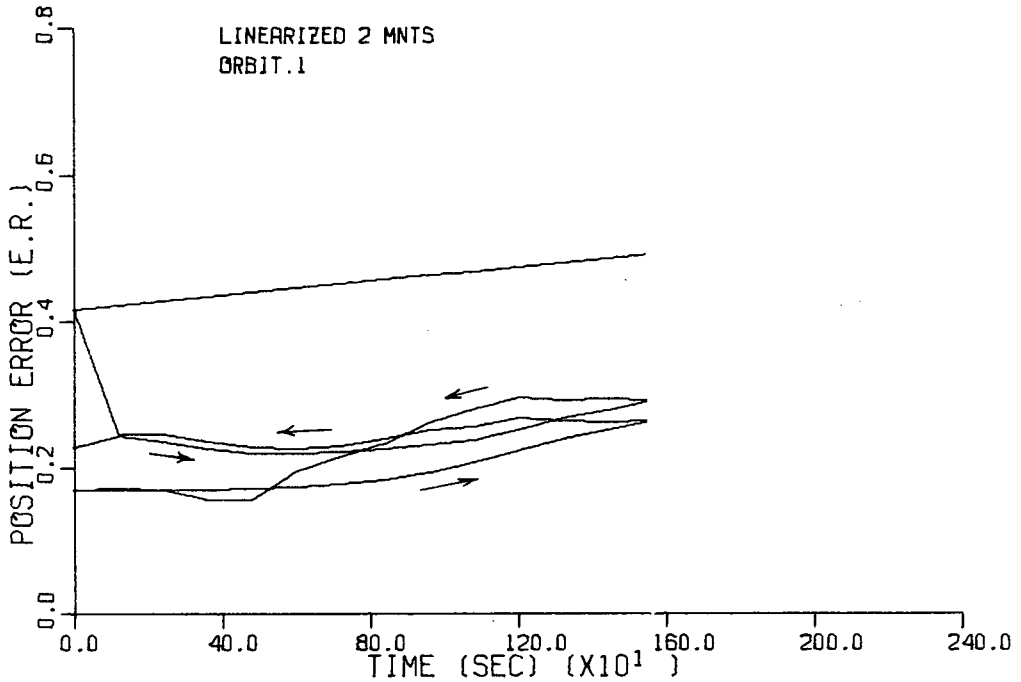

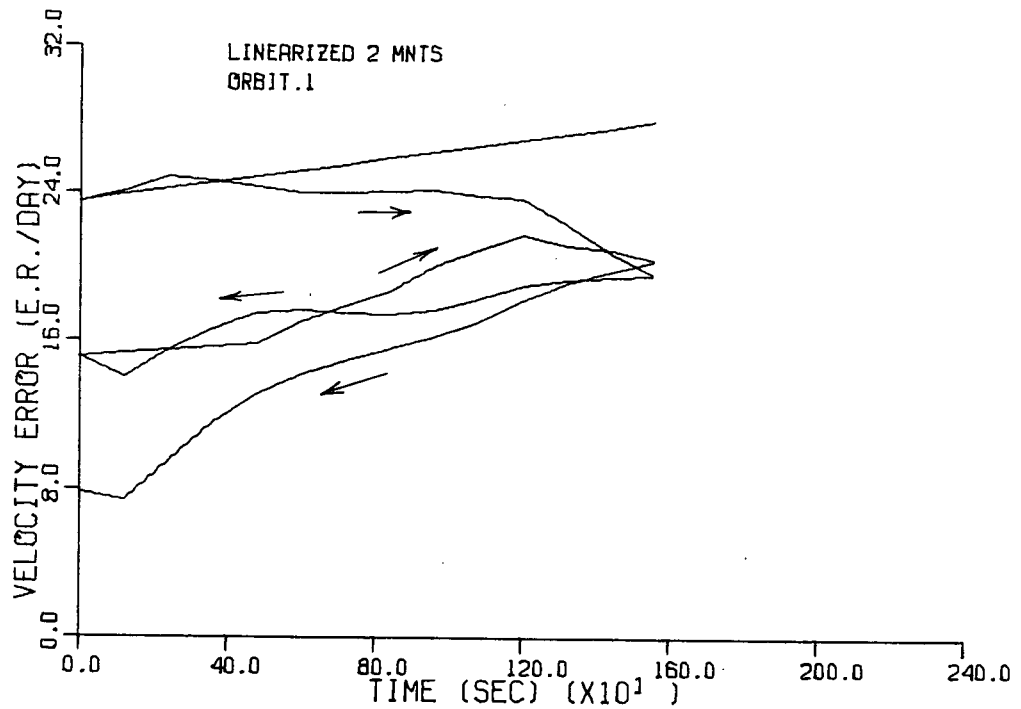

300 Km Error in "A"

Figure V.47

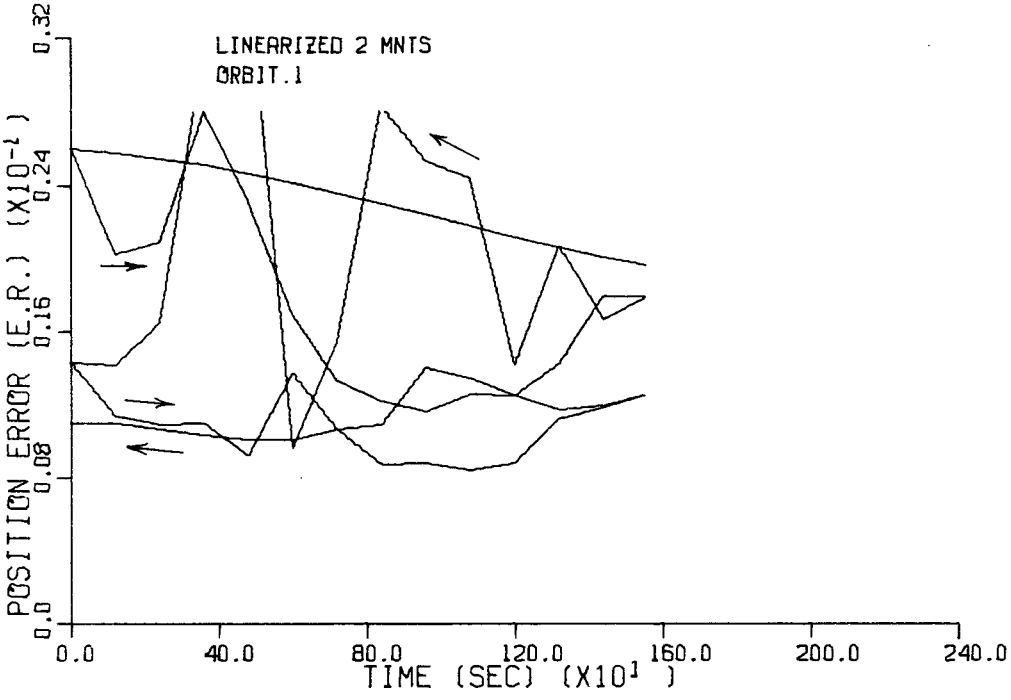

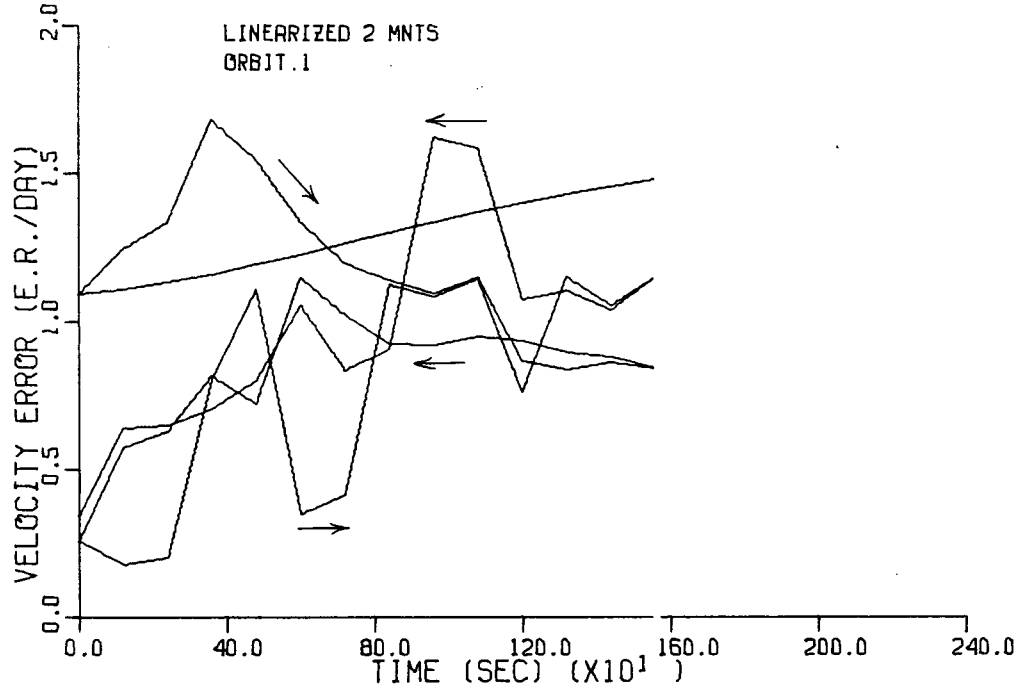

One Degree Error in "L"

Figure V.48

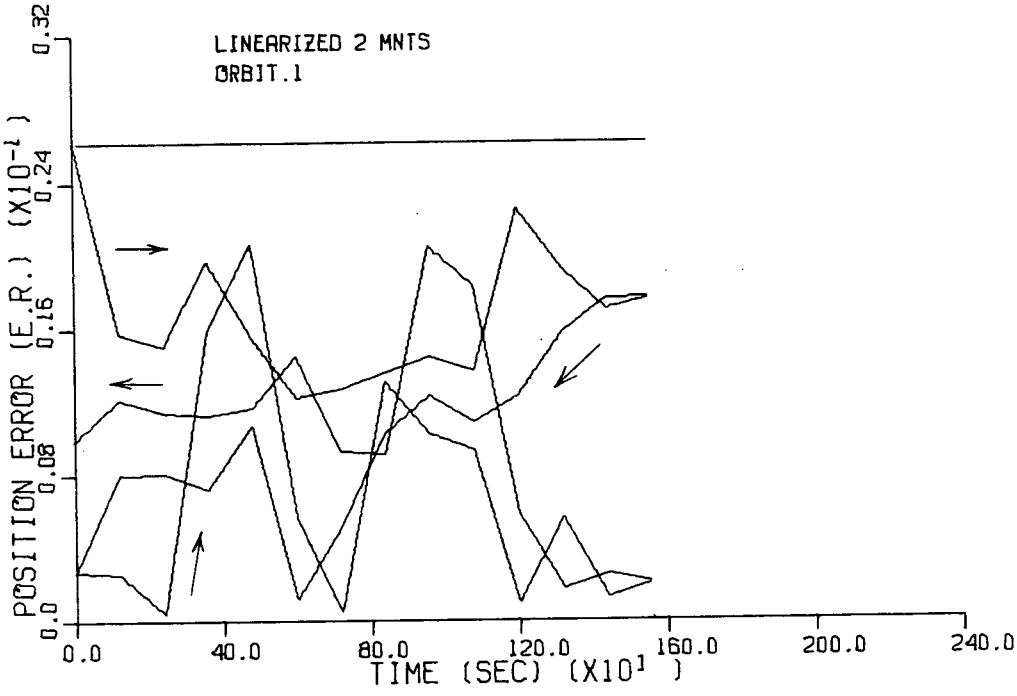

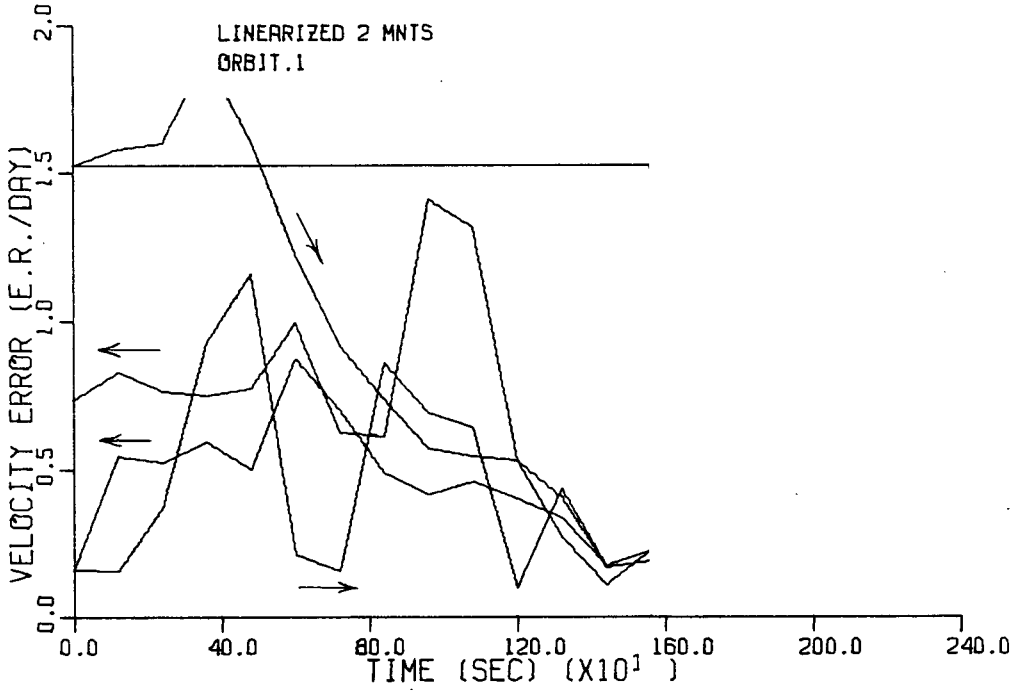

One Degree Error in "p"

Figure V.49

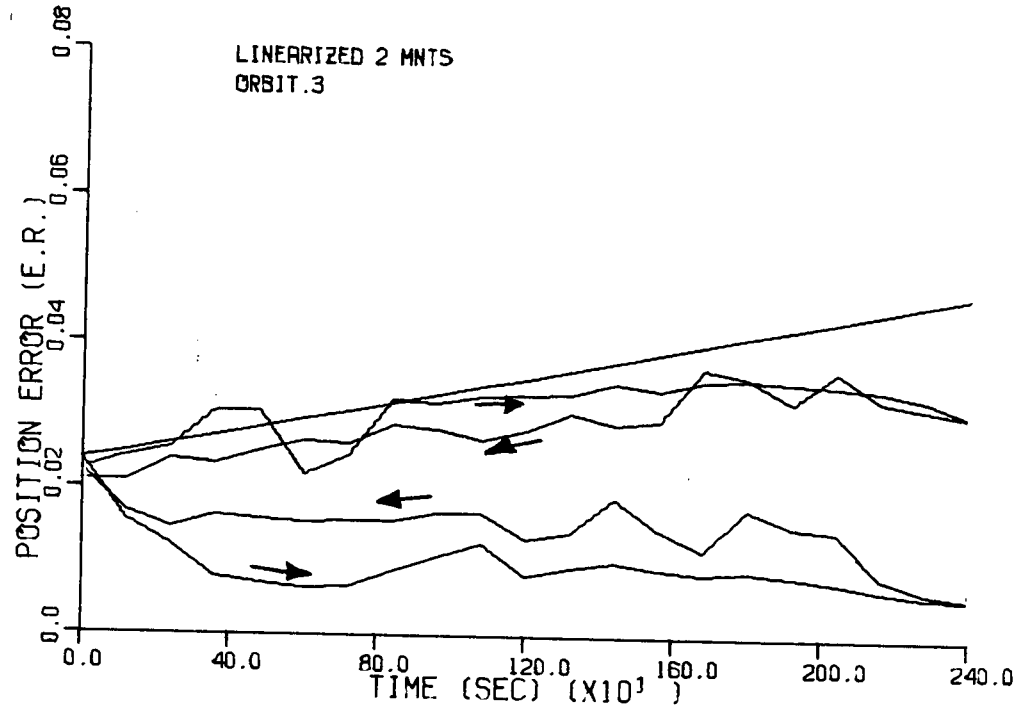

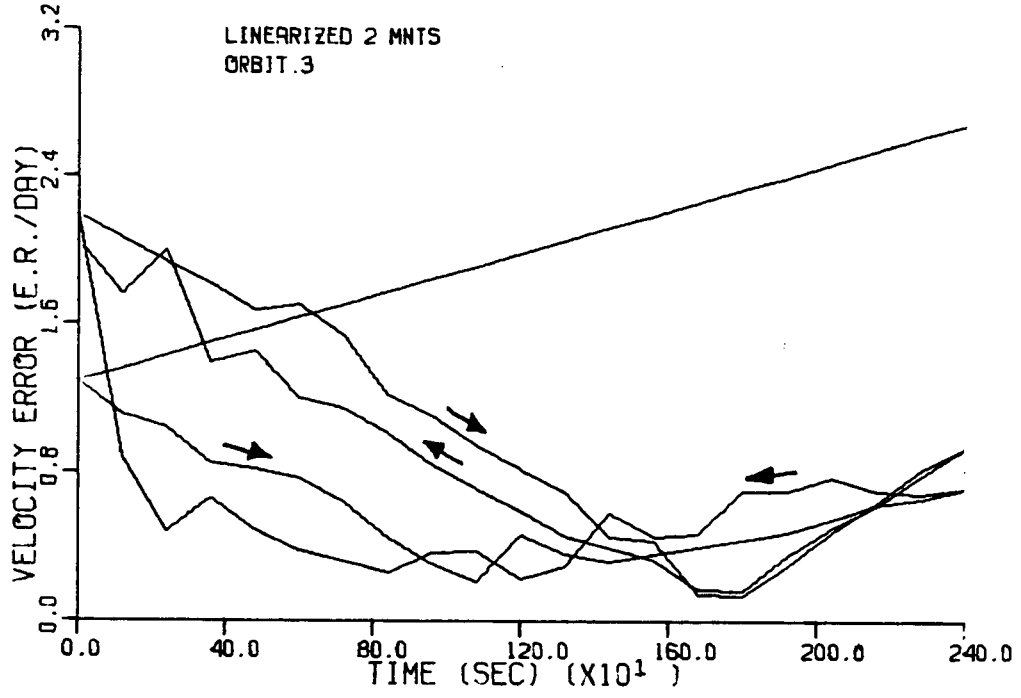

One Degree Error in "i" Orbit 3

Figure V.50

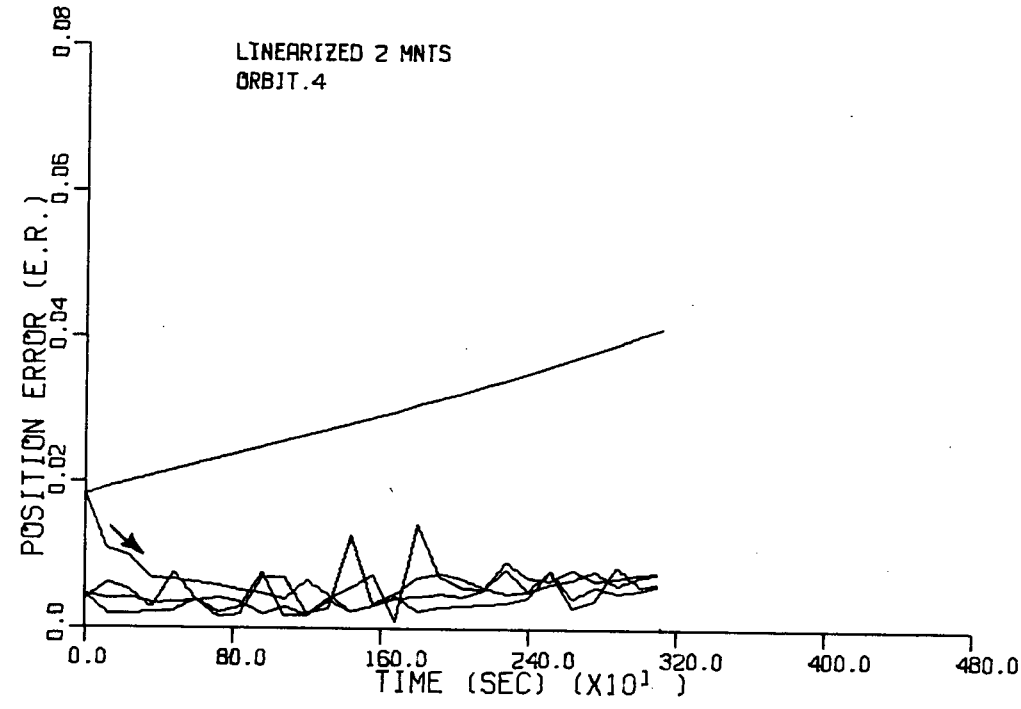

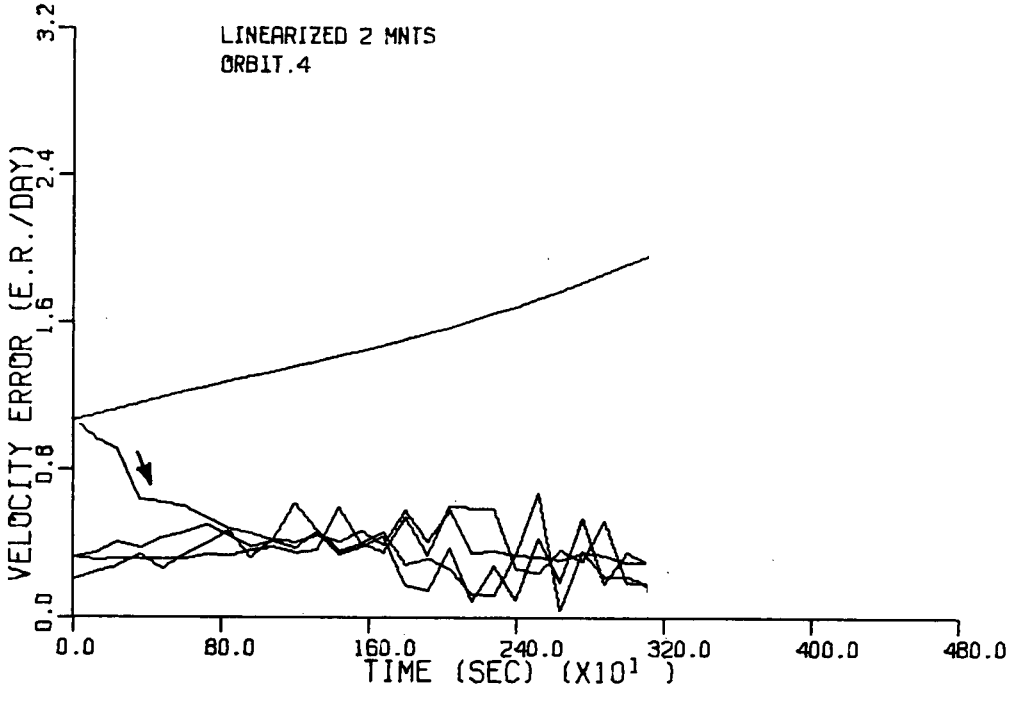

One Degree Error in "i" Orbit 4

Figure V.51

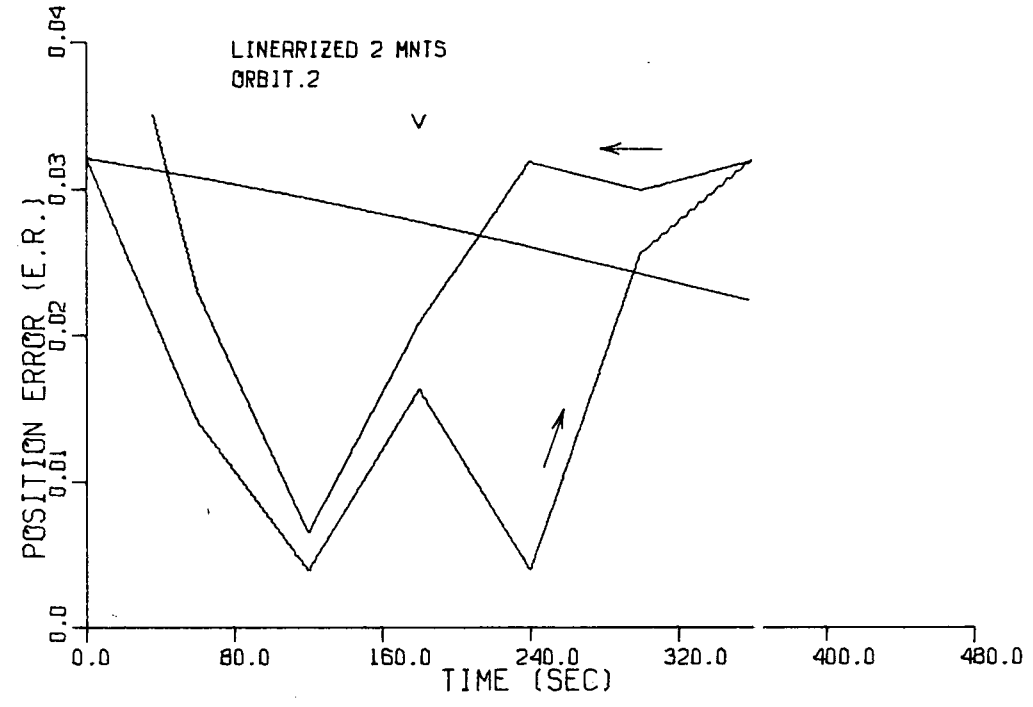

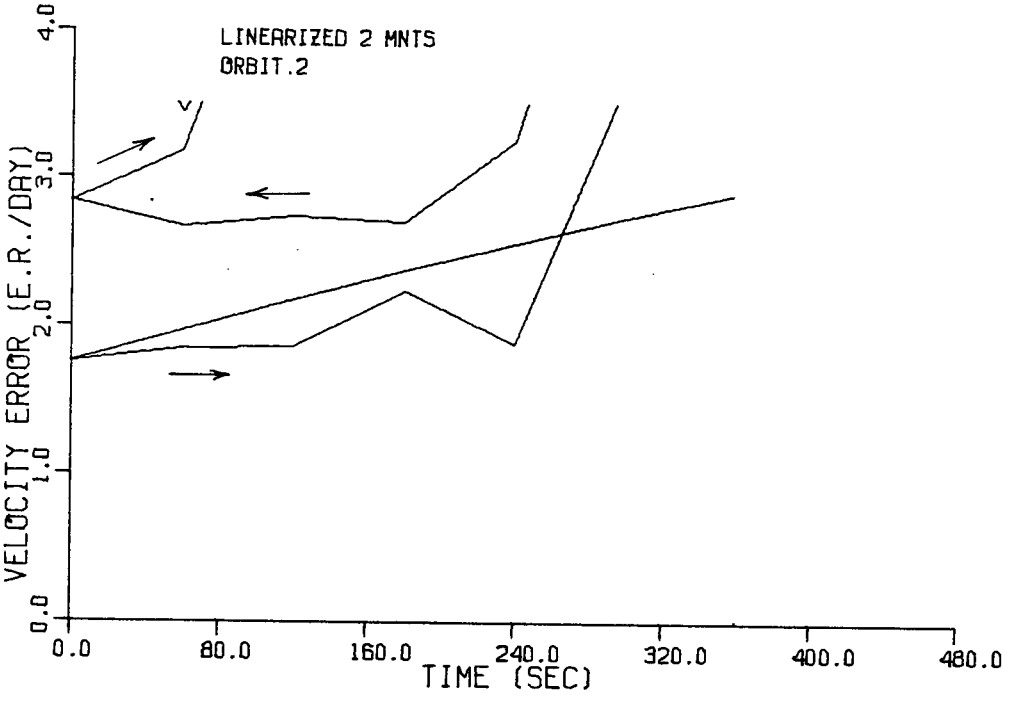

One Degree Error in "i"

Figure V.52

Finally Figure V.53 shows little or no improvement obtained when a one degree error in ascending node is assumed for a geosynchronous satellite. Some improvement can be obtained however if the error is in the semi-major axis as can be seen in Figure V.54 . The improvement is totally in the position, the velocity error already being so small the smoother cannot improve it.

The results indicate that while some improvement can be expected on the average, it is wise to simulate the correction procedure as has been done here, before applying it to any practical problem. This would enable the engineer to determine if the orbit geometry is of the correctable type.

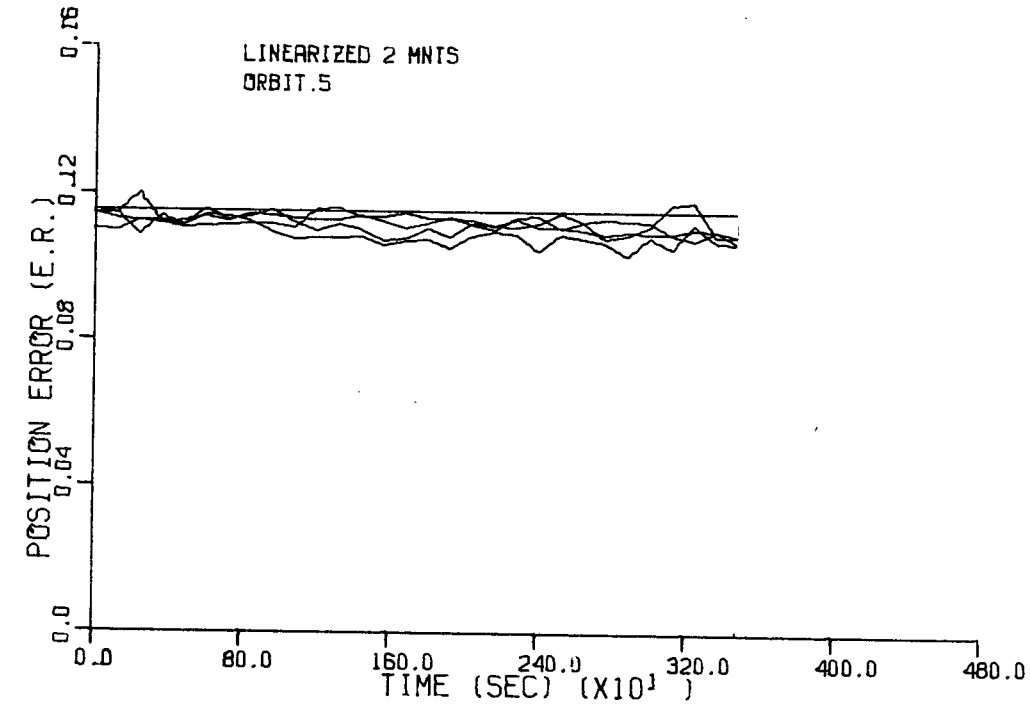

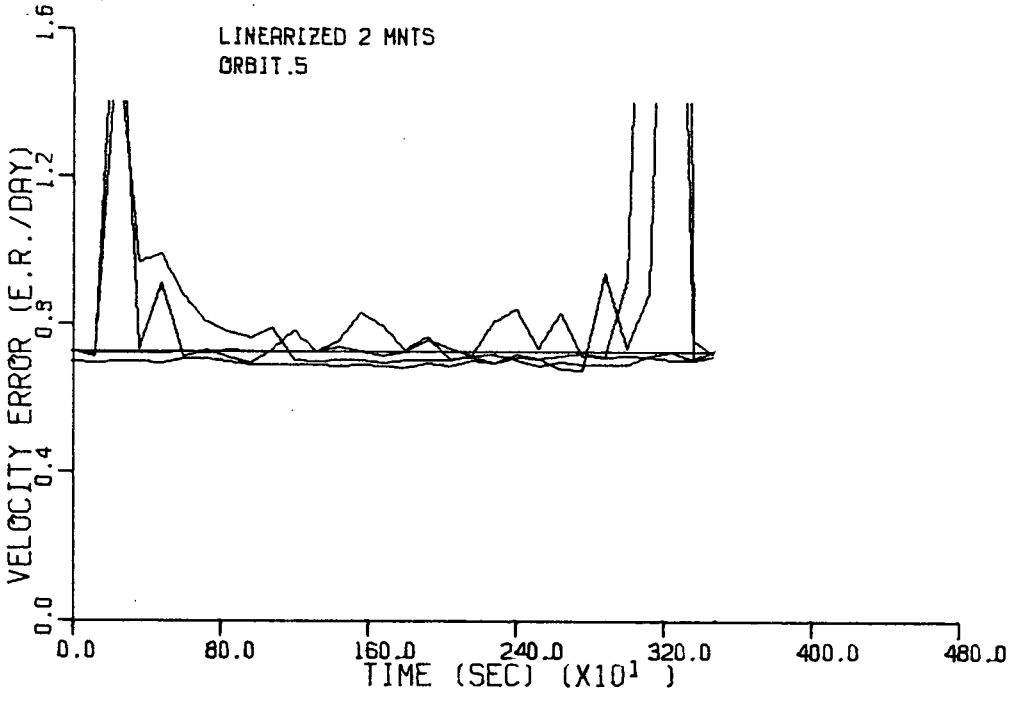

One Degree Error in "L"

Figure V.53

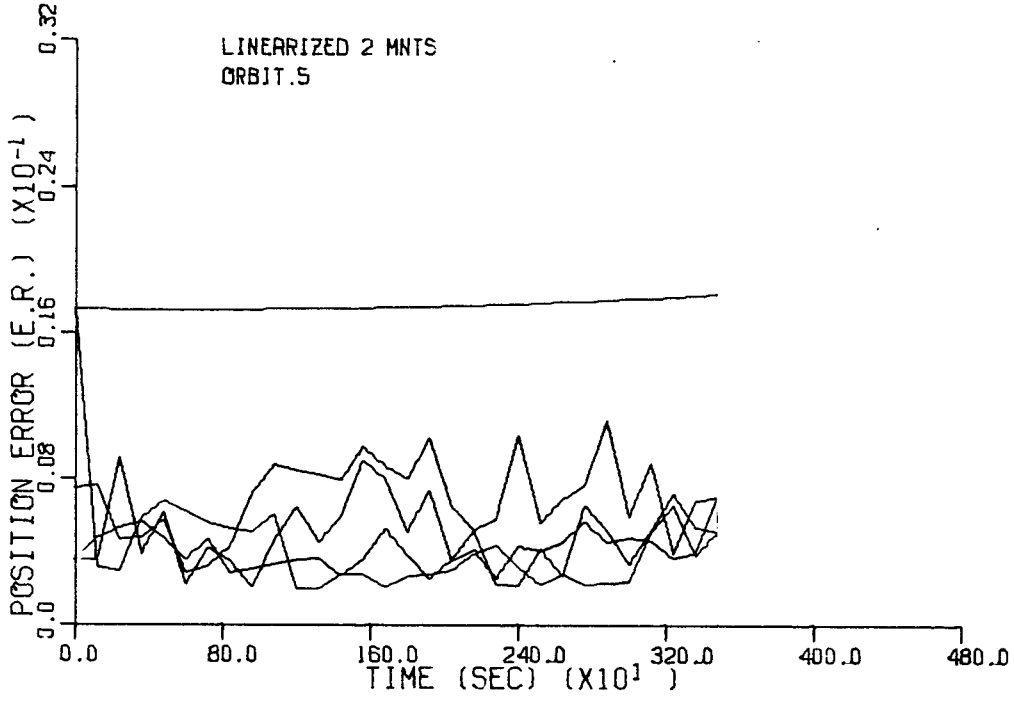

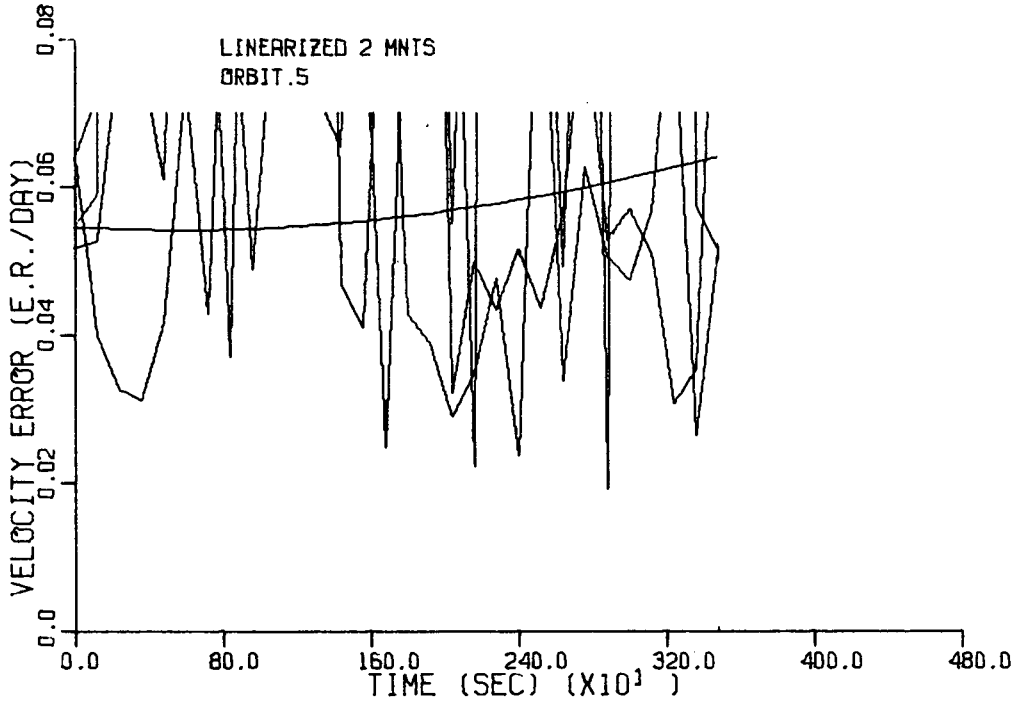

0.01 E.R. Error in "a"

Figure V.54

CHAPTER VI

CONCLUSIONS

A technique has been developed whereby the observability of a non-linear system can be determined through multiple simulation runs. As a good example of this technique, the observability of an earth satellite has been determined for a number of measurement sets. In this case, simulation showed that range and range-rate measurements alone were insufficient for orbit determination and that with the addition of azimuth angle measurements the system became observable. Similar runs showed that the addition of a second station also made the system observable and demonstrated the extended Kalman filter's sensitivity to initializaton. This sensitivity displayed itself in two ways, first within one simulation run only one or two of the four initializations tried would bring the smoother to the correct estimate, and second between simulation runs as the measurement equations were changed the best initialization for a given orbit would change as well. It is beyond the scope of this thesis to explore these instabilities in detail.

Finally, simulation has shown that it is possible in some cases to improve on orbital estimates arrived at by other means, using only range and range rate measurements from one station.

REFERENCES

[1] P.R. Escobal, Methods of Orbit Determination. New York: John Wiley & Sons, 1965.

[2] A. Gelb, Applied Optimal Estimation. Cambridge, Mass.: M.I.T. Press, 1974.

[3] R. Herman and A.J. Krener, "Nonlinear Controllability and Observability", IEEE Transactions on Automatic Control Oct 1977 vol AC-22 No. 5 p728

[4] A.H. Jazwinski, Stochastic Processes & Filtering Theory. New York: Academic Press, 1970.

[5] T.D. Moyer., "Mathematical Formulation of the Double Precision Orbit Determination Program, Jet Propulsion Lab May 1971.

[6] J.J. Pollard, " Orbital Parameter Determination by Weighted Least Square Error and Kalman Filtering Methods", MASc. Thesis Air Force Institute of Technology Dec 1972.

[7] B.E. Schutz, et al., "A Comparison of Estimation Methods for the Reduction of Laser Observations of a Near-Earth Satellite", AAS/AIAA Astrodynamics Conference, Vail Colorado / July 16-18,1973.

[8] P. Swerling, "Modern State Estimation Methods from the Viewpoint of the Method of Least Squares", IEEE Transactions on Automatic Control Dec 1971 vol AC-16 No. 6 p707.